CHANNEL ESTIMATION AND SIGNAL DETECTION FOR WIRELESS RELAY

A Dissertation
Presented to
The Academic Faculty

By

Jun Ma

In Partial Fulfillment
of the Requirements for the Degree
Doctor of Philosophy
in
Electrical and Computer Engineering

School of Electrical and Computer Engineering
Georgia Institute of Technology
December 2010

CHANNEL ESTIMATION AND SIGNAL DETECTION FOR WIRELESS RELAY

Approved by:

Dr. Geoffrey Ye Li, Advisor
Professor, School of Electrical and Computer Engineering
Georgia Institute of Technology

Dr. Erik I. Verriest
Professor, School of Electrical and Computer Engineering
Georgia Institute of Technology

Dr. John R. Barry
Professor, School of Electrical and Computer Engineering
Georgia Institute of Technology

Dr. Xingxing Yu
Professor, School of Mathematics
Georgia Institute of Technology

Dr. Mary Ann Ingram
Professor, School of Electrical and Computer Engineering
Georgia Institute of Technology

Date Approved: November 9, 2010

To Dafang Sun – my mother.

ACKNOWLEDGMENTS

I am most grateful to my research advisor, Professor Geoffrey Ye Li, who has taught me a lot and improved my research capabilities significantly. I have benefited a lot from his impressive insights in research. He also helped me improve my academic writing and oral presentation significantly. I appreciate his care and concern for my intellectual and personal growth. I would like to thank him for his support, encouragement, and invaluable advice during the course of my Ph.D. study.

I am also grateful to Dr. Philip Orlik and Dr. Jinyun Zhang, my supervisors during my research internship at Mitsubishi Electric Research Laboratories (MERL). It has been my pleasant and impressive experience to work with them at MERL in fall 2007 and summer 2008. My Ph.D. research has significantly benefited from their valuable guidance and constant encouragement. I would like to thank them for their everlasting support.

I would like to thank Professor John R. Barry, Professor Mary Ann Ingram, Professor Erik I. Verriest, and Professor Xingxing Yu for serving in my dissertation committee. Their broad perspectives and suggestions helped me a lot in refining this dissertation.

I would also like to thank Professor Wuyang Zhou at the University of Science and Technology of China for initializing my interest in wireless communications and shaping my research capabilities. I am thankful for all my labmates in the Information Transmission and Processing Laboratory and all my colleagues at Centergy One building for inspiring discussions. I thank all my friends at Georgia Institute of Technology. You make this place vivid, warm, and more attractive.

Finally, I would like to thank my parents. They have been supportive during my Ph.D. study. My mother has been educating me to work hard and overcome hardship since my childhood. It was she who has shaped my positive attitude in both work and life. This dissertation is dedicated to my parents.

TABLE OF CONTENTS

LIST OF FIGURES

SUMMARY

Wireless relay plays a critical role in realizing ubiquitous and reliable wireless communications. With wireless relay, signal coverage can be extended and transmission reliability can be enhanced. In practice, a wireless *relay station* (RS) can be utilized to boost the signal strength in a coverage hole, such as in thick buildings or underground tunnels, or to improve the *quality-of-service* (QoS) under adverse channel conditions, such as on high-speed trains. The application of wireless relay, especially the *amplify-and-forward* (AF) relay, entails advanced signal processing techniques to be implemented at both the RS and the *destination station* (DS). This thesis focuses on developing novel channel estimation and signal detection techniques to improve the performance of a wireless relay system.

Our work starts from signal processing in a two-hop *multi-input-multi-output* (MIMO) AF relay system consisting of a *source station* (SS), a DS, and an RS that simply amplifies and forwards its received signal to the DS without any further processing. Since noise is amplified and forwarded from the RS to the DS together with the signal, the overall noise at the DS is colored. To improve signal detection at the DS, we first propose a blind algorithm to estimate the noise correlation based on the statistics of the broadband channel when *orthogonal frequency division multiplexing* (OFDM) modulation is employed. Since no pilots are inserted at the RS, estimation of the backward and the forward relay channels over the SS-RS and the RS-DS hops becomes a challenging issue. To deal with this problem, we propose to estimate the two cascaded relay channels based on a predefined amplifying matrix sequence at the RS and the corresponding overall channel sequence obtained at the DS through conventional channel estimation algorithms. We derive rules to design low-complexity amplifying matrices to guarantee successful relay channel estimation at the DS. Both the blind noise correlation estimation and the indirect relay channel estimation effectively improve the overall performance of a two-hop MIMO AF relay system.

For a *channel-reuse-relay station* (CRRS) to work properly, the co-channel cross-talk

interference from the transmit to the receive antennas must be cancelled. To that end, the coupling channel between the transmit and the receive antennas needs to be estimated first. While the conventional coupling channel estimator requires the RS to transmit dedicated pilots, we propose to utilize the random forwarded signals of the RS as pilots for coupling channel estimation. Without making any modification to the signal structure in the physical layer and causing any in-band interference at the DS, the proposed cross-talk canceller achieves significant performance improvements over the conventional one.

When wireless relay is deployed on a high-speed train to improve the QoS provided to passengers, Doppler compensation techniques need to be implemented at the RS to shield mobile terminals from adverse channel conditions between the *base station* (BS) and the train. This is especially necessary when OFDM modulation is applied because the time-varying channel causes *inter-subchannel interference* (ICI). Since typically a *line-of-sight* (LOS) path exists between the BS and the train, there is strong correlation in and between the desired signal and the ICI. In light of this, we develop the Wiener filtering in the downlink and the transmit preprocessing in the uplink to mitigate ICI by utilizing such correlation. To mitigate ICI in the absence of a LOS path, we further develop a general reduced-rate OFDM transmission scheme to trade spectral efficiency for ICI self-cancellation in a high-mobility environment. By transmit and receive preprocessing, we transform the original N-subcarrier OFDM system into an equivalent K-subcarrier one with significantly reduced ICI. With the preprocessing coefficients optimized based on the statistics of the time-varying channel, the developed reduced-rate OFDM transmission achieves significant performance improvements over the existing ICI self-cancellation schemes.

CHAPTER 1

INTRODUCTION

1.1 Motivation

Wireless relay has become a hot research topic in wireless communication. As a repeater, a wireless *relay station* (RS) forwards signals from the *source station* (SS) to the *destination station* (DS). Wireless relay is suitable for realizing long-range communication or boosting the signal strength in coverage holes, such as in thick buildings or underground tunnels, or on the cell edge [1, 2, 3]. Such wireless RSs also provide flexibility in meeting temporary communication demands under certain scenarios. Furthermore, the coordination between the SS and one or more RSs can be utilized to achieve spatial diversity to enhance the reliability or the capacity of wireless links [4, 5, 6, 7, 8, 9, 10, 11, 12, 13]. With appropriate signal processing, wireless relay can also be utilized to shield a mobile terminal from adverse channel conditions over the direct SS-DS link, such as the time-varying channel between a *base station* (BS) and a high-speed train with a high Doppler frequency.

Depending on how much processing is performed at the RS, the existing relay mechanisms can be broadly categorized as *decode-and-forward* (DF) and *amplify-and-forward* (AF) [4]. An RS working in DF mode detects and demodulates its received signals, decodes the encoded data, re-modulates the data, and forwards them to the DS. In contrast, an RS in AF mode only amplifies and forwards its received signals without any other processing and thus has much simpler implementation than that in DF mode. Furthermore, the RS in AF mode does not require any *a priori* information of its received signal and can be applied to any scenario. Depending on whether channel translation is performed, an RS can be either a *channel-shift-relay station* (CSRS) or a *channel-reuse-relay station* (CRRS). While a CSRS utilizes two orthogonal channels over the SS-RS and the RS-DS links by time division or frequency division, a CRRS reuses the same channel over both links. Compared

to the conventional CSRS, a CRRS significantly increases the spectral efficiency at the expense of increased implementation complexity for canceling local cross-talk interference from the transmit antenna to the receive antenna [14, 15, 16].

To improve the overall performance of a wireless relay system, novel signal processing techniques need to be developed, among which channel estimation and signal detection play critical roles.

- Depending on the implementation complexity permitted and the *channel state information* (CSI) available, appropriate signal processing can be performed at an AF-based RS to improve the system performance. In a two-hop *multi-input-multi-output* (MIMO) AF relay system, the overall channel between the SS and the DS is a concatenated one combining the backward and forward relay channels over the SS-RS and the RS-DS links and the amplifying matrix at the RS. Therefore, optimization of the amplifying matrix is very important in improving the overall channel condition. With complete or partial CSI at the RS, the amplifying matrix can be designed appropriately to increase the capacity or improve the signal detection performance of the overall system [17, 18, 19].

- In a two-hop MIMO AF relay system, estimation of both the overall channel between the SS and the DS and the involved backward and forward relay channels is very important in the amplifying matrix design at the RS and signal detection at the DS [20]. Different from the conventional one-hop channel, the overall channel between the SS and the DS is a cascaded one combining the backward and the forward relay channels and the amplifying matrix at the RS, which makes estimation of the overall channel in a two-hop AF relay system a unique issue. Furthermore, in the presence of a low-complexity AF-based RS, the forward relay channel has to be estimated at the DS without help of any dedicated pilots from the RS. In general, dedicated channel estimation techniques need to be developed for AF-based wireless relay.

- While a CRRS improves spectral efficiency by reusing the same channel over both the SS-RS and the RS-DS hops, it suffers severe cross-talk interference from the transmit to the receive antenna [15, 21], which, if not cancelled, will prevent the CRRS from working properly. Therefore, design of advanced cross-talk cancellers is a critical issue in the application of CRRSs. In particular, novel algorithms need to be developed to estimate the coupling channel from the transmit to the receive antenna in a way that is completely transparent to both the SS and DS [22].

- When wireless relay is deployed on a high-speed train to improve the *quality-of-service* (QoS) provided to passengers, it is desired to perform Doppler compensation at the RS based on the statistics of the time-varying channel that can be obtained from the train system, such as the speed and the position of the train relative to the BS. With appropriate signal processing, such an RS shields mobile terminals from the severe Doppler spread in the wireless channel between the BS and the train [23].

1.2 Literature Review

In this section, we review state-of-the-art signal processing techniques for wireless relay, including AF wireless relay, cross-talk cancellation for wireless relay with channel reuse, and *inter-subchannel interference* (ICI) mitigation for wireless relay on high-speed trains with *orthogonal frequency division multiplexing* (OFDM) modulation.

1.2.1 AF Wireless Relay

1.2.1.1 Cooperative Relay

The QoS of wireless communication is mainly limited by the wireless medium. Since wireless channel is a broadcast one, only one user is allowed to transmit at any time, which significantly restricts the capacity of the wireless communication system. Moreover, time-varying fading caused by multiple paths in wireless channel further degrades the reliability of wireless links. In a rich scattering environment, multipath fading varies significantly on the scale of half wavelength. In light of this, it has been proposed to deploy multiple

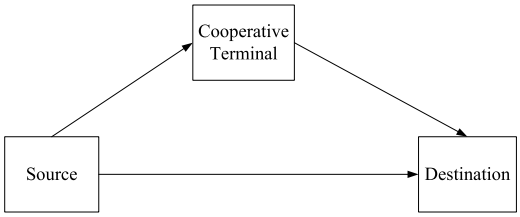

Figure 1.1. Schematic diagram of cooperative relay.

antennas at the receiver and/or the transmitter to enhance the reliability [24, 25, 26] or the capacity [27, 28, 29, 30] of a wireless communication system.

Multiple-antenna techniques improve the QoS of a wireless communication system at the expense of an increased implementation cost at mobile terminals. Usually deploying multiple sufficiently spaced antennas at a mobile terminal is a demanding task. Therefore, it has been suggested in [7, 8, 10, 11] to let single-antenna mobile terminals cooperate with each other to form a virtual multiple-antenna system. Figure 1.1 shows a schematic diagram of such a system in which the cooperative terminal relays signals for the source by the AF or the DF mechanism. Since the destination receives multiple independent copies of the desired signal from the source and one or more cooperative terminals, diversity is achieved by user cooperation without the need for deploying multiple antennas at mobile terminals. In [10], it has been demonstrated that the AF cooperation protocol in which one user acts as a relay for the other by amplifying and forwarding the signal received from its partner with a fixed gain, achieves full cooperative diversity. In [11], distributed space-time coded cooperation protocols have been developed in which cooperative terminals that fully decode the received signal utilize a space-time code to cooperatively relay to the destination. It has been demonstrated that such a *distributed space-time coding* (DSTC) scheme achieves full cooperative diversity in the number of cooperating terminals. Recently, cooperative diversity via fixed-gain AF relay and *maximum ratio combination* (MRC) and *equal gain combination* (EGC) at the destination over general Nakagami fading channels has been investigated in [31] and [32], respectively. Furthermore, the performance of multi-hop and multi-branch cooperative AF relay has also been investigated in [33] and [34].

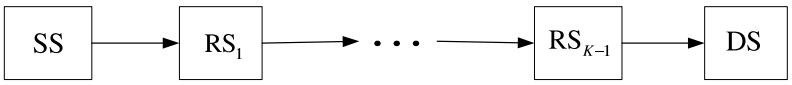

Figure 1.2. Schematic diagram of a K-hop relay system.

1.2.1.2 Multi-Hop AF Relay

Wireless relay can be utilized to achieve cooperative diversity when there already exists a direct link between the SS and the DS or there exist multiple RSs. On the other hand, wireless relay can also be utilized for multi-hop transmission in the absence of a direct link between the SS and the DS. Figure 1.2 shows a schematic diagram of such a multi-hop relay system. In cellular communication systems, relay-assisted two-hop transmission can be utilized to boost the signal strength in coverage holes, such as in thick buildings or underground tunnels, or on the cell edge, etc [1,2,3,35]. Furthermore, relay-assisted multi-hop transmission can also be utilized in wireless sensor networks to realize long-range communication with constrained transmit power [35].

For a single-antenna two-hop AF relay system consisting of an SS, an RS with a fixed gain or a fixed instantaneous transmit power, and a DS, the outage probability of the received *signal-to-noise ratio* (SNR) at the DS over various fading channels have been investigated in [36, 37, 38, 39]. In [40, 41, 42, 43], similar analysis has been conducted for multi-hop AF relay systems. When the CSI is only available at the DS, the ergodic capacity of a multi-hop AF relay system over Rayleigh fading channels has been investigated in [44] and [45]. The optimal power allocation between the SS and the RSs in a multi-hop AF relay system that minimizes the outage probability or maximizes the instantaneous received SNR at the DS has also been investigated in [46] and [47].

Recently, MIMO AF relay has been developed to enhance the reliability or increase the capacity of multi-hop transmission [48,49,50,51]. Different from a single-antenna RS with a scalar gain, a multiple-antenna RS has an amplifying matrix gain. When perfect CSI is available at both the SS and the RS, the optimal amplifying matrix and the corresponding

optimal power allocation at and between the SS and the RS have been proposed to maximize the instantaneous capacity [17, 18, 19] or minimize the *mean-square error* (MSE) of the symbol estimations [52] in a two-hop MIMO AF relay system with constrained overall transmit power. When different levels of partial CSI are available at the RS, various suboptimal amplifying matrices have also been investigated in [53].

1.2.1.3 Channel Estimation for AF Relay

While most of the aforementioned work on wireless relay assumes perfect or partial CSI at the RS and the DS, relay channel estimation has also received much attention recently. For the DF relay, the channels over the SS-RS and the RS-DS hops are required at the RS and the DS for signal detection, respectively. Therefore, the conventional single-hop channel estimation algorithms can be utilized directly for channel estimation for the DF relay. For the AF relay, the overall channel from the SS to the DS, which is a cascaded one consisting of the SS-RS and the RS-DS hops, is required at the DS for signal detection. Since the two-hop overall channel has different statistical properties from a single-hop wireless channel, the conventional channel estimation algorithms are suboptimal for the AF relay. In [54], the statistics of the overall channel in a single-antenna two-hop AF relay system, including the statistical distribution, the time-domain correlation, and the Doppler spectrum, have been investigated. Based on these statistical properties, pilot-aided *minimum mean-square error* (MMSE) overall channel estimation has been proposed in [55]. In [56], the optimal training sequence and the corresponding optimal amplifying matrix at the RS that minimize the MSE of the overall channel estimate have also been investigated. By utilizing the statistics of the broadband overall channel, a blind algorithm has been proposed in [57] to estimate the overall channel in a two-hop AF relay system up to a phase ambiguities vector, which can be estimated with a small number of pilot symbols. As an alternative to direct overall channel estimation at the DS, it has also been proposed to separately estimate the backward and the forward relay channels at the RS and the DS, respectively, and then let the RS feed forward the estimated backward relay channel to the DS to obtain the overall channel. With

additional feed-forwarding overhead, the separate overall channel estimation scheme has been demonstrated as being superior to the direct one, especially when there exists severe noise propagation from the RS to the DS [58].

1.2.2 Cross-Talk Cancellation for Wireless Relay with Channel Reuse

Conventionally, the RS receives data from the SS over one channel and forwards them to the DS over the other channel by time division or frequency division [10, 11]. In this way, interference between the SS-RS and the RS-DS hops is avoided, which, however, sacrifices spectral efficiency since the communication between the SS and the RS consumes half of the time or frequency resource allocated to the link. Alternatively, the RS may forward signals to the DS over the same channel as it receives. An RS working in this mode is called a *channel-reuse-relay station* (CRRS). In *digital video broadcasting* (DVB), on-channel repeaters [14, 15, 16] have been applied as in-band relays to extend the signal coverage. These on-channel repeaters amplify and forward their received signals without any channel translation, i.e., the same channel is utilized over both the source-to-repeater and the repeater-to-destination links. In contrast with the conventional RS, a CRRS not only significantly increases spectral efficiency but also avoids changing the existing physical and link layers to support relay mechanism. In practice, a CRRS is especially suitable for boosting the signal strength in coverage holes since, in this case, the transmit power of the RS is low due to a restricted coverage and directional transmission, which relaxes the requirements for a high isolation between the transmit and the receive antennas of the RS. While a CRRS is an attractive option, a critical issue involved is severe co-channel cross-talk interference from the transmit antenna to the receive antenna, which is shown in Figure 1.3 as the dashed line. Since the transmit power of an RS is dramatically greater than its received desired signal power, such cross-talk interference, if not cancelled properly, will keep the RS from receiving signals from the source. To mitigate cross-talk interference at a CRRS, a high isolation between the transmit and the receive antennas is required [59].

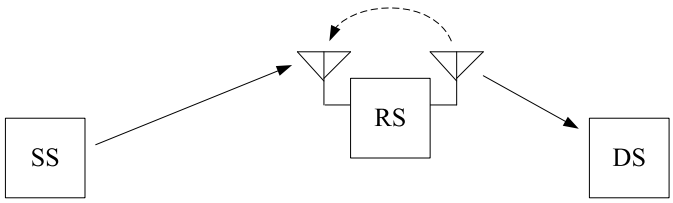

Figure 1.3. Cross-talk interference at a wireless CRRS.

To that end, directional transmission and reception is usually applied at the CRRS. Furthermore, a shield may also be put between the transmit and the receive antennas [60]. Besides high-isolation antennas, both analog [61,62] and digital [15,21] cancellers need to be implemented at the CRRS to further reduce the cross-talk interference.

Since cross-talk interference at a CRRS consists of its previously transmitted signal coupled with the channel from the transmit to the receive antenna, it can be reconstructed and cancelled if the coupling CSI is available. Therefore, it is natural to estimate the coupling channel and perform cross-talk cancellation accordingly. In contrast with the conventional wireless channel characterized by multipath (frequency-selective) and time-varying (time-selective) due to distantly located transmitter and receiver, the coupling channel at a CRRS is quasi-static and has very slow variation with both time and OFDM subcarriers since the transmit and the receive antennas of the CRRS are collocated. Such simplistic characteristics of the coupling channel greatly facilitate the coupling channel estimation and cross-talk cancellation at a CRRS [15, 16, 21]. In the literature, various digital cross-talk cancellation schemes based on the coupling channel estimation have been developed [15, 21]. It has been proposed to set dedicated pilots, such as the pseudo-random sequences, at a CRRS for local coupling channel estimation. Such dedicated pilots assisted coupling channel estimation usually consists of two phases. In the startup phase, the RS transmits dedicated pilots only and obtains an initial coupling channel estimate. In the update phase, low-power dedicated pilots are transmitted by the RS together with its forwarded signals for coupling channel estimate updating.

1.2.3 ICI Mitigation for OFDM-based Wireless Relay

Relay-assisted two-hop transmission can be utilized not only to extend the signal coverage but also to shield a mobile terminal from the adverse channel conditions over the direct SS-DS link by transferring the burden of signal processing to the wireless relay. Recently, high-speed train techniques have attracted lots of interests throughout the world. Next-generation wireless communication systems are expected to provide reliable data transmission to passengers on such high-speed trains. Since these trains travel at a maximum speed of around 500 km/h, the wireless channel between the BS and the train suffers a high Doppler frequency. When OFDM [63] modulation is utilized for broadband data transmission, the time-domain variation of wireless channel within an OFDM symbol caused by a high Doppler frequency destroys the orthogonality among subcarriers and causes ICI [64, 65, 66, 67, 68], which, if not cancelled, will severely degrade the system performance and result in an error floor. To improve the QoS provided to passengers, a wireless RS can be deployed on the train, which forwards signals from the BS to mobile users or vice versa after appropriate processing. The RS has one or multiple antennas on top of the train for communication with the BS, and multiple antennas distributed in carriages for communication with mobile users. With the burden of ICI mitigation transferred to the RS, mobile terminals on the train are shielded from the high Doppler frequency in the channel between the BS and the train.

1.2.3.1 Pilot-Assisted ICI Cancellation

In a high-mobility environment, the impulse response of channel varies with time even within an OFDM symbol. As a result, the *channel frequency response* (CFR) matrix is no longer diagonal and the off-diagonal elements are the interference gains among OFDM subchannels. In the literature, it has been proposed to estimate these interference gains with the help of pilots and then perform ICI cancellation accordingly. Since the CFR matrix is an approximately banded one with most of its power concentrated around the main diagonal, a clustered pilot structure has been proposed for interference gain estimation [69, 70, 71]. To

improve the interference gain estimation, various time-varying channel models have been established to reduce the number of to-be-estimated parameters in the multipath channel. In [72, 73, 74], it has been assumed that the channel over each path varies with time linearly in one or more OFDM symbols. As an extension, polynomial channel models have been developed in [75, 76]. In [69] and [77], various *basis expansion models* (BEMs), including the Karhunen-Loeve BEM, the prolate spheroidal BEM, and the complex-exponential BEM, have been introduced to approximate the time-varying channels in OFDM systems. Recently in [78], the time-varying channel has also been modeled as a linear combination of the dominant eigenvectors of the correlation matrix of the time-domain channel vector. Since the CFR matrix estimation requires lots of pilots, decision feedback assisted iterative ICI cancellation has also been developed in [79, 80, 81].

1.2.3.2 OFDM Transmission with ICI Mitigation

ICI cancellation based on the CFR matrix estimation requires lots of pilots, which significantly sacrifices spectral efficiency. Moreover, treating the generally full CFR matrix as a banded one results in an error floor in the interference gain estimation. As an alternative to pilot-assisted ICI cancellation, various OFDM transmission schemes with inherent ICI mitigation capabilities have been developed. In [82], two-order frequency-domain correlative coding has been proposed to mitigate the ICI by introducing correlation among transmitted symbols over neighboring OFDM subchannels. In [83], the optimal *partial response encoding* (PRC) at an OFDM transmitter that minimizes the ICI power has been proposed as an extension of the frequency-domain correlative coding developed in [82]. In [84], the frequency-domain correlative coding has been further extended to MIMO-OFDM systems over fast fading channels. In [85, 86, 87], various transmit and receive windowing techniques have been developed to mitigate ICI caused by time-varying channels or carrier frequency offsets. However, these pilot-free full-rate OFDM transmission schemes only have limited ICI mitigation capabilities and still suffer considerable residual ICI. To deal with this problem, an ICI self-cancellation transmission scheme has been

developed in [88], which significantly reduces ICI at the expense of a halved spectral efficiency. In [89] and [90], general ICI self-cancellation schemes have been proposed to achieve tradeoffs between ICI mitigation and spectral efficiency.

1.3 Our Approaches and Thesis Outline

The major goal of this research is to investigate novel channel estimation and signal detection algorithms to improve the performance of a wireless relay system. Depending on the specific application scenario, these algorithms are implemented at the RS or the DS for relay channel estimation, cross-talk interference cancellation, and Doppler compensation in the presence of a high-mobility terminal. With these algorithms, the end-to-end performance of the wireless relay system will be significantly improved.

As the first step, we consider a two-hop MIMO-OFDM AF relay system consisting of an SS, a DS, and an RS that simply amplifies and forwards its received signal to the DS without any further processing. Such a system can be utilized to extend the coverage of wireless communications in certain scenarios. Since the local noise at the RS is amplified and forwarded to the DS together with the signal, the overall noise vector at the DS is colored. In Chapter 2, we propose a blind noise correlation estimation algorithm so as to improve signal detection at the DS. Without requiring any dedicated pilots, such a blind algorithm takes advantages of the frequency-domain correlation of the broadbind wireless channel in an OFDM system. The proposed algorithm significantly improves signal detection at the DS especially over spatially correlated MIMO forward relay channels even in the presence of significant uncertainties in the channel statistics.

In a two-hop MIMO AF relay system, the overall channel from the SS to the DS is a cascade of the backward relay channel over the SS-RS hop, the amplifying matrix at the RS, and the forward relay channel over the RS-DS hop. While the overall CSI guarantees successful signal detection at the DS, the involved backward and forward relay CSI, if available, can be utilized to improve the overall system performance. However, no pilots are

inserted at the low-complexity AF-based RS to assist direct estimation of the forward relay channel at the DS. In Chapter 3, we investigate the estimation of the two cascaded relay channels at the DS based on a predefined amplifying matrix sequence at the RS and the corresponding overall channel sequence obtained through conventional channel estimation algorithms with the help of pilots transmitted by the SS. In particular, we find necessary and sufficient conditions on the pilot amplifying matrix sequence at the RS to ensure successful relay channel estimation at the DS. Based on these conditions, rules are presented to design diagonal or quasi-diagonal pilot amplifying matrices so that the cascaded relay channels can be successfully estimated with minimum complexity at the RS. With the estimated relay CSI at the DS, a significant performance improvement in signal detection is achieved.

While a CRRS enhances spectral efficiency by receiving and transmitting over the same channel, it suffers severe cross-talk interference from the transmit to the receive antennas. The existing cross-talk cancellation techniques usually require the RS to transmit dedicated pilots, such as the pseudo-random sequences, for estimation of the local coupling channel from the transmit to the receive antennas. However, inserting these dedicated pilots at the RS not only changes the original signal structure in the physical layer but also results in in-band interference at the DS. In Chapter 4, we propose a new cross-talk canceller that does not require the RS to transmit any dedicated pilots. In particular, the random forwarded signals of the RS are utilized as pilots for local coupling channel estimation. The proposed cross-talk canceller based on the least square coupling channel estimation can be applied to an RS with the AF, the DF, or any other relay mechanism. For an RS with the DF mechanism, we further propose a cross-talk canceller based on the MMSE coupling channel estimation, which is essentially an MMSE canceller. Without requiring any dedicated pilots and causing any in-band interference at the DS, the proposed cross-talk canceller achieves a significant performance improvement over the conventional one.

When a wireless RS is deployed on a high-speed train to improve the QoS provided to passengers, Doppler compensation at the RS is necessary so as to shield a mobile terminal

from the adverse channel conditions over the direct link. When OFDM modulation is employed, time-varying of the wireless channel between the BS and the high-speed train causes ICI among subchannels and results in an error floor. In Chapter 5, statistics-based ICI mitigation schemes are developed for OFDM-based wireless relay on high-speed trains. Without requiring any dedicated pilots, these schemes reduce ICI by taking advantages of the strong correlation in and between the desired signal and the ICI when there exists a *line-of-sight* (LOS) path between the BS and the train. In particular, we propose the Wiener filtering in the downlink and the transmit preprocessing in the uplink, respectively, both of which effectively mitigate ICI and lower the error floor even in the presence of significant uncertainties in the channel statistics.

The pilot-free full-rate ICI mitigation schemes proposed in Chapter 5 for OFDM-based wireless relay relies on the existence of a LOS path between the BS and the train. In the absence of a LOS path, it only has limited ICI mitigation capabilities and still suffers considerable residual ICI. In Chapter 6, we further develop a general reduced-rate OFDM transmission scheme for ICI mitigation at a high-mobility wireless relay. By transmit and receive preprocessing, we transform the original N-subcarrier OFDM system into an equivalent K-subcarrier one with the rate reduction factor $\frac{N}{K}$. At the expense of a reduced transmission rate, we are able to design the transmitted signal structure with inherent ICI self-cancellation capability. Without requiring the instantaneous CSI, we develop a general structure of transmit and receive preprocessing matrices so that the K equivalent subchannels in the equivalent OFDM system share a common average SIR. Based on the developed structure, we further optimize the preprocessing coefficients to maximize the SIR based on the statistics of the time-varying channel. The developed reduced-rate OFDM transmission achieves significant performance improvements over the existing ICI self-cancellation schemes in a high-mobility environment.

CHAPTER 2

BLIND NOISE CORRELATION ESTIMATION IN TWO-HOP MIMO-OFDM AF RELAY SYSTEMS

In cellular communication systems, the quality of received signal at a *mobile station* (MS) on the cell edge or in severely shadowed regions cannot be guaranteed. While this problem may be alleviated by decreasing the cell size, this solution is cost-inefficient since more BSs will have to be deployed in the network. As an alternative, wireless relay techniques have been proposed to boost signal strength in such coverage holes [1, 2, 3].

In this chapter, we are concerned with a two-hop MIMO-OFDM AF relay system, which can be utilized to extend the coverage of cellular communications via low-complexity wireless relay. Such a system consists of an SS, an RS, and a DS, all of which are equipped with multiple transmit/receive antennas. In this system, the SS communicates with the RS over one channel while the RS amplifies and forwards its received signals to the DS over the other channel. That is, there is no direct communication link between the SS and the DS and data is conveyed from source to destination via two orthogonal channel uses by time division or frequency division. Since the local noise is amplified and forwarded from the RS to the DS together with the signal, the overall noise vector at the DS is colored with its correlation matrix determined by the forward relay channel over the RS-DS hop. Therefore, estimation of the noise correlation at the DS is very important in improving signal detection. Conventionally, one may propose to estimate the forward relay channel at the DS and then obtain the noise correlation accordingly. However, this requires the RS to transmit pilots to assist forward relay channel estimation at the DS, which may not suitable for a low-complexity AF-based RS. To deal with this problem, we propose a blind noise correlation estimation algorithm in this chapter. Without requiring any pilots, this algorithm is based on the channel statistics such as the power delay profile of the time-domain

multipath channel. Simulation results demonstrate that the proposed noise correlation estimation algorithm effectively improves signal detection at the DS even in the presence of significant uncertainties in the channel statistics.

The remainder of this chapter is organized as follows. In Section 2.1, we describe the system model. In Section 2.2, we develop the blind noise correlation estimation algorithm. Simulation results are presented in Section 2.3. Finally Section 2.4 concludes this chapter.

2.1 System Model

In this chapter, we consider a two-hop MIMO-OFDM AF relay system. Suppose that there are N_s transmit antennas at the SS, N_r receive and transmit antenna pairs at the RS, and N_d receive antennas at the DS. Furthermore, K-subcarrier OFDM modulation is applied for broadband transmission. Denote $\mathbf{H}_1(k)$ as the $N_r \times N_s$ channel matrix between the SS and the RS over the kth ($0 \leq k \leq K-1$) OFDM subcarrier, $\mathbf{G}(k)$ as the $N_r \times N_r$ amplifying matrix at the RS, and $\mathbf{H}_2(k)$ as the $N_d \times N_r$ channel matrix between the RS and the DS, and then the received signal vector at the DS, $\mathbf{y}_d(k)$, can be expressed as

$$\begin{aligned} \mathbf{y}_d(k) &= \mathbf{H}_2(k)\mathbf{G}(k)\mathbf{H}_1(k)\mathbf{x}(k) + \mathbf{H}_2(k)\mathbf{G}(k)\mathbf{n}_r(k) + \mathbf{n}_d(k) \\ &= \mathbf{H}(k)\mathbf{x}(k) + \mathbf{n}(k), \quad 0 \leq k \leq K-1 \end{aligned} \tag{2.1}$$

where $\mathbf{x}(k)$ denotes the transmitted signal vector at the SS, $\mathbf{n}_r(k)$ and $\mathbf{n}_d(k)$ denote the noise vectors generated at the RS and the DS, respectively, $\mathbf{H}(k)$ denotes the overall channel matrix between the SS and the DS defined as

$$\mathbf{H}(k) = \mathbf{H}_2(k)\mathbf{G}(k)\mathbf{H}_1(k), \tag{2.2}$$

and $\mathbf{n}(k)$ denotes the overall noise vector at the DS defined as

$$\mathbf{n}(k) = \mathbf{H}_2(k)\mathbf{G}(k)\mathbf{n}_r(k) + \mathbf{n}_d(k), \tag{2.3}$$

which consists of the colored noise forwarded from the RS and the local white noise. Based on (2.1), we show the block diagram of the two-hop MIMO-OFDM AF relay system model over the kth subcarrier in Figure 2.1.

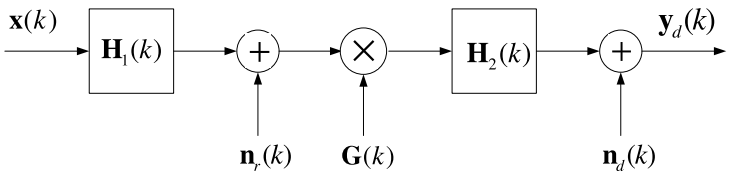

Figure 2.1. Two-hop MIMO-OFDM AF relay system model over the kth subcarrier

To simplify the relay structure as much as possible, we assume that $\mathbf{G}(k) = g\mathbf{I}_{N_r}, 0 \leq k \leq K-1$, where $\mathbf{I}_{N_r}$ denotes the $N_r \times N_r$ identity matrix and g denotes the constant amplifying gain of the RS. We further assume that the elements of $\mathbf{n}_r(k)$ and $\mathbf{n}_d(k)$ are *identical and independently distributed* (i.i.d.) complex Gaussian random variables with zero mean and variance σ_n^2, i.e.,

$$\mathbf{R}_{n_r}(k) = E_n\left\{\mathbf{n}_r(k)\mathbf{n}_r^H(k)\right\} = \sigma_n^2\mathbf{I}_{N_r}, \tag{2.4}$$

and

$$\mathbf{R}_{n_d}(k) = E_n\left\{\mathbf{n}_d(k)\mathbf{n}_d^H(k)\right\} = \sigma_n^2\mathbf{I}_{N_d}, \tag{2.5}$$

where $E_n\{\cdot\}$ denotes the expectation with respect to noise. Based on the above assumptions, the correlation matrix of the overall noise vector at the DS can be obtained as

$$\mathbf{R}_n(k) = E_n\left\{\mathbf{n}(k)\mathbf{n}^H(k)\right\} = g^2\sigma_n^2\mathbf{H}_2(k)\mathbf{H}_2^H(k) + \sigma_n^2\mathbf{I}_{N_d}, \tag{2.6}$$

which indicates that the noise components over different receive antennas of the DS are correlated unless $\mathbf{H}_2(k)$ has orthogonal row vectors.

2.1.1 White Noise Assumption

In the two-hop MIMO-OFDM AF relay system, the low-complexity RS simply amplifies and forwards its received signals to the DS without any further processing. Therefore, the forward relay channel between the RS and the DS cannot be estimated with the help of pilots. As a result, the correlation matrix of the overall noise vector at the DS, $\mathbf{R}_n(k)$, cannot be obtained. However, the knowledge on $\mathbf{R}_n(k)$ is very important in improving estimation of the overall channel between the SS and the DS and signal detection at the DS.

Conventionally, we may simply assume that the elements of $\mathbf{n}(k)$ are i.i.d. and approximate $\mathbf{R}_n(k)$ with

$$\begin{aligned}\overline{\mathbf{R}}_n(k) = E\{\mathbf{R}_n(k)\} &= g^2\sigma_n^2 E\left\{\mathbf{H}_2(k)\mathbf{H}_2^H(k)\right\} + \sigma_n^2\mathbf{I}_{N_d} \\ &= \sigma_n^2\left(N_r g^2\sigma_2^2 + 1\right)\mathbf{I}_{N_d}, \end{aligned} \tag{2.7}$$

where $E\{\cdot\}$ denotes the expectation with respect to $\mathbf{H}_2(k)$ and σ_2^2 denotes the average power gain over the second hop from the RS to the DS. Obviously, if $N_r g^2\sigma_2^2 \ll 1$, then the power of the colored noise forwarded from the RS is negligible compared to that of the local white noise at the DS. As a result, $\mathbf{R}_n(k) \approx \overline{\mathbf{R}}_n(k)$, i.e., the overall noise is approximately white. On the other hand, if N_r is large enough for a given N_d, then the rows of $\mathbf{H}_2(k)$ will be approximately orthogonal to one another according to the law of large numbers [91]. In this case, $\mathbf{R}_n(k)$ approximates diagonal and thus the overall noise is also approximately white. When *vertical bell laboratories layered space-time* (V-BLAST) transmission is applied in the two-hop MIMO-OFDM AF relay system, the approximate MMSE and *maximum likelihood* (ML) detection based on the white noise assumption in (2.7) can be implemented, as will be discussed in Section 2.3.

2.2 Blind Noise Correlation Estimation

As mentioned, the elements of the overall noise vector at the DS are correlated with the correlation matrix $\mathbf{R}_n(k)$ given in (2.6). Since the forward relay channel, $\mathbf{H}_2(k)$, is unavailable, the actual $\mathbf{R}_n(k)$ is unknown to the DS. While we have made the white noise assumption in Section 2.1, it is only applicable to certain scenarios and inevitably causes a performance degradation in general cases. In this section, we propose a blind algorithm to directly estimate the noise correlation matrix based on the channel statistics. Essentially, this algorithm takes advantages of the strong frequency-domain correlation of the broadband wireless channel in an OFDM system. Without requiring any pilots, the proposed blind noise correlation estimation algorithm is able to significantly improve signal detection at the DS. Since the proposed algorithm is based on the statistics of the forward relay

channel, $\mathbf{H}_2(k)$, we will first describe the statistical model of $\mathbf{H}_2(k)$.

2.2.1 Channel Statistics

Throughout this chapter, we assume that the wireless channel is constant within an OFDM symbol. Suppose that the maximum delay of the forward relay channel is $L-1$ OFDM sampling intervals. Without loss of generality, we model the time-domain forward relay channel as an L-tap one with each tap representing one path. Denote

$$\mathbf{g}_{ij} = [g_{ij,0}, g_{ij,1}, \cdots, g_{ij,L-1}]^T, \;\; 0 \le i \le N_r - 1, 0 \le j \le N_d - 1, \tag{2.8}$$

as the L-tap time-domain channel vector in the current OFDM symbol between the ith transmit antenna at the RS and the jth receive antenna at the DS. Without loss of generality, we assume that the $\mathbf{g}_{ij}$'s for different i's and j's are independent and follow the same statistical model. Assume that the channel gains over different paths are independent and the average power gain over each path decays exponentially with the delay, i.e.,

$$\begin{aligned} E\left\{g_{ij,l_1} g^*_{ij,l_2}\right\} &= \begin{cases} p_l & \text{if} l_1 = l_1 = l \\ 0 & \text{otherwise} \end{cases} \\ &= \begin{cases} \mu\sigma_2^2 e^{-\lambda l} & \text{if} l_1 = l_1 = l \\ 0 & \text{otherwise} \end{cases} \end{aligned} \tag{2.9}$$

where λ denotes the power decay exponent and μ denotes the normalization factor to ensure that the summation of $p_l, 0 \le l \le L-1$, equals the average power gain over the second hop, σ_2^2. Thus the correlation matrix of $\mathbf{g}_{ij}$ is given by

$$\mathbf{R}_g = E\left\{\mathbf{g}_{ij}\mathbf{g}_{ij}^H\right\} = \begin{bmatrix} p_0 & 0 & \cdots & 0 \\ 0 & p_1 & \cdots & 0 \\ \vdots & \vdots & \ddots & \vdots \\ 0 & 0 & \cdots & p_{L-1} \end{bmatrix}. \tag{2.10}$$

Denote $\mathbf{h}_{ij} = [h_{ij,0}, h_{ij,1}, \cdots, h_{ij,K-1}]^T, 0 \le i \le N_r - 1, 0 \le j \le N_d - 1$, as the corresponding frequency-domain channel vector, and then $\mathbf{h}_{ij} = \mathbf{F}\mathbf{g}_{ij}$ where $\mathbf{F}$ is the truncated $K \times L$

discrete Fourier transform (DFT) matrix defined as

$$\mathbf{F} = \frac{1}{\sqrt{K}} \begin{bmatrix} 1 & 1 & \cdots & 1 \\ 1 & e^{-j\frac{2\pi}{K}} & \cdots & e^{-j\frac{2\pi(L-1)}{K}} \\ \vdots & \vdots & \ddots & \vdots \\ 1 & e^{-j\frac{2\pi(K-1)}{K}} & \cdots & e^{-j\frac{2\pi(L-1)(K-1)}{K}} \end{bmatrix}. \tag{2.11}$$

Thus the correlation matrix of $\mathbf{h}_{ij}$ can be obtained as

$$\mathbf{R}_h = E\left\{\mathbf{h}_{ij}\mathbf{h}_{ij}^H\right\} = \begin{bmatrix} r_f(0) & r_f(-1) & \cdots & r_f\left(-(K-1)\right) \\ r_f(1) & r_f(0) & \cdots & r_f\left(-(K-2)\right) \\ \vdots & \vdots & \ddots & \vdots \\ r_f(K-1) & r_f(K-2) & \cdots & r_f(0) \end{bmatrix} = \mathbf{F}\mathbf{R}_g\mathbf{F}^H, \tag{2.12}$$

where $r_f(k) = E\left\{h_{ij,l+k}h_{ij,l}^*\right\}$ denotes the frequency-domain correlation of the channel gains over different OFDM subcarriers. Recall that the noise correlation matrix over the kth OFDM subcarrier is given by

$$\mathbf{R}_n(k) = g^2\sigma_n^2\mathbf{H}_2(k)\mathbf{H}_2^H(k) + \sigma_n^2\mathbf{I}_{N_d}, \;\; 0 \le k \le K-1. \tag{2.13}$$

where

$$\mathbf{H}_2\left(k\right) = \begin{bmatrix} h_{00,k} & h_{01,k} & \cdots & h_{0,N_r-1,k} \\ h_{10,k} & h_{11,k} & \cdots & h_{1,N_r-1,k} \\ \vdots & \vdots & \ddots & \vdots \\ h_{N_d-1,0,k} & h_{N_d-1,1,k} & \cdots & h_{N_d-1,N_r-1,k} \end{bmatrix} \tag{2.14}$$

Therefore, the correlation in the elements of $\mathbf{h}_{ij}$ can be utilized to estimate the noise correlation matrix in (2.13).

2.2.2 Estimation of the Noise Correlation Matrix

To facilitate analysis, we assume that the overall noise vector is obtained by perfectly subtracting the data part from the received signal at the DS, i.e.,

$$\begin{aligned} \mathbf{n}(k) = [n_0(k)\; n_1(k)\; \cdots\; n_{N_d-1}(k)]^T &= \mathbf{y}_d(k) - \mathbf{H}(k)\mathbf{x}(k) \\ &= g\mathbf{H}_2(k)\mathbf{n}_r(k) + \mathbf{n}_d(k). \end{aligned} \tag{2.15}$$

Define $r_{ij}(k) = E_n\left\{n_i(k)n_j^*(k)\right\}, 0 \le i, j \le N_d - 1$, and then $\mathbf{R}_n(k)$ can be expressed as

$$\mathbf{R}_n(k) = E_n\left\{\mathbf{n}(k)\mathbf{n}(k)^H\right\} = \begin{bmatrix} r_{00}(k) & r_{01}(k) & \cdots & r_{0,N_d-1}(k) \\ r_{10}(k) & r_{11}(k) & \cdots & r_{1,N_d-1}(k) \\ \vdots & \vdots & \ddots & \vdots \\ r_{N_d-1,0}(k) & r_{N_d-1,1}(k) & \cdots & r_{N_d-1,N_d-1}(k) \end{bmatrix}. \tag{2.16}$$

Instead of estimating $\mathbf{R}_n(k), 0 \le k \le K-1$, directly, we try to first estimate

$$\mathbf{r}_{ij} = [r_{ij}(0), r_{ij}(1), \cdots, r_{ij}(K-1)], \;\; 0 \le i, j \le N_d - 1, \tag{2.17}$$

and then obtain $\mathbf{R}_n(k)$ from $\mathbf{r}_{ij}$ based on (2.16). Based on the overall noise vector obtained in (2.15), we first get a temporal estimate of $\mathbf{r}_{ij}$ as

$$\widehat{\mathbf{r}}_{ij} = [\widehat{r}_{ij}(1), \widehat{r}_{ij}(2), \cdots, \widehat{r}_{ij}(K)], \tag{2.18}$$

where $\widehat{r}_{ij}(k) = n_i(k)n_j^*(k)$. Then a linear MMSE estimate of $\mathbf{r}_{ij}$ can be further obtained from $\widehat{\mathbf{r}}_{ij}$ as [92]

$$\widetilde{\mathbf{r}}_{ij} = \mathbf{C}_{ij}\widehat{\mathbf{r}}_{ij} = \mathbf{R}_{r\widehat{r},ij}\mathbf{R}^{-1}_{\widehat{r}\widehat{r},ij}\widehat{\mathbf{r}}_{ij}, \tag{2.19}$$

where $\mathbf{R}_{r\widehat{r},ij} = E\left\{\mathbf{r}_{ij}\widehat{\mathbf{r}}_{ij}^H\right\}$ denotes the cross correlation matrix of $\mathbf{r}_{ij}$ and $\widetilde{\mathbf{r}}_{ij}$ and $\mathbf{R}_{\widehat{r}\widehat{r},ij} = E\left\{\widehat{\mathbf{r}}_{ij}\widehat{\mathbf{r}}_{ij}^H\right\}$ denotes the correlation matrix of $\widetilde{\mathbf{r}}_{ij}$. The corresponding MSE matrix of $\widetilde{\mathbf{r}}_{ij}$ is given by [92]

$$\mathbf{R}_{\mathbf{e}} = E\left\{\left(\mathbf{r}_{ij} - \widetilde{\mathbf{r}}_{ij}\right)\left(\mathbf{r}_{ij} - \widetilde{\mathbf{r}}_{ij}\right)^H\right\} = \mathbf{R}_{rr,ij} - \mathbf{R}_{r\widehat{r},ij}\mathbf{R}^{-1}_{\widehat{r}\widehat{r},ij}\mathbf{R}^H_{r\widehat{r},ij}, \tag{2.20}$$

where $\mathbf{R}_{rr,ij} = E\left\{\mathbf{r}_{ij}\mathbf{r}_{ij}^H\right\}$. Since $\widehat{\mathbf{r}}_{ij}$ is a temporal estimate of $\mathbf{r}_{ij}$ depending on the instantaneous forward relay channel, it can be easily shown that $\mathbf{R}_{rr,ij} = \mathbf{R}_{r\widehat{r},ij}$.

Define $p_{ij}(k) = E\left\{r_{ij}(l+k)\widehat{r}_{ij}^*(l)\right\}$ and $o_{ij}(k) = E\left\{\widehat{r}_{ij}(l+k)\widehat{r}_{ij}^*(l)\right\}$, and then

$$\mathbf{R}_{\widehat{r}\widehat{r},ij} = \begin{bmatrix} p_{ij}(0) & p_{ij}(-1) & \cdots & p_{ij}(-(K-1)) \\ p_{ij}(1) & p_{ij}(0) & \cdots & p_{ij}(-(K-2)) \\ \vdots & \vdots & \ddots & \vdots \\ p_{ij}(K-1) & p_{ij}(K-2) & \cdots & p_{ij}(0) \end{bmatrix} \tag{2.21}$$

and

$$\mathbf{R}_{\widetilde{rr},ij} = \begin{bmatrix} o_{ij}(0) & o_{ij}(-1) & \cdots & o_{ij}(-(K-1)) \\ o_{ij}(1) & o_{ij}(0) & \cdots & o_{ij}(-(K-2)) \\ \vdots & \vdots & \ddots & \vdots \\ o_{ij}(K-1) & o_{ij}(K-2) & \cdots & o_{ij}(0) \end{bmatrix}. \tag{2.22}$$

Without loss of generality, assume that $g^2 = \sigma_n^2 = 1$, and then, based on the channel statistics described in Section 2.2.1, we have shown in Appendix A.1 that

$$p_{ij}(k) = M\sigma_2^4 |r_f(k)|^2 + \left(1 + M\sigma_2^2\right)^2 \delta(i-j), \tag{2.23}$$

and

$$o_{ij}(k) = M\sigma_2^4 |r_f(k)|^2 + \left(1 + M\sigma_2^2\right)^2 \delta(k) + \left[M\sigma_2^4 + \left(1 + M\sigma_2^2\right)^2 \delta(k)\right] \delta(i-j), \tag{2.24}$$

where $r_f(k)$ is defined in (2.12) and $\delta(\cdot)$ denotes the Kronecker delta function.

After getting $\widetilde{\mathbf{r}}_{ij}, 0 \le i, j \le N_d$, through (2.19), the noise correlation matrix over each OFDM subcarrier can be further obtained based on (2.16).

2.3 Simulation Results

In this section, we present simulation results to demonstrate the performance improvements achieved by blind noise correlation estimation in a two-hop MIMO-OFDM AF relay system. In our simulation, we consider a 256-subcarrier ($K = 256$) OFDM system and assume that there are 4 antennas at the SS, the RS, and the DS, i.e., $N_s = N_r = N_d = 4$. Without loss of generality, we further normalize the power amplifying gain of the RS and the average power gain over the second hop to get $g^2 = \sigma_2^2 = 1$. As a result, $N_r g^2 \sigma_2^2 \gg 1$ and according to the discussion in Section 2.1.1, the white overall noise assumption is inaccurate and noise correlation estimation is necessary. Furthermore, V-BLAST transmission with QPSK modulation is applied at the SS and perfect overall CSI between the RS and the DS, $\mathbf{H}(k)$, is assumed available at the DS for signal detection. In our simulation, the *zero-forcing* (ZF) detection, the approximate MMSE and ML detection based on the white noise assumption,

the estimated MMSE and ML detection based on the estimated noise correlation matrix, and the ideal MMSE and ML detection based on the actual noise correlation matrix are simulated. As mentioned, we assume that the transmitted signal is perfectly detected and subtracted from the received signal to get the overall noise at the DS when estimating the noise correlation matrix.

Figure 2.2 shows the contrastive BER versus SNR curves of different detection schemes over ideal channels. Here *ideal channels* means that the channels are generated exactly according to the statistical model described in Section 2.2.1 with $L = 32$ and $\lambda = 0.3$. Figure 2.3 shows the contrastive BER versus SNR curves of different detection schemes over B4 and B3 WINNER *clustered delay line* (CDL) channels [93] that are specially developed for wireless relay to enhance signal coverage in indoor hot spots. In Figure 2.3, we still use the statistical channel model described in Section 2.2.1 with $L = 32$ and $\lambda = 0.3$ to estimate the noise correlation matrix. It can be observed from Figures 2.2 and 2.3 that the MMSE detection based on the estimated noise correlation matrix achieves almost the same performance as the ideal MMSE detection, with an SNR gain of 2 dB over the approximate MMSE detection based on the white overall noise assumption. Compared to the approximate ML detection based on the white overall noise assumption, that based on the estimated noise correlation matrix achieves SNR gains of about 1 dB over ideal channels when BER=10^{-3} and about 3 dB over WINNER channels when BER=10^{-2}. In particular, we notice that although there is a mismatch between the conjectured and the actual statistics in the WINNER channels, the noise correlation estimation still achieves significant performance improvements. While the ideally generated channels assume that different elements of the MIMO channel matrix are uncorrelated, this assumption is not true in practical WINNER channels where the spatial correlation in multiple antennas is considered. As a result, the overall noise vector over WINNER channels has relatively strong autocorrelation and thus the proposed blind noise correlation estimation is expected to significantly improve the system performance, as verified in Figure 2.3.

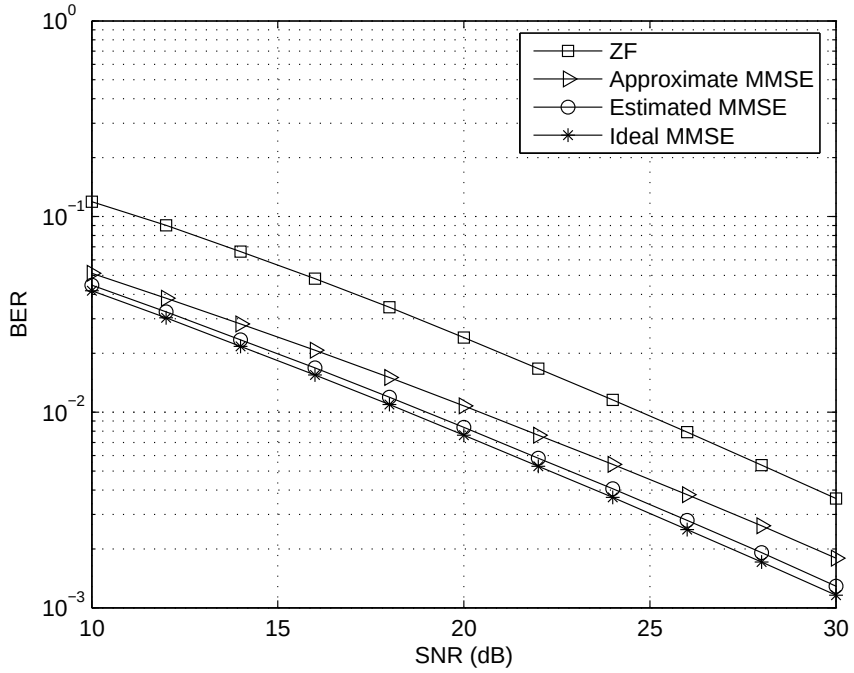

(a) ZF and MMSE detection

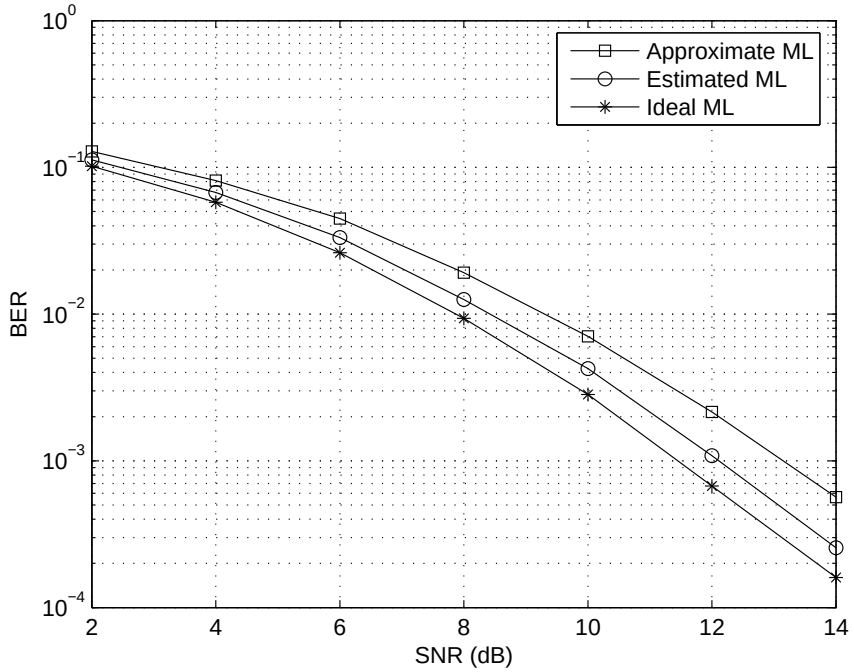

(b) ML detection

Figure 2.2. BER curves of different detection schemes over ideal channels

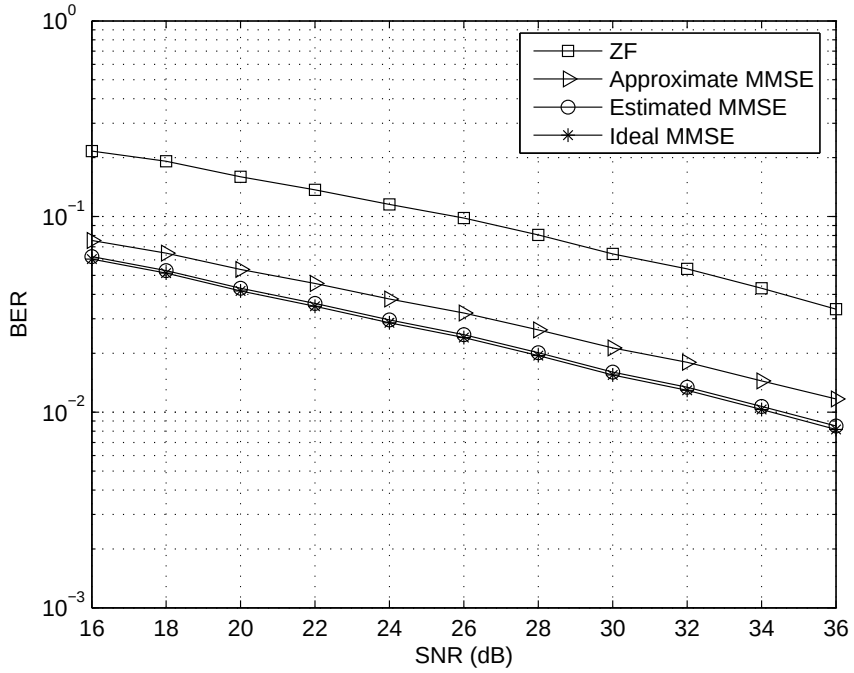

(a) ZF and MMSE detection

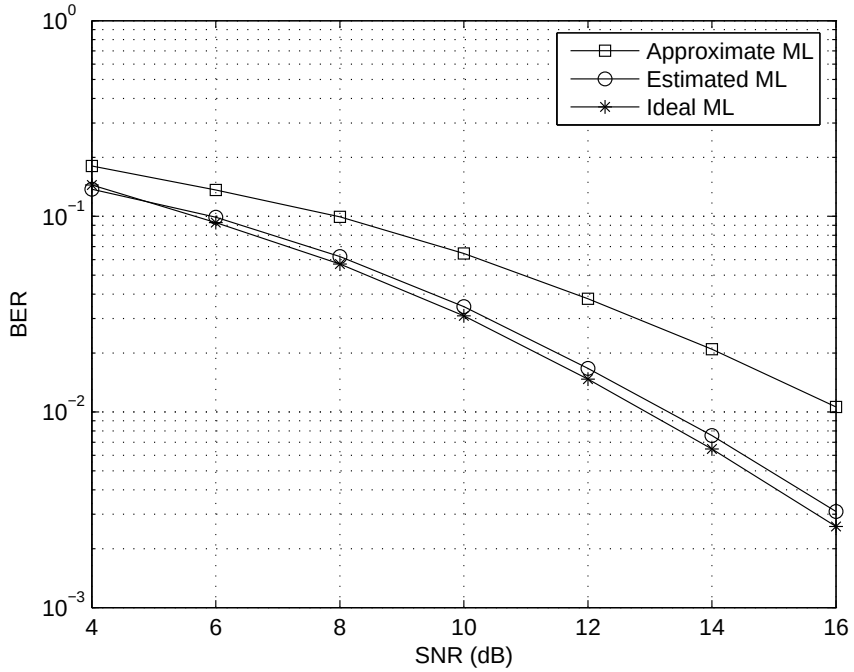

(b) ML detection

Figure 2.3. BER curves of different detection schemes over B4 and B3 WINNER channels

2.4 Conclusion

In this chapter, we have proposed a blind algorithm to estimate the correlation matrix of the overall noise vector at the DS of a two-hop MIMO-OFDM AF relay system. Without requiring any pilots, such an algorithm takes advantages of the frequency-domain correlation of the broadband wireless channel in an OFDM system. Simulation results have demonstrated that the proposed noise correlation estimation algorithm effectively improves signal detection at the DS especially over spatially correlated MIMO forward relay channels even in the presence of significant uncertainties in the channel statistics.

CHAPTER 3

PILOT MATRIX DESIGN FOR ESTIMATING CASCADED CHANNELS IN TWO-HOP MIMO AF RELAY SYSTEMS

In this chapter, we consider a narrowband two-hop MIMO AF relay system in which data are conveyed from the SS to the DS via two cascaded orthogonal channels by frequency division or time division. In this system, the overall channel between the SS and the DS is a cascade of the backward relay channel over the SS-RS hop, the amplifying matrix at the RS, and the forward relay channel over the RS-DS hop. With the help of pilots inserted at the SS, the overall channel from the SS to the DS can be obtained at the DS through conventional channel estimation algorithms that have been proposed for regular MIMO systems [92, 94, 95, 96]. While the overall CSI guarantees successful data detection at the DS, the involved relay CSI, if available, can be utilized to improve the overall system performance. As analyzed in Chapter 2, the overall noise vector at the DS is colored with its correlation determined by the forward relay channel over the RS-DS hop. Although a blind noise correlation estimation algorithm has been proposed in Chapter 2, it requires the statistics of the broadbind wireless channel over the RS-DS hop and is only applicable to certain scenarios. Alternatively, we may estimate the forward relay channel and then obtain the correlation matrix of the overall noise vector at the DS accordingly. Conventionally, the relay channels over the SS-RS and RS-DS hops can be estimated directly at the RS and the DS with the help of pilots inserted at the SS and the RS, respectively. However, such direct relay channel estimation is based on the assumption that the RS is aware of the structure of its received signal and capable of performing further signal processing. In practice, it is attractive to keep minimum complexity at the RS that is supposed to be cost-efficient and undertakes no task except simply amplifying and forwarding its received signals. In this chapter, we investigate estimating the two cascaded relay channels at the DS based on a predefined pilot amplifying matrix sequence at the RS and the corresponding overall

channel sequence obtained at the DS through conventional channel estimation algorithms. In particular, we find necessary and sufficient conditions on the pilot amplifying matrix sequence at the RS to ensure successful relay channel estimation at the DS. Based on these conditions, we derive rules to design diagonal or quasi-diagonal pilot amplifying matrices so that the relay channels can be successfully estimated with minimum complexity at the RS.

The remainder of this chapter is organized as follows. In Section 3.1, we present the system model and the principle of estimating the cascaded relay channels at the DS. In Section 3.2, we investigate necessary and sufficient conditions for successful relay channel estimation. In Section 3.3, we derive rules to design diagonal or quasi-diagonal pilot amplifying matrices meeting these conditions. In Section 3.4, we develop approximate linear *least-square* (LS) estimation of the relay channels in the presence of imperfect overall CSI. In Section 3.5, we extend relay channel estimation to a general two-hop MIMO AF system. In Section 3.6, we present simulation results on the approximate linear LS relay channel estimation in a noisy environment. Finally we conclude this chapter in Section 3.7.

3.1 Problem Formulation

In this chapter, we are concerned with a narrowband two-hop MIMO AF relay system, which can be directly used in a broadband multicarrier system like OFDM, as discussed in Chapter 2. The block diagram of such a system is shown in Figure 3.1. As indicated, this system consists of an SS, an RS, and a DS, all of which utilize multiple transmit/receive antennas. In this system, data are conveyed from the SS to the DS via two cascaded orthogonal channels by frequency division or time division.

3.1.1 System Model

Suppose there are N_s transmit antennas at the SS, N_r receive and transmit antenna pairs at the RS, and N_d receive antennas at the DS. Denote $\mathbf{H}_1$ as the $N_r \times N_s$ backward relay channel matrix between the SS and the RS, $\mathbf{H}_2$ as the $N_d \times N_r$ forward relay channel matrix between

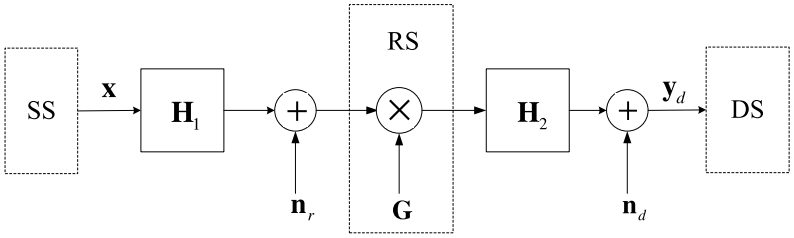

Figure 3.1. Two-hop MIMO AF relay system model

the RS and the DS, both of which are assumed nonsingular throughout this chapter, and $\mathbf{G}$ as the $N_r \times N_r$ amplifying matrix at the RS, and then the received signal vector at the DS can be expressed as

$$\mathbf{y}_d = \mathbf{H}_2\mathbf{G}\mathbf{H}_1\mathbf{x} + \mathbf{H}_2\mathbf{G}\mathbf{n}_r + \mathbf{n}_d = \mathbf{H}\mathbf{x} + \mathbf{n}, \tag{3.1}$$

where $\mathbf{x}$ denotes the transmitted signal vector of the SS, and $\mathbf{n}_r$ and $\mathbf{n}_d$ denote the local noise vectors at the RS and the DS, respectively. In (3.1), $\mathbf{H}$ denotes the $N_d \times N_s$ overall channel matrix between the SS and the DS defined as $\mathbf{H} = \mathbf{H}_2\mathbf{G}\mathbf{H}_1$, and $\mathbf{n}$ denotes the overall noise vector at the DS defined as $\mathbf{n} = \mathbf{H}_2\mathbf{G}\mathbf{n}_r + \mathbf{n}_d$, which consists of the colored noise forwarded from the RS and the local white noise at the DS. In order for the overall channel to be nonsingular, we assume $N_r \geq \min\{N_s, N_d\}$ throughout this chapter. Furthermore, to maintain a constant power amplifying gain at the RS, we let $\mathbf{G} = g\mathbf{P}$ where g is the fixed amplifying gain of the RS and $\mathbf{P}$ is a unitary matrix. In practice, $\mathbf{P}$ is usually a diagonal matrix or a permutation of a diagonal matrix, also called a quasi-diagonal matrix in this chapter, so as to reduce the complexity in the matrix multiplication manipulation at the RS. Without loss of generality, we further assume $g = 1$ throughout this chapter for notational convenience and thus $\mathbf{H} = \mathbf{H}_2\mathbf{P}\mathbf{H}_1$. Assume that the elements of $\mathbf{n}_r$ and $\mathbf{n}_d$ are i.i.d. complex Gaussian random variables with zero mean and variances σ_r^2 and σ_d^2, respectively, and then the correlation matrix of the overall noise vector, $\mathbf{n}$, is given by

$$\mathbf{R}_n = E\left\{\mathbf{n}\mathbf{n}^H\right\} = \sigma_r^2\mathbf{H}_2\mathbf{H}_2^H + \sigma_d^2\mathbf{I}_{N_d}, \tag{3.2}$$

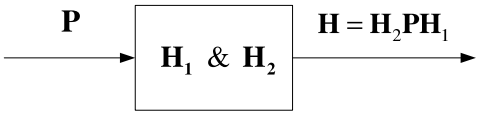

Figure 3.2. Equivalent system for estimating cascaded relay channels at the DS

which indicates that the noise correlation at the DS is determined by the forward relay channel over the RS-DS hop, $\mathbf{H}_2$.

In a practical two-hop MIMO AF relay system, it is attractive to keep minimum complexity at the RS that is supposed to be cost-effective. Thus it is desired that the RS does not undertake any task except simply amplifying and forwarding its received signals. In other words, no pilots are inserted at the RS to assist direct estimation of the forward relay channel at the DS. As a result, only the overall channel between the SS and the DS, $\mathbf{H}$, can be estimated directly with the help of pilots inserted at the SS while the two cascaded relay channels over the SS-RS and the RS-DS hops, $\mathbf{H}_1$ and $\mathbf{H}_2$, remain unknown. However, Equation (3.2) indicates that the correlation matrix of the overall noise vector at the DS, based on which the ML and the MMSE detection of a V-BLAST [29] system are performed, is determined by the forward relay channel over the RS-DS hop. Therefore, indirect estimation of the two cascaded relay channels at the DS of a two-hop MIMO AF system will effectively improve the system performance.

3.1.2 Principle of Estimating Cascaded Relay Channels at the DS

Figure 3.2 shows an equivalent system for estimating cascaded relay channels at the DS. Our objective is to estimate the relay channels, $\mathbf{H}_1$ and $\mathbf{H}_2$, based on the predefined amplifying matrix at the RS, $\mathbf{P}$, and the corresponding overall channel, $\mathbf{H} = \mathbf{H}_2\mathbf{P}\mathbf{H}_1$, which is assumed available at the DS through conventional channel estimation algorithms with the help of pilots inserted at the SS. Since the input $\mathbf{P}$ is known and works like a pilot for relay channel estimation, it is called the pilot amplifying matrix in this chapter. By varying

$\mathbf{H}_{o,1} = \mathbf{H}_2\mathbf{P}_1\mathbf{H}_1$	$\mathbf{H}_{o,2} = \mathbf{H}_2\mathbf{P}_2\mathbf{H}_1$	$\bullet\ \bullet\ \bullet$	$\mathbf{H}_{o,L} = \mathbf{H}_2\mathbf{P}_L\mathbf{H}_1$

Figure 3.3. Principle of relay channel estimation

the pilot amplifying matrix within several consecutive time slots[1], multiple equations *with respect to* (w.r.t.) $\mathbf{H}_1$ and $\mathbf{H}_2$ can be established and once the number of independent equations is large enough, successful relay channel estimation will be guaranteed. The principle of relay channel estimation is further illustrated in Figure 3.3, in which $\mathbf{P}_1, \mathbf{P}_2, \cdots, \mathbf{P}_L$ denote the pilot amplifying matrices for L consecutive time slots, and $\mathbf{H}_{o,1}, \mathbf{H}_{o,2}, \cdots, \mathbf{H}_{o,L}$ denote the corresponding overall channel matrices, i.e.,

$$\mathbf{H}_{o,l} = \mathbf{H}_2\mathbf{P}_l\mathbf{H}_1, \quad 1 \le l \le L. \tag{3.3}$$

Throughout this chapter, we let $\mathbf{P}_1 = \mathbf{I}_{N_r}$ since, from the perspective of relay channel estimation, the pilot amplifying matrix sequence, $(\mathbf{P}_1, \mathbf{P}_2, \cdots, \mathbf{P}_L)$, is equivalent to

$$\left(\mathbf{I}_{N_r}, \mathbf{P}_1^{-1}\mathbf{P}_2, \cdots, \mathbf{P}_1^{-1}\mathbf{P}_L\right). \tag{3.4}$$

Obviously only $\alpha\mathbf{H}_2$ and $\frac{1}{\alpha}\mathbf{H}_1$, where α denotes an unknown complex scalar, can be obtained from (3.3) no matter how many different pilot amplifying matrices are utilized at the RS. However, since $\mathbf{H}_2$ (or $\mathbf{H}_1$) and $\alpha\mathbf{H}_2$ (or $\frac{1}{\alpha}\mathbf{H}_1$) share the same matrix structure, the knowledge of $\alpha\mathbf{H}_2$ and $\frac{1}{\alpha}\mathbf{H}_1$ at the DS can effectively improve the overall system performance, as will be demonstrated in Section 3.6.

Given the framework of relay channel estimation in Figure 3.3, it is our objective to investigate what and how many pilot amplifying matrices are needed to guarantee successful estimation of the two cascaded MIMO [2] relay channels. In the rest of this chapter, we will first assume perfect overall CSI at the DS and focus on the identifiability of the two

[1] A *time slot* is defined as a period of time it takes to estimate the overall channel, $\mathbf{H}$. Here we assume slow fading channel so that the two relay channels remain constant during the whole estimation process.

[2] In the trivial case that either of the two relay channels is *single-input-single-output* (SISO), the pilot matrix at the RS reduces to a scalar and thus only one time slot is enough for successful relay channel estimation.

relay channels for a given pilot amplifying matrix sequence. In particular, necessary and sufficient conditions for successful relay channel estimation will be found and rules for designing low-complexity pilot amplifying matrices will be given accordingly.

3.2 Necessary and Sufficient Conditions for Successful Relay Channel Estimation

In this section, we will investigate the identifiability of the two cascaded relay channels from matrix equation (3.3) for a given pilot amplifying matrix sequence. Since the equation w.r.t. $\mathbf{H}_1$ and $\mathbf{H}_2$ in (3.3) is nonlinear and difficult to analyze directly, we will first transform it into a linear one. For analytical convenience, we first consider a special case, $N_r = \min\{N_s, N_d\}$. The extension to the general case that $N_r \geq \min\{N_s, N_d\}$ will be discussed in Section 3.5.

3.2.1 Transformation into a Linear Matrix Equation

When $N_r = \min\{N_s, N_d\}$, transformation of (3.3) into a linear equation is straightforward. We first express $\mathbf{H}_2$ in terms of $\mathbf{H}_1$ or vice versa; then a linear matrix equation w.r.t. one of the two relay channels can be established by eliminating the other. To be brief, the original nonlinear matrix equation in (3.3) can be transformed into a linear one as[3]

$$\mathbf{P}_l \mathbf{H}_x = \mathbf{H}_x \mathbf{Q}_l, \quad 2 \leq l \leq L, \tag{3.5}$$

where

$$\mathbf{H}_x = \begin{cases} \mathbf{H}_1, & \text{if } N_r = N_s \leq N_d, \\ \mathbf{H}_2^{-1}, & \text{if } N_r = N_d \leq N_s, \end{cases} \tag{3.6}$$

denotes the $N_r \times N_r$ channel matrix to estimate, and

$$\mathbf{Q}_l = \begin{cases} \left(\mathbf{H}_{o,1}^H \mathbf{H}_{o,1}\right)^{-1} \mathbf{H}_{o,1}^H \mathbf{H}_{o,l}, & \text{if } N_r = N_s \leq N_d, \\ \mathbf{H}_{o,l} \mathbf{H}_{o,1}^H \left(\mathbf{H}_{o,1} \mathbf{H}_{o,1}^H\right)^{-1}, & \text{if } N_r = N_d \leq N_s. \end{cases} \tag{3.7}$$

Given the linear matrix equation in (3.5), we need to estimate $\mathbf{H}_x$ based on the pilot matrix sequence, $\{\mathbf{P}_l, 2 \leq l \leq L\}$, and the corresponding observed matrix sequence, $\{\mathbf{Q}_l, 2 \leq l \leq L\}$.

[3]Note that we have assumed $L \geq 2$ since in the general case that both the two relay channels are MIMO, relay channel estimation cannot be performed within only one time slot.

3.2.2 First Necessary and Sufficient Condition

The original matrix equation in (3.5) for relay channel estimation can be rewritten as [97]

$$\left(\mathbf{I}_{N_r} \otimes \mathbf{P}_l - \mathbf{Q}_l^T \otimes \mathbf{I}_{N_r}\right) \cdot \mathbf{h}_x = 0, \;\; 2 \leq l \leq L, \tag{3.8}$$

where $\mathbf{h}_x = \text{vec}(\mathbf{H}_x)$ denotes the vectorization of $\mathbf{H}_x$ formed by stacking the columns of $\mathbf{H}_x$ into a single column vector, and $\otimes$ denotes the Kronecker product [97], [98].

Define

$$\mathbf{A} = \begin{bmatrix} \mathbf{A}_2 \\ \mathbf{A}_3 \\ \vdots \\ \mathbf{A}_L \end{bmatrix} = \begin{bmatrix} \mathbf{I}_{N_r} \otimes \mathbf{P}_2 - \mathbf{Q}_2^T \otimes \mathbf{I}_{N_r} \\ \mathbf{I}_{N_r} \otimes \mathbf{P}_3 - \mathbf{Q}_3^T \otimes \mathbf{I}_{N_r} \\ \vdots \\ \mathbf{I}_{N_r} \otimes \mathbf{P}_L - \mathbf{Q}_L^T \otimes \mathbf{I}_{N_r} \end{bmatrix}, \tag{3.9}$$

which is an $(L-1)N_r^2 \times N_r^2$ matrix, and then (3.8) can be rewritten in a compact manner as

$$\mathbf{A} \cdot \mathbf{h}_x = 0. \tag{3.10}$$

As the relay channel to estimate, $\mathbf{h}_x$ is not a zero vector. Consequently, $\mathbf{A}$ is not of full column rank, i.e., $\text{rank}\,(\mathbf{A}) \leq N_r^2 - 1$. As a result, Equation (3.10) has an infinite number of solutions, including $\mathbf{h}_x$. In other words, the exact value of $\mathbf{h}_x$ cannot be determined no matter how many different pilot amplifying matrices are utilized at the RS, which coincides with our earlier analysis. For relay channel estimation, our objective is to obtain $\alpha\mathbf{h}_x$ from (3.10), where α denotes an unknown complex scalar, so as to learn about the matrix structure of $\mathbf{H}_x$. Therefore, the necessary and sufficient condition for successful relay channel estimation is $\text{rank}\,(\mathbf{A}) = N_r^2 - 1$, i.e., the solutions to (3.10) have only one *degree of freedom* (DoF) embodied in the unknown α. Since $\mathbf{A}$ depends on not only the pilot amplifying matrix sequence, $\{\mathbf{P}_l, 2 \leq l \leq L\}$, but also the relay channel to estimate, $\mathbf{H}_x$, it is inconvenient to control the rank of $\mathbf{A}$ directly to meet this necessary and sufficient condition. To deal

with this problem, we further define

$$\mathbf{B} = \begin{bmatrix} \mathbf{B}_2 \\ \mathbf{B}_3 \\ \vdots \\ \mathbf{B}_L \end{bmatrix} = \begin{bmatrix} \mathbf{I}_{N_r} \otimes \mathbf{P}_2 - \mathbf{P}_2^T \otimes \mathbf{I}_{N_r} \\ \mathbf{I}_{N_r} \otimes \mathbf{P}_3 - \mathbf{P}_3^T \otimes \mathbf{I}_{N_r} \\ \vdots \\ \mathbf{I}_{N_r} \otimes \mathbf{P}_L - \mathbf{P}_L^T \otimes \mathbf{I}_{N_r} \end{bmatrix}. \tag{3.11}$$

Similar to $\mathbf{A}$, $\mathbf{B}$ is also an $(L-1)N_r^2 \times N_r^2$ matrix. Furthermore, we have shown in Appendix B.1 that matrices $\mathbf{A}$ and $\mathbf{B}$ have the same rank, i.e., $\text{rank}\,(\mathbf{A}) = \text{rank}\,(\mathbf{B})$. Thus we obtain the following proposition.

Proposition 3.2.1 *Given $\{\boldsymbol{P}_l, 2 \le l \le L\}$, the necessary and sufficient condition for successful relay channel estimation is*

$$rank\,(\boldsymbol{B}) = N_r^2 - 1. \tag{3.12}$$

Different from $\mathbf{A}$, $\mathbf{B}$ depends only on the pilot amplifying matrix sequence, independent of the relay channel to estimate. Therefore, given $\{\mathbf{P}_l, 2 \le l \le L\}$, it is convenient to decide on the identifiability of the two cascaded relay channels by checking the rank of $\mathbf{B}$.

Although Proposition 3.2.1 enables us to decide on the qualification of a given pilot amplifying matrix sequence, it does not provide any clue on rules to design qualified pilot matrices directly since it is still rather difficult to establish an explicit relationship between the pilot amplifying matrix sequence and the rank of $\mathbf{B}$. To deal with this problem, we will define a new problem that is equivalent to the original problem of relay channel estimation. Based on the equivalent problem, rules will be developed conveniently to design qualified pilot amplifying matrices for relay channel estimation.

3.2.3 Equivalent Problem and Second Necessary and Sufficient Condition

Up to now, we have described the original problem of relay channel estimation, the definition of which is given below.

Original problem: Solve

$$\mathbf{H}_{o,l} = \mathbf{H}_2 \mathbf{P}_l \mathbf{H}_1, \quad 1 \le l \le L, \tag{3.13}$$

to get $\mathbf{H}_1$ and $\mathbf{H}_2$.

To facilitate further analysis of the original problem, we define its equivalent problem as follows.

Equivalent problem: Solve

$$\mathbf{P}_l = \mathbf{T}_2\mathbf{P}_l\mathbf{T}_1, \quad 1 \leq l \leq L, \tag{3.14}$$

to get $N_r \times N_r$ square matrices $\mathbf{T}_1$ and $\mathbf{T}_2$.

It must be mentioned that both the original and the equivalent problems have an infinite number of solutions [4]. In Appendix B.2, we have proved the following proposition.

Proposition 3.2.2 *The solutions to the original problem and those to the equivalent problem have the same DoF.*

The equivalence between the two problems indicated in Proposition 3.2.2 significantly facilitates analysis of the identifiability of the two relay channels for a given pilot amplifying matrix sequence. As mentioned, the necessary and sufficient condition for successful relay channel estimation is that the solutions to the original problem have only one DoF. Thus, from Proposition 3.2.2, we obtain the second necessary and sufficient condition for successful relay channel estimation as follows.

Proposition 3.2.3 *Given $\{\boldsymbol{P}_l, 2 \leq l \leq L\}$, successful relay channel estimation is guaranteed if and only if $\boldsymbol{T}_1 = \alpha\boldsymbol{I}_{N_r}$ and $\boldsymbol{T}_2 = \frac{1}{\alpha}\boldsymbol{I}_{N_r}$, where α denotes an arbitrary complex scalar, are the sole solutions to the equivalent problem.*

In practice, the RS in the two-hop MIMO AF relay system needs to maintain a minimum complexity. Therefore, it is attractive to set the pilot amplifying matrices as the permutations of an identity matrix since, in this case, the matrix multiplication manipulation at the RS can be realized with minimum complexity by switching the connection

[4]Note that $\mathbf{T}_1 = \alpha\mathbf{I}_{N_r}$ and $\mathbf{T}_2 = \frac{1}{\alpha}\mathbf{I}_{N_r}$, where α denotes an arbitrary complex scalar, are always solutions to the equivalent problem.

between the receive and the transmit antennas of the RS. Unfortunately, with the help of Proposition 3.2.3, we have proved in Appendix B.3 that it is impossible to estimate the two cascaded relay channels at the DS with such pilot amplifying matrices.

3.2.4 Third Necessary and Sufficient Condition

Considering Proposition 3.2.3, we will reinvestigate the identifiability of the two relay channels for a given pilot amplifying matrix sequence by examining the DoF of the solutions to the equivalent problem.

Since $\mathbf{P}_1 = \mathbf{T}_2\mathbf{P}_1\mathbf{T}_1$ and $\mathbf{P}_1 = \mathbf{I}_{N_r}$, $\mathbf{T}_1 = \mathbf{T}_2^{-1}$. Thus Equation (3.14) can be rewritten as

$$\mathbf{T}_2 = \mathbf{P}_l\mathbf{T}_2\mathbf{P}_l^{-1}, \ \ 2 \le l \le L. \tag{3.15}$$

Perform eigenvalue decomposition on $\mathbf{T}_2$ to get $\mathbf{T}_2 = \mathbf{U}\Lambda\mathbf{U}^{-1}$ [5], where $\mathbf{U}$ and Λ denote the eigenvector and the eigenvalue matrices of $\mathbf{T}_2$, respectively. Then (3.15) can be rewritten as

$$\mathbf{T}_2 = \mathbf{P}_l\mathbf{U} \cdot \Lambda \cdot (\mathbf{P}_l\mathbf{U})^{-1}, \ \ 2 \le l \le L, \tag{3.16}$$

which indicates that, for any $2 \le l \le L$, $\mathbf{P}_l\mathbf{U}$ is also an eigenvector matrix of $\mathbf{T}_2$.

According to Proposition 3.2.3, successful relay channel estimation is guaranteed if and only if $\mathbf{T}_2$ in (3.16) has only one DoF. To find the necessary and sufficient condition for that, we first perform eigenvalue decomposition on each pilot matrix to get

$$\mathbf{P}_l = \mathbf{V}_l\Lambda_l\mathbf{V}_l^{-1}, \ \ 2 \le l \le L, \tag{3.17}$$

where $\mathbf{V}_l = (\mathbf{v}_{l1}, \mathbf{v}_{l2}, \cdots, \mathbf{v}_{lN_r})$ and $\mathbf{v}_{ln}, 1 \le n \le N_r$, denotes the nth eigenvector of $\mathbf{P}_l$. Then we group the N_r [6] eigenvectors of $\mathbf{P}_l$ into K clusters with n_k eigenvectors in the kth cluster V_{lk}, $1 \le k \le K$, such that V_{lk}'s for different l's span the same n_k-dimension space S_k with the bases, $\mathbf{e}_{k1}, \mathbf{e}_{k2}, \cdots, \mathbf{e}_{kn_k}$. Given the above eigenvector grouping rule, we have proved the following third necessary and sufficient condition for successful relay channel estimation in Appendix B.4.

[5] Since $\mathbf{P}_l$ is unitary and $\mathbf{P}_l = \mathbf{T}_2\mathbf{P}_l\mathbf{T}_1$, $\mathbf{T}_2$ and $\mathbf{T}_1$ must be nonsingular.

[6] In the case that $\mathbf{P}_l$ has an n-dimension ($n > 1$) eigenspace associated with an n-order repeated eigenvalue, arbitrary n eigenvectors are chosen from this eigenspace for grouping.

Proposition 3.2.4 *Given* $\{\boldsymbol{P}_l, 2 \leq l \leq L\}$*, successful relay channel estimation is guaranteed if and only if the maximum number of their eigenvector clusters is one, i.e.,* $K_{max} = 1$.

The third necessary and sufficient condition given by Proposition 3.2.4 can be used not only to determine whether a given pilot matrix sequence can ensure successful relay channel estimation, but also to design qualified pilot matrix sequence directly. According to Proposition 3.2.4, it is impossible to successfully estimate the two MIMO relay channels within two time slots since, in this case, $L = 2$ and the maximum number of eigenvector clusters of $\mathbf{P}_2$ alone is N_r, which is greater than one. On the other hand, for appropriately designed $\mathbf{P}_2$ and $\mathbf{P}_3$, the maximum number of their eigenvector clusters can be as small as one. In other words, the minimum number of time slots required for successful relay channel estimation is 3, i.e., $L_{min} = 3$. In Section 3.3, specific rules will be developed to design low-complexity $\mathbf{P}_2$ and $\mathbf{P}_3$ meeting the third necessary and sufficient condition such that the two cascaded relay channels can be successfully estimated within three time slots.

3.3 Design Rules

In this section, we develop rules to design low-complexity pilot amplifying matrices so that the relay channels can be successfully estimated with minimum complexity at the RS. According to Proposition 3.2.4, what we need to do is to ensure that the maximum number of eigenvector clusters of the designed pilot matrix sequence is one.

As mentioned, it is always attractive to use a diagonal matrix or a quasi-diagonal matrix (a permutation of a diagonal matrix) as the pilot amplifying matrix at the RS so as to reduce the complexity in the matrix multiplication manipulation. Before giving the specific design rules, we first present the following definitions regarding a permutation operation.

Denote $\mathbf{D}$ and $\mathbf{F}$ as two $N_r \times N_r$ square matrices. Let $\mathbf{F}$ be a permutation of $\mathbf{D}$, i.e., $\mathbf{F}$ is obtained by switching the row order of $\mathbf{D}$, and then we define

- If the ith row of $\mathbf{F}$ comes from the jth row of $\mathbf{D}$, i is *directly reachable* from j,

$1 \leq i, j \leq N_r$, which is denoted as $f(j) = i$ and $f^{-1}(i) = j$ [7].

- If i is directly reachable from j and j is directly reachable from k, i is *reachable* from k.

- A permutation is *indivisible* if any i and j ($1 \leq i, j \leq N_r$) reach each other.

Given the above definitions, we present the following design rules.

- Let $\mathbf{P}_1 = \mathbf{I}_{N_r}$.

- Generate N_r distinct complex numbers, each with unit magnitude, to get a diagonal $\mathbf{P}_2$.

- Let $\mathbf{P}_3$ be an indivisible permutation of $\mathbf{P}_2$.

With the above design rules, we have shown in Appendix B.5 that $\mathbf{P}_2$ and $\mathbf{P}_3$ have only one eigenvector cluster and thus the two cascaded relay channels can be successfully estimated within three time slots. Among all of the $N_r!$ permutations of $\mathbf{P}_2$, there are $(N_r - 1)!$ indivisible ones that qualify as $\mathbf{P}_3$ candidates. In practice, $\mathbf{P}_3$ can be obtained by simply cyclically shifting the rows of $\mathbf{P}_2$. To illustrate the above design rules, we give a pilot amplifying matrix sequence candidate for relay channel estimation in a two-hop MIMO AF relay system with $N_r = 2$ as follows.

$$\mathbf{P}_1 = \begin{bmatrix} 1 & 0 \\ 0 & 1 \end{bmatrix}, \mathbf{P}_2 = \begin{bmatrix} 1 & 0 \\ 0 & -1 \end{bmatrix}, \mathbf{P}_3 = \begin{bmatrix} 0 & 1 \\ -1 & 0 \end{bmatrix}. \tag{3.18}$$

The above design rules are especially attractive in practice because, firstly, the two relay channels can be successfully estimated within the minimum three time slots, secondly, application of diagonal and quasi-diagonal pilot amplifying matrices maintains a minimum complexity at the RS, and thirdly, the orthogonality of these pilot amplifying matrices ensures a constant power amplifying gain at the RS.

[7] Note that, for any permutation, there exists a unique j that directly reaches i and a unique k that is directly reachable from i.

3.4 Linear Least-Square Estimation of Relay Channels in a Noisy Environment

So far, we have assumed perfect overall CSI at the DS and focused on the design of the pilot matrix sequence to ensure successful relay channel estimation. In this section, we will consider imperfect overall CSI at the DS and develop a specific algorithm to estimate the relay channels in such a noisy environment.

In practice, the overall channel between the SS and the DS, $\mathbf{H}_{o,l}$, has to be estimated at the DS. Therefore, it is always corrupted by noise, i.e.,

$$\mathbf{H}_{o,l}^{N} = \mathbf{H}_{o,l} + \mathbf{N}_{o,l}, \quad 1 \leq l \leq L, \tag{3.19}$$

where $\mathbf{H}_{o,l}$ is the actual overall channel, $\mathbf{H}_{o,l}^{N}$ denotes its estimate at the DS, and $\mathbf{N}_{o,l}$ denotes an additive noise matrix. Accordingly, the corrupted version of $\mathbf{Q}_l$ in (3.7) is given by

$$\mathbf{Q}_l^N = \begin{cases} \left(\left(\mathbf{H}_{o,1}^{N}\right)^H \mathbf{H}_{o,1}^{N}\right)^{-1} \left(\mathbf{H}_{o,1}^{N}\right)^H \mathbf{H}_{o,l}^{N}, & \text{if } N_r = N_s \leq N_d, \\ \mathbf{H}_{o,l}^{N} \left(\mathbf{H}_{o,1}^{N}\right)^H \left(\mathbf{H}_{o,1}^{N} \left(\mathbf{H}_{o,1}^{N}\right)^H\right)^{-1}, & \text{if } N_r = N_d \leq N_s, \end{cases} \tag{3.20}$$

which can be equivalently rewritten as $\mathbf{Q}_l^N = \mathbf{Q}_l + \mathbf{N}_{Q,l}$ where $\mathbf{N}_{Q,l}$ denotes an equivalent additive noise matrix. As a result, the original linear matrix equation in (3.5) is revised as

$$\mathbf{P}_l \mathbf{H}_x - \mathbf{H}_x \mathbf{Q}_l^N + \mathbf{H}_x \mathbf{N}_{Q,l} = 0, \quad 2 \leq l \leq L, \tag{3.21}$$

Define

$$\mathbf{A}_N = \begin{bmatrix} \mathbf{A}_2^N \\ \mathbf{A}_3^N \\ \vdots \\ \mathbf{A}_L^N \end{bmatrix} = \begin{bmatrix} \mathbf{I}_{N_r} \otimes \mathbf{P}_2 - \left(\mathbf{Q}_2^N\right)^T \otimes \mathbf{I}_{N_r} \\ \mathbf{I}_{N_r} \otimes \mathbf{P}_3 - \left(\mathbf{Q}_3^N\right)^T \otimes \mathbf{I}_{N_r} \\ \vdots \\ \mathbf{I}_{N_r} \otimes \mathbf{P}_L - \left(\mathbf{Q}_L^N\right)^T \otimes \mathbf{I}_{N_r} \end{bmatrix}, \mathbf{n}_{H_x} = \begin{bmatrix} \text{vec}\left(\mathbf{H}_x \mathbf{N}_{Q,2}\right) \\ \text{vec}\left(\mathbf{H}_x \mathbf{N}_{Q,3}\right) \\ \vdots \\ \text{vec}\left(\mathbf{H}_x \mathbf{N}_{Q,L}\right) \end{bmatrix}, \tag{3.22}$$

and then (3.21) can be rewritten as

$$\mathbf{A}_N \cdot \mathbf{h}_x + \mathbf{n}_{H_x} = 0, \tag{3.23}$$

where $\mathbf{h}_x = \text{vec}(\mathbf{H}_x) = \left(h_{x,1}, h_{x,2}, \cdots, h_{x,N_r^2}\right)^T$ denotes the vectorization of $\mathbf{H}_x$. As mentioned, we can only obtain $\alpha \mathbf{h}_x$, where α denotes an unknown complex scalar, through

relay channel estimation. Considering this, we try to estimate the value of $\mathbf{h}_x$ normalized to $h_{x,1}$, namely $\mathbf{h}_{x,n} = \frac{1}{h_{x,1}}\mathbf{h}_x$, by adding an extra equation to (3.23) to get

$$\begin{bmatrix} \mathbf{A}_N \\ \mathbf{e} \end{bmatrix} \cdot \mathbf{h}_{x,n} + \begin{bmatrix} \mathbf{n}_{H_x} \\ 0 \end{bmatrix} = \mathbf{y}, \tag{3.24}$$

where $\mathbf{e} = (1, 0, 0, \cdots, 0)$ is an N_r^2-dimension row vector, and $\mathbf{y} = (0, 0, \cdots, 1)^T$ is an $(L-1)N_r^2 + 1$-dimension column vector. Thus $\mathbf{h}_{x,n}$ can be estimated as an approximate LS solution [97] to (3.24) [8] as

$$\hat{\mathbf{h}}_{x,n,LS} = \left(\mathbf{C}^H\mathbf{C}\right)^{-1}\mathbf{C}^H\mathbf{y}, \tag{3.25}$$

where $\mathbf{C} = \left[\mathbf{A}_N^T \ \ \mathbf{e}^T\right]^T$. According to (3.24), the estimation error of $\hat{\mathbf{h}}_{x,n,LS}$ is given by

$$\hat{\mathbf{h}}_{x,n,LS} - \mathbf{h}_{x,n} = \left(\mathbf{C}^H\mathbf{C}\right)^{-1}\mathbf{C}^H\mathbf{n}'_{H_x}, \tag{3.26}$$

where $\mathbf{n}'_{H_x} = \left[\mathbf{n}_{H_x}^T \ \ 0\right]^T$. Accordingly, the *mean-square error* (MSE) of $\hat{\mathbf{h}}_{x,n,LS}$ can be expressed as

$$\xi = E\left\{\left(\hat{\mathbf{h}}_{x,n,LS} - \mathbf{h}_{x,n}\right)^H\left(\hat{\mathbf{h}}_{x,n,LS} - \mathbf{h}_{x,n}\right)\right\}, \tag{3.27}$$

where $E\{\cdot\}$ denotes expectation w.r.t. both the random noise and the relay channel to estimate. Since both $\mathbf{C}$ and $\mathbf{n}'_{H_x}$ depend on not only the random noise but also the relay channel to estimate, it is rather difficult to obtain a closed-form expression for ξ. Therefore, it can only be evaluated numerically. While the focus of this chapter is on investigating the feasibility of estimating the cascaded relay channels at the DS and designing low-complexity pilot amplifying matrices at the RS, it will be a potential future research topic to design the optimal pilot matrices to minimize the MSE in a noisy environment.

3.5 Extension to General Case

In order for the overall channel to be nonsingular, we have assumed $N_r \geq \min\{N_s, N_d\}$, which consists of Case I: $N_r = \min\{N_s, N_d\}$ and Case II: $N_r > \min\{N_s, N_d\}$. In the previous

[8] Since the noise part, $\mathbf{n}_{H_x}$, also depends on the unknown channel $\mathbf{H}_x$, $\hat{\mathbf{h}}_{x,n,LS}$ is not an exact LS solution to (3.24). Actually, in the presence of imperfect overall CSI, Equation (3.24) turns out to be a nonlinear equation w.r.t $\mathbf{h}_{x,n}$ and is hard to solve. When a relatively accurate overall channel is available, the power of $\mathbf{n}_{H_x}$ is low. In this case, $\hat{\mathbf{h}}_{x,n,LS}$ is an approximate linear LS solution to (3.24).

sections, we have investigated relay channel estimation at the DS in Case I; in this section, we will extend it to Case II.

In Case II, the original nonlinear matrix equation in (3.3) cannot be transformed into a linear one w.r.t either one of the two cascaded relay channels. Therefore, we propose to estimate the relay channels via multiple steps. In each step, the relay channel estimation procedure in Case I is applied. Specifically, we divide the receive and transmit antenna pairs at the RS into multiple groups so that the number of antenna pairs in each group, $N_r^{'}$, equals $\min\{N_s, N_d\}$. Obviously there will be overlapping antenna pairs in different groups if $I = \frac{N_r}{N_r^{'}}$ is not an integer. Without loss of generality, we assume I is an integer to facilitate explanations. By grouping the receive and transmit antenna pairs at the RS, the original two-hop MIMO AF relay system is decomposed into I parallel subsystems with still N_s and N_d antennas at the SS and the DS, respectively, but $N_r^{'}$ receive and transmit antenna pairs at the RS. Let $\mathbf{H}_{1,i}$ and $\mathbf{H}_{2,i}, 1 \leq i \leq I$, denote the backward and the forward relay channels of the ith subsystem, respectively, and then the overall relay channels are given by $\mathbf{H}_1 = \left(\mathbf{H}_{1,1}^T, \mathbf{H}_{1,2}^T, \cdots, \mathbf{H}_{1,I}^T\right)^T$ and $\mathbf{H}_2 = (\mathbf{H}_{2,1}, \mathbf{H}_{2,2}, \cdots, \mathbf{H}_{2,I})$. Since $N_r^{'} = \min\{N_s, N_d\}$, $\mathbf{H}_{1,i}$ and $\mathbf{H}_{2,i}$ can be estimated following the procedure in Case I by switching off all of the antenna pairs of the RS that are outside the ith group. Then the overall relay channels, $\mathbf{H}_1$ and $\mathbf{H}_2$, can be obtained by combining $\mathbf{H}_{1,i}$'s and $\mathbf{H}_{2,i}$'s, respectively. Since we can only get the values of $\mathbf{H}_{1,i}$ and $\mathbf{H}_{2,i}$ normalized to one of their respective elements, J extra antenna groups are needed to obtain the amplitude and phase relationship between the relay channels of different subsystems, where the specific value of J depends on I and $N_r^{'}$.

3.6 Simulation Results

In this section, we will give some simulation results to demonstrate the performance of the approximate linear LS estimation of the relay channels presented in Section 3.4. In our simulation, a 4/4/4 ($N_s = N_r = N_d = 4$) two-hop MIMO AF relay system is considered. The elements of $\mathbf{H}_1$, $\mathbf{H}_2$, $\mathbf{n}_r$, and $\mathbf{n}_d$ are all modeled as i.i.d. complex Gaussian random

variables with zero mean and unit variance. Furthermore, the power amplifying gain of the RS is set to one, i.e., $g = 1$. Denote P_s to be the transmit power of each antenna at the SS, the value of which represents the system SNR of the overall system. Three pilot amplifying matrices are generated randomly for relay channel estimation according to the design rules given in Section 3.3. The normalized relay channels, $\overline{\mathbf{H}}_1 = \frac{1}{\mathbf{H}_1(1,1)}\mathbf{H}_1$ and $\overline{\mathbf{H}}_2 = \frac{1}{\mathbf{H}_2(1,1)}\mathbf{H}_2$, where $\mathbf{H}_i(1,1)$ denotes the element at the first row and the first column of $\mathbf{H}_i, 1 \leq i \leq 2$, are estimated through the approximate linear LS estimation procedure given in Section 3.4. The corresponding normalized MSE of estimate $\overline{\mathbf{H}}_{i,E}$ is defined as

$$\xi_i = E\left\{\frac{\|\overline{\mathbf{H}}_i - \overline{\mathbf{H}}_{i,E}\|^2}{\|\overline{\mathbf{H}}_i\|^2}\right\}, \quad 1 \leq i \leq 2, \tag{3.28}$$

where $\|\cdot\|^2$ denotes the sum power of all elements of a matrix.

Figure 3.4 shows the normalized MSE curves of the estimated relay channels, $\overline{\mathbf{H}}_{1,E}$ and $\overline{\mathbf{H}}_{2,E}$. In Figure 3.4(a), we apply the imperfect overall channel model in (3.19) and define its equivalent SNR as the ratio of the average power of the overall channel to that of the additive white Gaussian noise. In contrast, the imperfect overall channel in Figure 3.4(b) is obtained by employing the linear-MMSE-based channel estimation algorithm under a certain system SNR. Figure 3.4 indicates that an acceptable estimation performance, such as a normalized MSE smaller than -5 dB, can be achieved when the equivalent SNR of the overall channel (in Figure 3.4(a)), or the system SNR (in Figure 3.4(b)), is greater than 15 dB. This suggests that the accuracy of the overall channel is significant to the relay channel estimation. While $\overline{\mathbf{H}}_{1,E}$ and $\overline{\mathbf{H}}_{2,E}$ have the same normalized MSE under the imperfect overall channel model with additive white Gaussian noise, it is interesting to notice that $\overline{\mathbf{H}}_{1,E}$ has a smaller normalized MSE than $\overline{\mathbf{H}}_{2,E}$ when the overall channel is obtained through the conventional channel estimation algorithms. This is actually reasonable since the overall system model in (3.1) indicates that $\mathbf{H}_1$ and $\mathbf{H}_2$ are not playing interchangeable roles in the original system. Specifically, $\mathbf{H}_1$ is independent of the overall noise at the DS while $\mathbf{H}_2$ is not since it conveys $\mathbf{n}_r$, the noise vector at the RS, to the DS. While the focus of this chapter is on pilot matrix design for estimating cascaded relay channels based on available overall

CSI, it will be a potential future research topic to jointly estimate $\mathbf{H}_1$, $\mathbf{H}_2$, and the overall channel.

Figure 3.5 demonstrates the performance improvements of the two-hop MIMO AF relay system when the estimated forward relay channel is utilized to improve the data detection at the DS. In our simulation, V-BLAST transmission with QPSK modulation is applied at the SS and no error correcting coding is utilized. Imperfect overall channel is obtained through the linear-MMSE-based channel estimation algorithm and, based on that, the ML and MMSE detection schemes are applied at the DS. In order to get accurate overall channel estimation for system performance optimization, we assume that the SNR of the pilot for overall channel estimation is 10 dB higher than that of the data. In particular, we assume that the average power gain over the RS-DS hop, σ_2^2, which equals one in our simulation, is known at the DS since it is static and thus can be easily obtained. When the relay CSI over the RS-DS hop is unavailable, we simply assume that the overall noise at the DS is white and estimate its correlation matrix as

$$\tilde{\mathbf{R}}_n = \sigma_r^2 E\left\{\mathbf{H}_2\mathbf{H}_2^H\right\} + \sigma_d^2\mathbf{I}_{N_d} = \left(N_r\sigma_r^2\sigma_2^2 + \sigma_d^2\right)\mathbf{I}_{N_d}, \tag{3.29}$$

based on which approximate ML and MMSE detection schemes are applied at the DS. In contrast, with relay channel estimation at the DS, we estimate the correlation matrix of the overall noise vector as

$$\hat{\mathbf{R}}_n = \sigma_r^2\frac{N_dN_r\sigma_2^2}{||\overline{\mathbf{H}}_{2,E}||^2}\overline{\mathbf{H}}_{2,E}\overline{\mathbf{H}}_{2,E}^H + \sigma_d^2\mathbf{I}_{N_d}, \tag{3.30}$$

based on which improved approximate ML and MMSE detection schemes can be applied at the DS. From Figure 3.5, we observe that when BER is around 10^{-3}, the ML and the MMSE detection schemes based on the estimated relay channels achieve about 1.0 dB performance gains over those based on the white overall noise assumption, respectively. While the initial simulation results have justified estimating the cascaded relay channels at the DS, further utilization of the estimated relay channels for system performance improvements will be a future research topic.

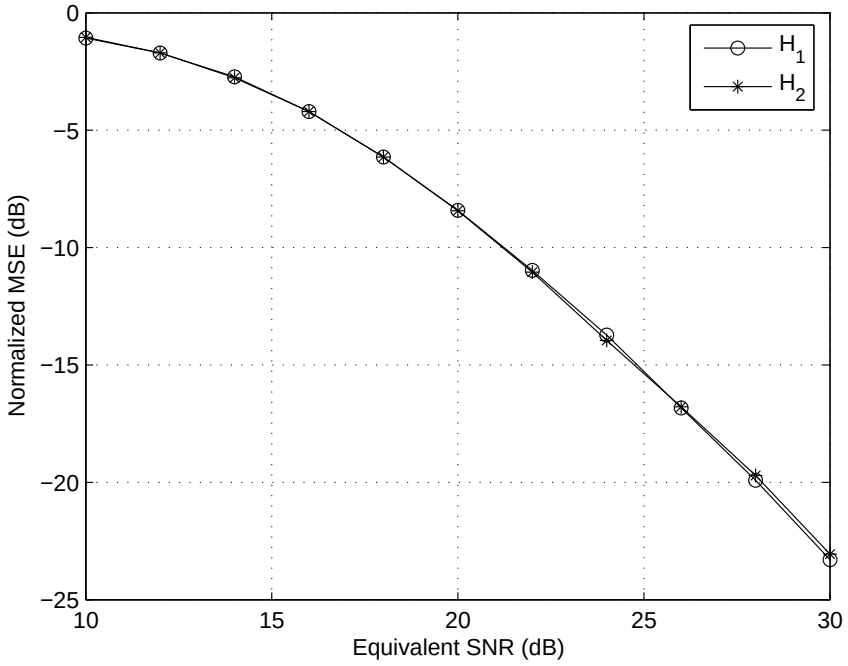

(a) Normalized MSE versus equivalent SNR of the overall channel

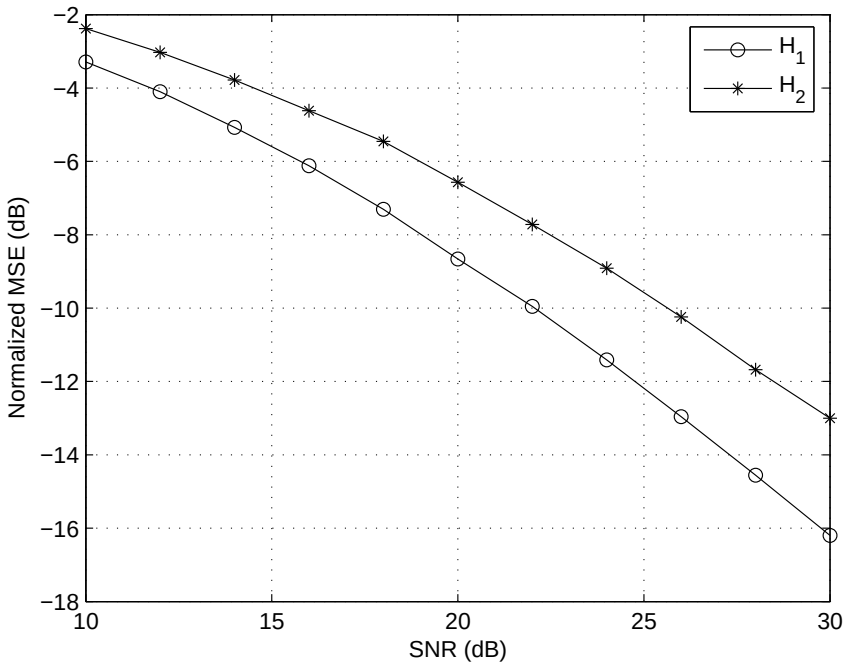

(b) Normalized MSE versus system SNR

Figure 3.4. Normalized MSE curves of the estimated relay channels

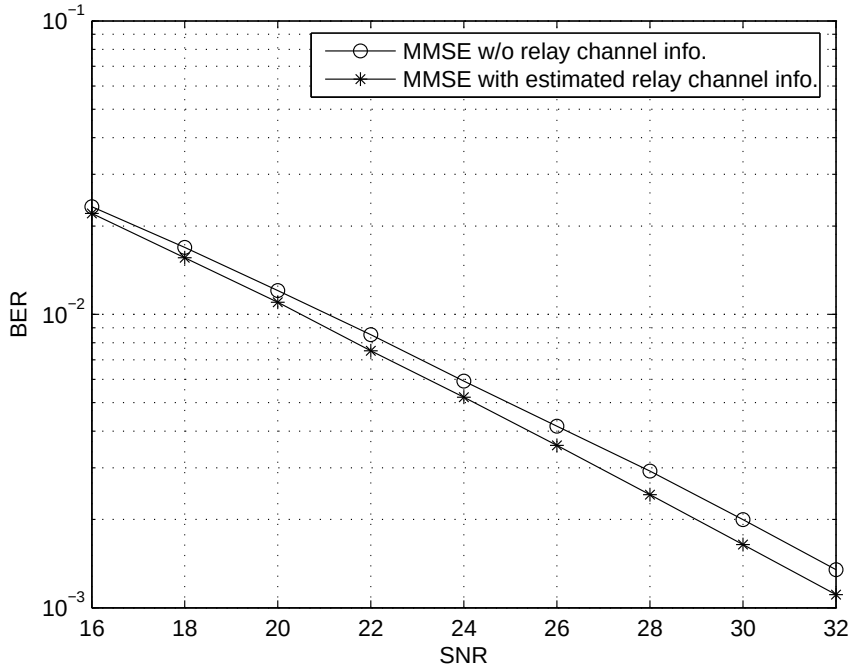

(a) MMSE detection

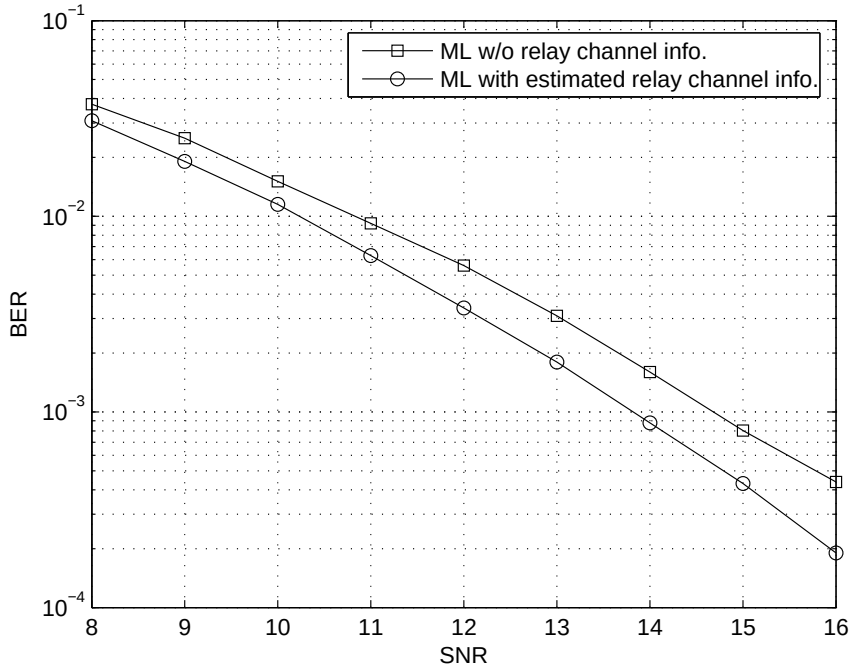

(b) ML detection

Figure 3.5. BER performance improvements achieved by relay channel estimation

3.7 Conclusion

In this chapter, we have investigated estimating the cascaded backward and forward relay channels at the final destination of a two-hop MIMO AF relay system based on a predefined pilot amplifying matrix sequence at the RS and the corresponding overall channel sequence obtained at the DS through conventional channel estimation algorithms. Such a relay channel estimation scheme is applicable to a minimum-complexity relay that simply amplifies and forwards its received signals. We have found the necessary and sufficient conditions on the pilot matrix sequence to ensure successful relay channel estimation and presented rules to design diagonal or quasi-diagonal pilot amplifying matrices to meet these conditions. In the presence of imperfect overall CSI at the DS, we have further developed the approximate linear LS estimation of the relay channels and evaluated its performance by simulation results. Furthermore, initial simulation results have also demonstrated the system performance improvements achieved by relay channel estimation.

CHAPTER 4

CROSS-TALK CANCELLATION FOR WIRELESS RELAY WITH CHANNEL REUSE

Conventionally, a wireless RS receives data from the SS over one channel and forwards them to the DS over the other channel by time division or frequency division [10, 4]. In contrast, a CRRS forwards signals to the DS over the same channel as it receives, thus significantly increasing spectral efficiency. However, a critical issue with a CRRS is severe co-channel cross-talk interference from its transmit antenna to its receive antenna.

In this chapter, we focus on digital cross-talk cancellation techniques for a CRRS. With the help of high isolation antennas [59, 60] and analog cancellers [61, 62], the strength of cross-talk interference at the RS can be significantly reduced, paving the way for further digital cancellation. In the literature, various techniques for digital cross-talk cancellation based on the estimation of the coupling channel from the transmit to the receive antenna of the RS have been proposed [15, 16, 21]. However, all of these techniques require the RS to transmit dedicated pilots, such as the pseudo-random sequences, for local coupling channel estimation. Inserting these dedicated pilots at the RS not only changes the original signal structure in the physical layer but also results in in-band interference at the destination. In practice, cross-talk cancellation at the RS is supposed to be completely transparent to the existing wireless standard, i.e., no modifications need to be made to the signal structure in the physical layer, to the BS, and to the MS. In light of this, we propose a new cross-talk canceller in this chapter, which does not require the RS to transmit any dedicated pilots. Specifically, the proposed canceller utilizes the random forwarded signals of the RS as pilots for coupling channel estimation. We propose the LS coupling channel estimation for cross-talk cancellation at a general RS with any relay mechanism, and present qualitative performance analysis. For a DF-based RS with constant amplitude modulation, we further develop the MMSE coupling channel estimation and quantitatively analyze the

performance of the proposed cross-talk canceller, including the correlation matrix of the residual error and the post *signal-to-interference ratio* (SIR) after cross-talk cancellation.

The remainder of this chapter is organized as follows. In Section 4.1, cross-talk interference at a wireless CRRS is modeled. Then we develop a new cross-talk canceller based on the LS coupling channel estimation without dedicated pilots in Section 4.2. In Section 4.3, we develop the MMSE coupling channel estimation for cross-talk cancellation at a DF-based RS with constant amplitude modulation. Then we present numerical and simulation results in Section 4.4. Finally we conclude this chapter in Section 4.5.

4.1 System Model and Problem Formulation

In this chapter, we are concerned with cross-talk interference from the transmit to the receive antenna of a wireless CRRS that is designed to boost signal strength in a coverage hole. Figure 1.3 in Chapter 1 shows a schematic description of such a CRRS where the dashed line denotes the co-channel cross-talk interference since the RS transmits signals over the same channel as it receives. Throughout this chapter, we assume that the RS is working in a wireless network with OFDM modulation. After receiving a whole OFDM symbol, the RS forwards it to the DS after appropriate processing according to the specific relay mechanism. To facilitate analysis, we assume that there is exactly one OFDM symbol delay at the RS due to signal processing[1]. Thus the currently received OFDM symbol of the RS is a summation of the desired symbol from the source and the cross-talk symbol from itself, which is a forwarded version of its previous received symbol.

Without loss of generality, we consider an RS equipped with M_r receive antennas and M_t transmit antennas. When $M_r \neq M_t$, appropriate signal dimension expansion or reduction is applied at the RS. In general, for an AF-based RS, a non-square matrix transformation is applied when $M_t \neq M_r$; for a DF-based RS, redundant receive or transmit antennas

[1]Since the cross-talk cancellation scheme proposed in this chapter works whether there is one or more OFDM symbols of delay at the RS, the one OFDM symbol delay assumption does not lose generality and the analysis framework presented in this chapter based on this assumption can be easily extended to the general case when there exists an arbitrary number of OFDM symbols of delay at the RS.

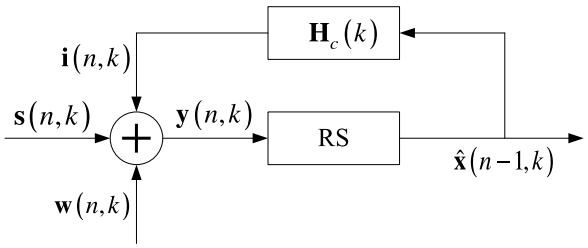

Figure 4.1. Mathematical model of cross-talk interference at the RS.

may be utilized for reliable signal transmission and in this case it is likely that $M_t \neq M_r$. Denote K as the number of OFDM subcarriers, $\mathbf{s}(n,k)$ as the M_r-dimensional desired signal vector at the RS received from the SS over the kth ($0 \leq k \leq K-1$) subcarrier of the nth OFDM symbol, and $\mathbf{w}(n,k)$ as the white noise vector independent of $\mathbf{s}(n,k)$, and then the corresponding received signal vector of the RS can be expressed as

$$\mathbf{y}(n,k) = \mathbf{s}(n,k) + \mathbf{i}(n,k) + \mathbf{w}(n,k), \tag{4.1}$$

where $\mathbf{i}(n,k)$ denotes the cross-talk interference vector. Based on (4.1), we show a mathematical model of cross-talk interference at the RS in Figure 4.1. Denote $\mathbf{H}_c(k)$ as the frequency-domain $M_r \times M_t$ coupling channel matrix over the kth OFDM subcarrier from the transmit to the receive antenna of the RS. Without loss of generality, we incorporate the power gain of the RS in the coupling channel and denote $\hat{\mathbf{x}}(n-1,k)$ as the M_t-dimensional transmitted signal vector of the RS in the nth OFDM symbol before power amplification, which is a forwarded version of $\mathbf{s}(n-1,k)$, and then $\mathbf{i}(n,k)$ can be expressed as

$$\mathbf{i}(n,k) = \mathbf{H}_c(k)\,\hat{\mathbf{x}}(n-1,k). \tag{4.2}$$

Throughout this chapter, we model the time-domain coupling channel as a multiple-tap one with the delay of each tap equal to integer OFDM sampling intervals. Suppose the maximum delay of the coupling channel is L ($< K$) OFDM sampling intervals and denote $\mathbf{H}_{c,l}$ as the time-domain $M_r \times M_t$ coupling channel matrix over the lth ($0 \leq l \leq L-1$) tap,

and then $\mathbf{i}(n,k)$ can be expressed as

$$\begin{aligned}\mathbf{i}\,(n,k) &= \sum_{l=0}^{L-1}\mathbf{H}_{c,l}e^{-j\frac{2\pi lk}{K}}\hat{\mathbf{x}}\,(n-1,k)\\ &= \sum_{l=0}^{L-1}\left[e^{-j\frac{2\pi lk}{K}}\hat{\mathbf{x}}^{T}\,(n-1,k)\otimes\mathbf{I}_{M_r}\right]\mathrm{vec}\,(\mathbf{H}_{c,l}),\end{aligned} \tag{4.3}$$

where $\mathbf{I}_{M_r}$ denotes the $M_r \times M_r$ identity matrix, $\otimes$ denotes the Kronecker product [98], and $\mathrm{vec}\,(\mathbf{H}_{c,l})$ denotes the vectorization of $\mathbf{H}_{c,l}$ formed by stacking the columns of $\mathbf{H}_{c,l}$ into a single column vector, i.e., $\mathrm{vec}\,(\mathbf{H}_{c.l}) = \left(\mathbf{h}_{c,l,1}^{T}, \mathbf{h}_{c,l,2}^{T}, \cdots, \mathbf{h}_{c,l,M_t}^{T}\right)^{T}$ where $\mathbf{h}_{c,l,m}, 1 \le m \le M_t$, denotes the mth column vector of $\mathbf{H}_{c.l}$. If we define

$$\hat{\mathbf{X}}\,(n-1,k,l) = e^{-j\frac{2\pi lk}{K}}\hat{\mathbf{x}}^{T}\,(n-1,k)\otimes\mathbf{I}_{M_r}, \tag{4.4}$$

$$\hat{\mathbf{X}}\,(n-1,k) = \left(\hat{\mathbf{X}}\,(n-1,k,0)\,,\hat{\mathbf{X}}\,(n-1,k,1)\,,\cdots,\hat{\mathbf{X}}\,(n-1,k,L-1)\right), \tag{4.5}$$

and the composite coupling channel vector as

$$\mathbf{h}_c = \left(\mathrm{vec}\,(\mathbf{H}_{c,0})^{T}\,,\mathrm{vec}\,(\mathbf{H}_{c,1})^{T}\,,\cdots,\mathrm{vec}\,(\mathbf{H}_{c,L-1})^{T}\right)^{T}, \tag{4.6}$$

and then $\mathbf{i}(n,k)$ can be expressed as

$$\mathbf{i}\,(n,k) = \hat{\mathbf{X}}\,(n-1,k)\,\mathbf{h}_c. \tag{4.7}$$

Further define the $KM_r \times LM_rM_t$ overall forwarded signal matrix of the RS as

$$\hat{\mathbf{X}}\,(n-1) = \left(\hat{\mathbf{X}}\,(n-1,0)^{T}\,,\hat{\mathbf{X}}\,(n-1,1)^{T}\,,\cdots,\hat{\mathbf{X}}\,(n-1,K-1)^{T}\right)^{T}, \tag{4.8}$$

and then the KM_r-dimensional overall cross-talk interference vector in the nth OFDM symbol can be expressed as

$$\mathbf{i}\,(n) = \left(\mathbf{i}\,(n,0)^{T}\,,\mathbf{i}\,(n,1)^{T}\,,\cdots,\mathbf{i}\,(n,K-1)^{T}\right)^{T} = \hat{\mathbf{X}}\,(n-1)\,\mathbf{h}_c. \tag{4.9}$$

Correspondingly, the overall received signal vector of the RS in the nth OFDM symbol is

$$\mathbf{y}\,(n) = \mathbf{s}\,(n) + \mathbf{i}\,(n) + \mathbf{w}\,(n)\,, \tag{4.10}$$

where

$$\mathbf{s}(n) = \left(\mathbf{s}(n,0)^T, \mathbf{s}(n,1)^T, \cdots, \mathbf{s}(n,K-1)^T\right)^T, \tag{4.11}$$

and

$$\mathbf{w}(n) = \left(\mathbf{w}(n,0)^T, \mathbf{w}(n,1)^T, \cdots, \mathbf{w}(n,K-1)^T\right)^T. \tag{4.12}$$

Based on (4.10), we define the SIR as

$$\text{SIR} = \frac{E\left\{\|\mathbf{s}(n)\|^2\right\}}{E\left\{\|\mathbf{i}(n)\|^2\right\}}, \tag{4.13}$$

and the *signal-to-noise ratio* (SNR) as

$$\text{SNR} = \frac{E\left\{\|\mathbf{s}(n)\|^2\right\}}{E\left\{\|\mathbf{w}(n)\|^2\right\}}, \tag{4.14}$$

where $E\left\{\|\mathbf{s}(n)\|^2\right\}$, $E\left\{\|\mathbf{i}(n)\|^2\right\}$, and $E\left\{\|\mathbf{w}(n)\|^2\right\}$ denote the average sum powers of the desired signal vector, the cross-talk interference vector, and the noise vector, respectively. Since the transmit power of the RS is dramatically greater than its received desired signal power, the SIR at the RS is so low that cross-talk interference must be cancelled before the RS can work properly.

4.2 Cross-Talk Cancellation based on Least Square Coupling Channel Estimation

Since cross-talk interference at the RS consists of its previously transmitted signal coupled with the channel from the transmit to the receive antenna, it can be reconstructed and cancelled if the coupling CSI is available. Therefore, it is natural to estimate the coupling channel and perform cross-talk cancellation accordingly. In contrast with the conventional wireless channel that is characterized by multipath (frequency-selective) and time-varying (time-selective) due to distantly located transmitter and receiver and movements of the MS, the coupling channel at the RS is quasi-static in the sense that it has very slow variation with both time and OFDM subcarriers since the transmit and the receive antennas of the RS are collocated. Such simplistic characteristics of the coupling channel greatly facilitate the

coupling channel estimation and cross-talk cancellation at the RS, as demonstrated in [15] and [21].

It has been proposed to set dedicated pilots, such as the pseudo-random sequences, at the RS transmitter for estimation of the quasi-static coupling channel [15, 21]. Such dedicated pilots assisted coupling channel estimation usually consists of two phases. In the startup phase, the RS transmits dedicated pilots only and obtains an initial coupling channel estimate. In the rest update phase, low-power dedicated pilots are transmitted by the RS together with its forwarded signals. While specially designed pilots help improve coupling channel estimation, treating the RS's forwarded signal as noise significantly decreases the *pilot-to-noise ratio* (PNR) in the update phase and, as a result, it takes a long time to obtain a sufficiently accurate coupling channel estimate for a stable cross-talk canceller at an AF-based RS [15]. Moreover, inserting these dedicated pilots at the RS not only changes the original signal structure in the physical layer but also results in in-band interference at the DS.

In this chapter, we propose a new coupling channel estimation scheme for cross-talk cancellation at the RS, a block diagram of which is shown in Figure 4.2. Different from the existing schemes that require the RS to transmit dedicated pilots, the proposed scheme utilizes the random forwarded signals of the RS, which are exactly known to the RS itself, as equivalent pilots for coupling channel estimation. Without inserting any dedicated pilots, the proposed scheme is especially attractive in practice because firstly, no modification to the existing signal structure is incurred; secondly, no in-band interference is caused at the DS; and thirdly, an accurate coupling channel estimate can be achieved rapidly since the PNR is significantly increased relative to the conventional scheme and every forwarded signal of the RS can be utilized as a pilot to improve coupling channel estimation. Different from the specially designed pilots with an optimized structure, the structure of the RS's forwarded signal is random and therefore is suboptimal. However, since every forwarded signal of the RS can be utilized as an equivalent pilot, the utilization of sufficient pilots

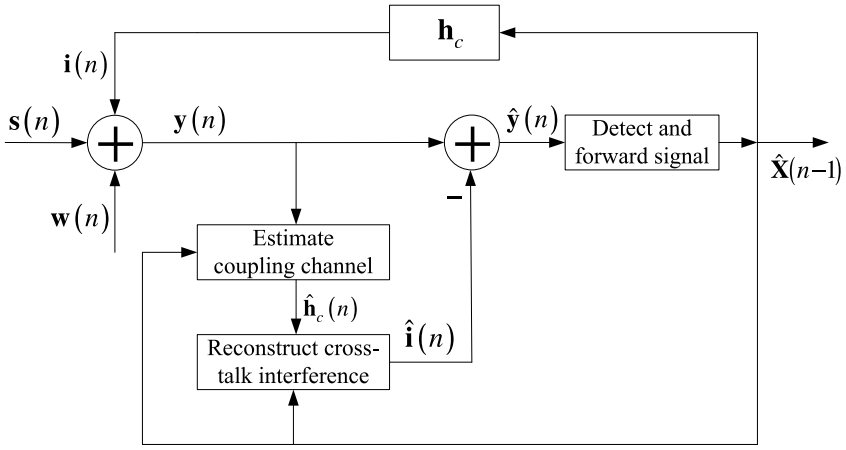

Figure 4.2. Block diagram of cross-talk cancellation based on coupling channel estimation without dedicated pilots.

makes up for its suboptimal structure. Furthermore, when the DF relay mechanism is applied at the RS, the existing optimized pilot structure contained in the forwarded signals for conventional channel estimation at the DS also benefits the coupling channel estimation at the RS.

Mathematically, the proposed scheme estimates $\mathbf{h}_c$ from

$$\mathbf{y}(n) = \hat{\mathbf{X}}(n-1)\,\mathbf{h}_c + \mathbf{s}(n) + \mathbf{w}(n), \tag{4.15}$$

where $\hat{\mathbf{X}}(n-1)$ works as the equivalent pilot matrix, and the unknown desired signal, $\mathbf{s}(n)$, is regarded as noise just like $\mathbf{w}(n)$ in the coupling channel estimation phase. Since the quasi-static coupling channel has very slow variation with time due to a low Doppler frequency, we assume throughout this chapter that it is block-fading and remains unchanged for a number of consecutive OFDM symbols during which joint coupling channel estimation can be performed. Suppose $N(>1)$ recently received OFDM symbols of the RS are utilized for joint coupling channel estimation; denote the composite equivalent pilot matrix of the RS in the previous N OFDM symbols as

$$\hat{\mathbf{X}}_N(n) = \left(\hat{\mathbf{X}}(n-1)^T, \hat{\mathbf{X}}(n-2)^T, \cdots, \hat{\mathbf{X}}(n-N)^T\right)^T, \tag{4.16}$$

and then the corresponding received signal vector of the RS is given by

$$\begin{aligned}\mathbf{y}_N(n) &= \left(\mathbf{y}(n)^T, \mathbf{y}(n-1)^T, \cdots, \mathbf{y}(n-(N-1))^T\right)^T \\ &= \mathbf{i}_N(n) + \mathbf{s}_N(n) + \mathbf{w}_N(n), \end{aligned} \tag{4.17}$$

where $\mathbf{i}_N(n) = \hat{\mathbf{X}}_N(n)\,\mathbf{h}_c$ denotes the composite cross-talk interference vector,

$$\mathbf{s}_N(n) = \left(\mathbf{s}(n)^T, \mathbf{s}(n-1)^T, \cdots, \mathbf{s}(n-(N-1))^T\right)^T, \tag{4.18}$$

and

$$\mathbf{w}_N(n) = \left(\mathbf{w}(n)^T, \mathbf{w}(n-1)^T, \cdots, \mathbf{w}(n-(N-1))^T\right)^T. \tag{4.19}$$

As will be analyzed in Section IV, $\mathbf{s}_N(n)$ for a given $\hat{\mathbf{X}}_N(n)$ is a random variable whose distribution depends on imperfect cross-talk cancellation and desired signal detection at the RS. Here we treat $\mathbf{s}_N(n)$ as noise and obtain the LS estimate of $\mathbf{h}_c$ in the nth OFDM symbol from (4.17) as [92]

$$\hat{\mathbf{h}}_{c,\mathrm{LS}}(n) = \left[\hat{\mathbf{X}}_N^H(n)\,\hat{\mathbf{X}}_N(n)\right]^{-1}\hat{\mathbf{X}}_N^H(n)\,\mathbf{y}_N(n) = \left[\mathbf{F}(n)\right]^{-1}\mathbf{g}(n), \tag{4.20}$$

where

$$\mathbf{F}(n) = \sum_{i=1}^{N}\hat{\mathbf{X}}^H(n-i)\,\hat{\mathbf{X}}(n-i), \tag{4.21}$$

and

$$\mathbf{g}(n) = \sum_{i=1}^{N}\hat{\mathbf{X}}^H(n-i)\,\mathbf{y}(n-i+1). \tag{4.22}$$

Based on $\hat{\mathbf{h}}_{c,\mathrm{LS}}(n)$, the cross-talk interference vector at the RS is reconstructed as

$$\hat{\mathbf{i}}(n) = \hat{\mathbf{X}}(n-1)\,\hat{\mathbf{h}}_{c,\mathrm{LS}}(n), \tag{4.23}$$

and the estimate of the desired signal is obtained by

$$\hat{\mathbf{y}}(n) = \mathbf{y}(n) - \hat{\mathbf{i}}(n) = \mathbf{s}(n) + \mathbf{w}(n) + \mathbf{e}(n), \tag{4.24}$$

where

$$\begin{aligned}\mathbf{e}(n) &= \hat{\mathbf{X}}(n-1)\left[\mathbf{h}_c - \hat{\mathbf{h}}_{c,\mathrm{LS}}(n)\right] \\ &= -\hat{\mathbf{X}}(n-1)\left[\hat{\mathbf{X}}_N^H(n)\,\hat{\mathbf{X}}_N(n)\right]^{-1}\hat{\mathbf{X}}_N^H(n)\left[\mathbf{s}_N(n) + \mathbf{w}_N(n)\right] \end{aligned} \tag{4.25}$$

denotes the residual error vector after cross-talk cancellation. The forwarded symbol matrix of the RS in the next OFDM symbol, $\hat{\mathbf{X}}(n)$, is then obtained from $\hat{\mathbf{y}}(n)$ according to the specific relay mechanism applied. When N is large enough for a given L, a sufficiently accurate coupling channel estimate will be obtained so that the amplitude of $\mathbf{e}(n)$ is less than that of $\hat{\mathbf{X}}(n-1)$, thus leading to a stable cross-talk canceller at an AF-based RS[2]. Different from the conventional low-power dedicated pilots assisted coupling channel estimation schemes, the proposed scheme based on random forwarded signals of the RS has a much higher PNR and therefore takes much less time to achieve a sufficiently accurate coupling channel estimate for a stable cross-talk canceller.

Equation (4.25) indicates that the amplitude of $\mathbf{e}(n)$ is proportional to the amplitude of the desired signal mixed with noise. On the other hand, the amplitude of $\mathbf{e}(n)$ is independent of the average transmit power of the RS, namely the average amplitude of $\hat{\mathbf{X}}_N(n)$ and $\hat{\mathbf{X}}(n-1)$, and is also independent of the amplitude of the coupling channel, $\mathbf{h}_c$. In other words, the amplitude of the residual error after cross-talk cancellation with the LS coupling channel estimation is independent of the average strength of the original cross-talk interference at the RS. While this conclusion seems contra-intuitive at first glance, it is actually reasonable since the cross-talk interference plays two different roles in this system. In the coupling channel estimation phase, the cross-talk symbols work as the pilots; in the cross-talk cancellation phase, they again work as the interference to cancel. As a result, the residual error is a product of the cross-talk symbol and the relay channel estimation error whose amplitude, according to the LS coupling channel estimation, is inversely proportional to that of the cross-talk symbol which works as pilot in the proposed scheme. Generally, $\mathbf{e}(n)$ and $\mathbf{s}(n)$ in (4.24) are statistically correlated because, as indicated in (4.18), $\mathbf{s}(n)$ constitutes $\frac{1}{N}$ part of $\mathbf{s}_N(n)$, which works as noise during joint coupling channel estimation in N consecutive OFDM symbols. However, since the coupling channel is quasi-static, N

[2]A cross-talk canceller at an AF-based RS is stable when the effect of its residual error after cross-talk cancellation in the current symbol gradually dies away in upcoming symbols and the average transmit power of the RS converges at a finite value.

is usually much larger than one and therefore $\mathbf{e}(n)$ is approximately independent of $\mathbf{s}(n)$. Based on that, we define the post SIR after cross-talk cancellation as

$$\mathrm{SIR}_{\mathrm{Post}} = \frac{E\left\{\|\mathbf{s}(n)\|^2\right\}}{E\left\{\|\mathbf{e}(n)\|^2\right\}}, \tag{4.26}$$

which, according to the above analysis, is independent of the original SIR level before cross-talk cancellation. Obviously the post SIR converges at a finite value even if the SNR goes to infinity. Intuitively, the specific value of the post SIR for a given SNR level depends on how autocorrelated the coupling channel is in the frequency-domain and in the time-domain; more precisely, it depends on the maximum delay spread of the coupling channel, L, and the maximum number of consecutive OFDM symbols during which the coupling channel remains unchanged.

As a final remark, cross-talk cancellation based on the LS coupling channel estimation proposed in this section is applicable to a wireless RS with the DF, the AF, or any other relay mechanism.

4.3 Coupling Channel Estimation and Cross-Talk Cancellation at DF-based RS

In the last section, we have investigated cross-talk cancellation based on the LS coupling channel estimation. Since the LS estimation does not require any *a priori* knowledge on the coupling channel, the desired signal, and the noise, it is applicable to any relay scenario. In this section, we will show that, when a DF-based RS is applied, the statistical characteristics of the coupling channel, the desired signal, and the noise can be conveniently utilized to perform the MMSE coupling channel estimation. With these statistics, we will also quantitatively analyze the performance of the proposed cross-talk canceller.

Recall that the composite received signal vector of the RS in the previous N OFDM symbols is

$$\mathbf{y}_N(n) = \hat{\mathbf{X}}_N(n)\,\mathbf{h}_c + \mathbf{s}_N(n) + \mathbf{w}_N(n), \tag{4.27}$$

where $\mathbf{s}_N(n)$ and $\hat{\mathbf{X}}_N(n)$ denote the composite desired signal vector and the corresponding composite forwarded signal matrix of the RS, respectively. Since $\hat{\mathbf{X}}_N(n)$ is a forwarded version of $\mathbf{s}_N(n)$ with one OFDM symbol delay, they are generally statistically correlated. For a general RS with any relay mechanism, however, determining the statistical distribution of $\mathbf{s}_N(n)$ for a given $\hat{\mathbf{X}}_N(n)$ is rather difficult since it involves imperfect cross-talk cancellation and desired signal detection at the RS in a noisy environment. As a result, quantitative performance analysis of the proposed cross-talk cancellation scheme at a general RS cannot be delivered. However, when the DF relay mechanism and constant amplitude modulation are applied, the statistical correlation between $\mathbf{s}_N(n)$ and $\hat{\mathbf{X}}_N(n)$ disappears, which greatly facilitates further performance analysis of the proposed cross-talk canceller. To show this, we will first present the desired signal model in the following.

4.3.1 Desired Signal Model

Suppose that there are M_s transmit antennas at the SS. Denote the M_s-dimensional transmitted signal vector of the SS over the kth subcarrier of the nth OFDM symbol as $\mathbf{x}(n,k)$, and the $M_r \times M_s$ channel matrix from the SS to the RS as $\mathbf{H}_r(n,k)$, and then the corresponding desired signal vector at the RS is

$$\mathbf{s}(n,k) = \mathbf{H}_r(n,k)\,\mathbf{x}(n,k). \tag{4.28}$$

Similarly, the overall desired signal vector at the RS defined in (4.11) can be expressed as

$$\mathbf{s}(n) = \mathbf{H}_r(n)\,\mathbf{x}(n), \tag{4.29}$$

where

$$\mathbf{x}(n) = \left(\mathbf{x}(n,0)^T, \mathbf{x}(n,1)^T, \cdots, \mathbf{x}(n,K-1)^T\right)^T, \tag{4.30}$$

and

$$\mathbf{H}_r(n) = \mathrm{diag}\left\{\mathbf{H}_r(n,0), \mathbf{H}_r(n,1), \cdots, \mathbf{H}_r(n,K-1)\right\} \tag{4.31}$$

denotes the block diagonal channel matrix from the SS to the RS in the nth OFDM symbol.

When the DF relay mechanism is applied, the channel from the SS to the RS needs to be estimated at the RS for desired signal detection unless noncoherent demodulation is adopted. Intuitively, the estimated channel from the SS to the RS together with the corresponding decoded transmitted symbols may be utilized to estimate $\mathbf{s}_N(n)$ for decision feedback assisted coupling channel estimation. However, we do not consider such decision feedback in this chapter and assume that the RS only knows the statistics of the channel from the SS to the RS when estimating the coupling channel and, as a result, $\mathbf{s}_N(n)$ is a random variable whose distribution generally depends on both the transmitted symbols and the statistics of the channel from the SS to the RS. Assume that constant amplitude modulation like *multiple phase-shift keying* (MPSK) is applied on each OFDM subcarrier, and then we have proved in Appendix C.1 that $\mathbf{s}_N(n)$ is statistically independent of both the transmitted symbols at the SS and their forwarded version at the RS, $\hat{\mathbf{X}}_N(n)$, which enables the following MMSE coupling channel estimation.

4.3.2 MMSE Coupling Channel Estimation

The MMSE coupling channel estimation minimizes the MSE of the estimate $\hat{\mathbf{h}}_c(n)$,

$$\phi_{\mathbf{h}_c} = E\left\{\left(\mathbf{h}_c - \hat{\mathbf{h}}_c(n)\right)^H \left(\mathbf{h}_c - \hat{\mathbf{h}}_c(n)\right)\right\}. \tag{4.32}$$

Since the residual error after cross-talk cancellation is

$$\mathbf{e}(n) = \hat{\mathbf{X}}(n-1)\left[\mathbf{h}_c - \hat{\mathbf{h}}_c(n)\right], \tag{4.33}$$

it can be shown that the cross-talk canceller based on the MMSE coupling channel estimation also minimizes the MSE of $\mathbf{e}(n)$ for a given $\hat{\mathbf{X}}(n-1)$, and thus is essentially an MMSE canceller. Therefore, it is always a preferred option when the statistics of the coupling channel, the desired signal, and the noise are available.

Denote $\mathbf{R}_{\mathbf{h}_c} = E\left\{\mathbf{h}_c\mathbf{h}_c^H\right\}$, $\mathbf{R}_{\mathbf{s}} = E\left\{\mathbf{s}_N(n)\,\mathbf{s}_N^H(n)\right\}$, and $\mathbf{R}_{\mathbf{w}} = E\left\{\mathbf{w}_N(n)\,\mathbf{w}_N^H(n)\right\}$ as the correlation matrices of $\mathbf{h}_c$, $\mathbf{s}_N(n)$, and $\mathbf{w}_N(n)$, respectively. For the MMSE coupling channel estimation, $\mathbf{R}_{\mathbf{h}_c}$ is known to the RS. Denote σ_r^2 as the white noise power at the RS, and then

$\mathbf{R}_{\mathbf{w}} = \sigma_r^2 \mathbf{I}_{NKM_r}$ where $\mathbf{I}_{NKM_r}$ denotes the $NKM_r \times NKM_r$ identity matrix. Furthermore, since $\mathbf{s}_N(n)$ is statistically independent of the equivalent pilot matrix $\hat{\mathbf{X}}_N(n)$, $\mathbf{R}_{\mathbf{s}}$ does not vary with $\hat{\mathbf{X}}_N(n)$. To provide insights with a simple expression for $\mathbf{R}_{\mathbf{s}}$, we assume that the transmitted signals of the SS are independent across different subcarriers and OFDM symbols with constant unit amplitude, and that the multi-tap time-domain channel from the SS to the RS has independent channel gains over different taps with the $M_r \times M_s$ channel matrix over each tap consisting of independently and identically distributed elements. With these assumptions, it can be shown that $\mathbf{R}_{\mathbf{s}} = M_s \sigma_h^2 \mathbf{I}_{NKM_r}$ where σ_h^2 denotes the average power gain over the channel from the SS to the RS. Then, from (4.27), we obtain an MMSE estimate of $\mathbf{h}_c$ in the nth OFDM symbol as [92]

$$\begin{aligned}\hat{\mathbf{h}}_{c,\mathrm{MMSE}}(n) &= \left[\mathbf{R}_{\mathbf{h}_c}^{-1} + \hat{\mathbf{X}}_N^H(n)\left(\mathbf{R}_{\mathbf{s}} + \mathbf{R}_{\mathbf{w}}\right)^{-1}\hat{\mathbf{X}}_N(n)\right]^{-1}\hat{\mathbf{X}}_N^H(n)\left(\mathbf{R}_{\mathbf{s}} + \mathbf{R}_{\mathbf{w}}\right)^{-1}\mathbf{y}_N(n), \\ &= \left[\left(\sigma_r^2 + M_s\sigma_h^2\right)\mathbf{R}_{\mathbf{h}_c}^{-1} + \mathbf{F}(n)\right]^{-1}\mathbf{g}(n), \end{aligned} \tag{4.34}$$

where $\mathbf{F}(n)$ and $\mathbf{g}(n)$ are defined in (4.21) and (4.22), respectively. The corresponding MSE matrix of estimate $\hat{\mathbf{h}}_{c,\mathrm{MMSE}}(n)$ is given by [92]

$$\begin{aligned}\mathbf{\Phi}_{\mathrm{MMSE}}(n) &= E\left\{\left[\mathbf{h}_c - \hat{\mathbf{h}}_{c,\mathrm{MMSE}}(n)\right]\left[\mathbf{h}_c - \hat{\mathbf{h}}_{c,\mathrm{MMSE}}(n)\right]^H\right\} \\ &= \left[\mathbf{R}_{\mathbf{h}_c}^{-1} + \hat{\mathbf{X}}_N^H(n)\left(\mathbf{R}_{\mathbf{s}} + \mathbf{R}_{\mathbf{w}}\right)^{-1}\hat{\mathbf{X}}_N(n)\right]^{-1} \\ &= \left[\mathbf{R}_{\mathbf{h}_c}^{-1} + \frac{1}{\left(\sigma_r^2 + M_s\sigma_h^2\right)}\mathbf{F}(n)\right]^{-1}. \end{aligned} \tag{4.35}$$

Utilize $\hat{\mathbf{h}}_{c,\mathrm{MMSE}}(n)$ for cross-talk cancellation at the RS, and then the corresponding residual error vector can be expressed as

$$\mathbf{e}_{\mathrm{MMSE}}(n) = \hat{\mathbf{X}}(n-1)\left[\mathbf{h}_c - \hat{\mathbf{h}}_{c,\mathrm{MMSE}}(n)\right]. \tag{4.36}$$

Since $\hat{\mathbf{X}}(n-1)$ is exactly known to the RS, the correlation matrix of $\mathbf{e}_{\mathrm{MMSE}}(n)$ is given by

$$\begin{aligned}\mathbf{R}_{\mathbf{e},\mathrm{MMSE}}(n) &= E\left\{\mathbf{e}_{\mathrm{MMSE}}(n)\,\mathbf{e}_{\mathrm{MMSE}}^H(n)\right\} \\ &= \hat{\mathbf{X}}(n-1)\,\mathbf{\Phi}_{\mathrm{MMSE}}(n)\,\hat{\mathbf{X}}^H(n-1). \end{aligned} \tag{4.37}$$

When the LS coupling channel estimation is applied, the correlation matrix of the residual error vector in the nth OFDM symbol can be similarly obtained as

$$\mathbf{R}_{\mathbf{e},\mathrm{LS}}(n) = \hat{\mathbf{X}}(n-1)\,\mathbf{\Phi}_{\mathrm{LS}}(n)\,\hat{\mathbf{X}}^H(n-1), \tag{4.38}$$

where

$$\begin{aligned}\mathbf{\Phi}_{\mathrm{LS}}(n) &= E\left\{\left[\mathbf{h}_c - \hat{\mathbf{h}}_{c,\mathrm{LS}}(n)\right]\left[\mathbf{h}_c - \hat{\mathbf{h}}_{c,\mathrm{LS}}(n)\right]^H\right\} \\ &= \left[\hat{\mathbf{X}}_N^H(n)\,\hat{\mathbf{X}}_N(n)\right]^{-1}\hat{\mathbf{X}}_N^H(n)\,(\mathbf{R}_{\mathbf{s}}+\mathbf{R}_{\mathbf{w}})\,\hat{\mathbf{X}}_N(n)\left[\hat{\mathbf{X}}_N^H(n)\,\hat{\mathbf{X}}_N(n)\right]^{-1} \\ &= \left(\sigma_r^2 + M_s\sigma_h^2\right)\mathbf{F}^{-1}(n). \end{aligned} \tag{4.39}$$

Since the residual error after cross-talk cancellation acts as noise, $\mathbf{R}_{\mathbf{e},\mathrm{MMSE}}(n)$ and $\mathbf{R}_{\mathbf{e},\mathrm{LS}}(n)$ can be utilized to further improve the desired signal detection at the RS, for example, by whitening the noise containing the residual error, or by performing MMSE detection of the transmitted signal of the SS.

4.3.3 Post SIR Analysis

According to (4.26), the post SIR after cross-talk cancellation in the nth OFDM symbol is given by

$$\mathrm{SIR}_{\mathrm{Post}}(n) = \frac{\mathrm{tr}\{\mathbf{R}_{\mathbf{s}}(n)\}}{\mathrm{tr}\{\mathbf{R}_{\mathbf{e}}(n)\}}, \tag{4.40}$$

where $\mathrm{tr}\{\cdot\}$ denotes the trace of a square matrix, $\mathbf{R}_{\mathbf{s}}(n) = E\left\{\mathbf{s}(n)\,\mathbf{s}^H(n)\right\}$, and $\mathbf{R}_{\mathbf{e}}(n)$ is given in (4.37) or (4.38). According to the desired signal model, $\mathbf{R}_{\mathbf{s}}(n) = M_s\sigma_h^2\mathbf{I}_{KM_r}$ and therefore $\mathrm{tr}\{\mathbf{R}_{\mathbf{s}}(n)\} = KM_rM_s\sigma_h^2$. Since $\mathbf{F}(n) = \hat{\mathbf{X}}_N^H(n)\,\hat{\mathbf{X}}_N(n)$, we see from (4.37) and (4.38) that $\mathrm{tr}\{\mathbf{R}_{\mathbf{e}}(n)\}$ is generally a function of $\hat{\mathbf{X}}_N(n)$. In other words, $\mathrm{SIR}_{\mathrm{Post}}(n)$ varies with $\hat{\mathbf{X}}_N(n)$, the random equivalent pilot matrix for coupling channel estimation. However, it is rather difficult to obtain a closed-form expression for the expectation of $\mathrm{SIR}_{\mathrm{Post}}(n)$ with respect to $\hat{\mathbf{X}}_N(n)$. As a result, the average post SIR after cross-talk cancellation at a general DF-based RS can only be evaluated numerically based on (4.40) and (4.37) or (4.38).

To further investigate the post SIR at a DF-based RS, we consider a special case that there is only one transmit antenna and one receive antenna at both the SS and the RS, i.e.,

$M_s = M_r = M_t = 1$. In this case, it can be shown from (4.4), (4.5), and (4.8) that

$$\hat{\mathbf{X}}(n-i) = \hat{\mathbf{X}}_d(n-i)\,\mathbf{F}_L, \quad 1 \le i \le N, \tag{4.41}$$

where $\mathbf{F}_L$ denotes the $K \times L$ truncated DFT matrix defined as

$$\mathbf{F}_L = \begin{bmatrix} 1 & 1 & \cdots & 1 \\ 1 & e^{-j\frac{2\pi}{K}} & \cdots & e^{-j\frac{2\pi(L-1)}{K}} \\ \vdots & \vdots & \ddots & \vdots \\ 1 & e^{-j\frac{2\pi(K-1)}{K}} & \cdots & e^{-j\frac{2\pi(L-1)(K-1)}{K}} \end{bmatrix}, \tag{4.42}$$

and $\hat{\mathbf{X}}_d(n-i)$ denotes the diagonal forwarded signal matrix of the RS in the $(n-i)$th OFDM symbol defined as

$$\hat{\mathbf{X}}_d(n-i) = \mathrm{diag}\Big\{\hat{x}(n-i,0), \hat{x}(n-i,1), \cdots, \hat{x}(n-i,K-1)\Big\}, \tag{4.43}$$

in which $\hat{x}(n-i,k)$ denotes the forwarded symbol over the kth subcarrier. Without loss of generality, we assume $\hat{x}(n-i,k)$ has constant unit amplitude. Thus $\hat{\mathbf{X}}_d(n-i)$ is unitary and

$$\begin{aligned} \mathbf{F}(n) &= \sum_{i=1}^{N} \hat{\mathbf{X}}^H(n-i)\,\hat{\mathbf{X}}(n-i) \\ &= \mathbf{F}_L^H \left(\sum_{i=1}^{N} \hat{\mathbf{X}}_d^H(n-i)\,\hat{\mathbf{X}}_d(n-i) \right) \mathbf{F}_L \\ &= NK\mathbf{I}_L, \end{aligned} \tag{4.44}$$

where $\mathbf{I}_L$ denotes the $L \times L$ identity matrix.

Substitute (4.44) in (4.37), and then we obtain

$$\mathbf{R}_{\mathbf{e},\mathrm{MMSE}}(n) = \hat{\mathbf{X}}_d(n-1)\,\mathbf{F}_L \left[\mathbf{R}_{\mathbf{h}_c}^{-1} + \frac{NK}{\left(\sigma_r^2 + \sigma_h^2\right)} \mathbf{I}_L \right]^{-1} \mathbf{F}_L^H \hat{\mathbf{X}}_d^H(n-1). \tag{4.45}$$

Suppose $\mathbf{R}_{\mathbf{h}_c} = \mathrm{diag}\{\lambda_0, \lambda_1, \cdots, \lambda_{L-1}\}$, where λ_l's for $0 \le l \le L-1$ denote the average power gains over L independent taps of the time-domain coupling channel, and then it can be shown that

$$\mathrm{tr}\{\mathbf{R}_{\mathbf{e},\mathrm{MMSE}}(n)\} = K\left(\sigma_r^2 + \sigma_h^2\right) \sum_{l=0}^{L-1} \frac{1}{NK + \frac{\sigma_r^2 + \sigma_h^2}{\lambda_l}}. \tag{4.46}$$

Therefore, the post SIR after cross-talk cancellation with the MMSE coupling channel estimation does not depend on $\hat{\mathbf{X}}_N(n)$ and can be obtained based on (4.40) as

$$\mathrm{SIR}_{\mathrm{Post-MMSE}} = \frac{\mathrm{tr}\{\mathbf{R}_{\mathbf{s}}(n)\}}{\mathrm{tr}\{\mathbf{R}_{\mathbf{e},\mathrm{MMSE}}(n)\}} = \frac{1}{\sum_{l=0}^{L-1} \frac{1}{NK + \frac{(\sigma_r^2+\sigma_h^2)}{\lambda_l}}} \frac{\sigma_h^2}{\sigma_r^2+\sigma_h^2}. \tag{4.47}$$

If the LS coupling channel estimation is applied, the corresponding post SIR can be obtained similarly as

$$\mathrm{SIR}_{\mathrm{Post-LS}} = \frac{NK}{L}\frac{\sigma_h^2}{\sigma_r^2+\sigma_h^2} = \frac{NK}{L}\frac{1}{1+\frac{1}{\mathrm{SNR}}}, \tag{4.48}$$

where $\mathrm{SNR} = \frac{\sigma_h^2}{\sigma_r^2}$. In contrast, the original SIR before cross-talk cancellation is given by $\mathrm{SIR} = \frac{\sigma_h^2}{\sum_{l=0}^{L-1}\lambda_l}$. Equation (4.48) indicates that $\mathrm{SIR}_{\mathrm{Post-LS}}$ is independent of the original SIR level and increases with the SNR. In contrast, $\mathrm{SIR}_{\mathrm{Post-MMSE}}$ increases with both the original SIR and the SNR. Comparison between (4.47) and (4.48) indicates that the MMSE coupling channel estimation achieves a higher post SIR than the LS estimation. However, the performance gap between them diminishes as the original SIR decreases. When the original SIR is low enough where the MMSE coupling channel estimation reduces to the LS estimation, they will have the same performance. Furthermore, Equations (4.47) and (4.48) indicate that, for a given K, both $\mathrm{SIR}_{\mathrm{Post-MMSE}}$ and $\mathrm{SIR}_{\mathrm{Post-LS}}$ increase with N but decrease with L, i.e., the performance of cross-talk cancellation improves as the coupling channel turns more and more autocorrelated in the time-domain and the frequency-domain.

4.4 Numerical and Simulation Results

In this section, we present numerical and simulation results to demonstrate the performance of the proposed cross-talk cancellation scheme at an RS with the AF or the DF relay mechanism. Without loss of generality, we assume that both the SS and the RS are equipped with two transmit antennas and two receive antennas, i.e., $M_s = M_r = M_t = 2$. In our simulation, 64-subcarrier ($K = 64$) OFDM modulation is utilized for broadband transmission and independent QPSK modulated symbols are loaded on different subcarriers and OFDM symbols. The maximum delay of the multiple-tap coupling channel at the RS is L OFDM

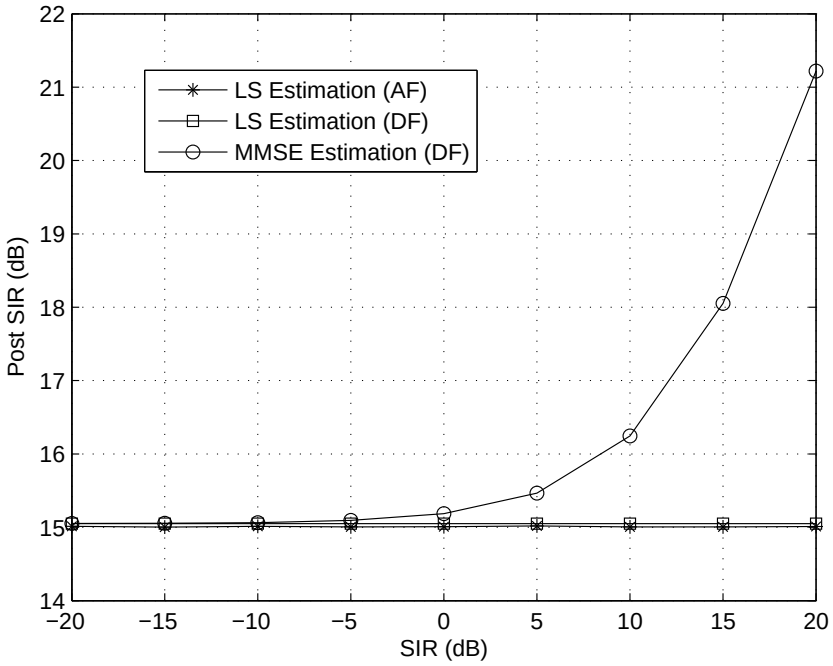

Figure 4.3. Post SIR versus original SIR when the 4-tap ($L = 4$) coupling channel is jointly estimated from 4 ($N = 4$) recently received OFDM symbols.

sampling intervals. While the proposed cross-talk canceller and its performance analysis throughout this chapter are applicable to any multi-input-multi-output coupling channel model, we assume in our simulation that the time-domain coupling channel has the same average power gain over L independent taps with the 2×2 coupling channel matrix over each tap consisting of independently and identically distributed complex Gaussian random variables. Such a coupling channel is jointly estimated from N recently received OFDM symbols during which the coupling channel remains unchanged. Similarly, the channel between the SS and the RS is also with Rayleigh fading and simulated as a 8-tap one. Without loss of generality, the received SNR at each antenna of the RS is fixed at 40 dB throughout the simulation.

Figure 4.3 shows the post SIR versus original SIR curves when $L = 4$ and $N = 4$. Both an AF-based RS and a DF-based RS are considered. For an AF-based RS, only the LS coupling channel estimation is applied and the post SIR after cross-talk cancellation

is obtained experimentally. For a DF-based RS, both the LS and the MMSE estimation are applied and their average post SIR's are calculated based on (4.38), (4.37), and (4.40). These numerically evaluated post SIR's perfectly match the simulated ones which are omitted in the figures to make them clear. Figure 4.3 indicates that, whether for an AF-based RS or a DF-based RS, the post SIR after cross-talk cancellation based on the LS coupling channel estimation does not vary with the original SIR level before cross-talk cancellation, which verifies the earlier analysis. Specifically, the post SIR is always about 15 dB for both the AF-based RS and the DF-based RS regardless of the original SIR level. In other words, when the original SIR is 0 dB, a 15 dB improvement gain is achieved by cross-talk cancellation; when the original SIR is -20 dB, a 35 dB improvement gain is achieved. However, the LS coupling channel estimation fails to obtain an SIR gain when the original SIR is greater than 15 dB. This is because that in high SIR region, the PNR is rather low for given L and N, and the LS estimation amplifies the noise and results in a bad coupling channel estimate. In practice, the original SIR before digital cross-talk cancellation is usually low and therefore the low-complexity LS coupling channel estimation is a feasible option. Furthermore, Figure 4.3 also indicates that the post SIR after cross-talk cancellation based on the MMSE coupling channel estimation at a DF-based RS increases with the original SIR level. It is observed that the MMSE estimation achieves a higher SIR gain than the LS estimation especially in high SIR region. In particular, when the original SIR is higher than 15 dB, the MMSE coupling channel estimation still achieves an SIR gain while the LS estimation can not.

Figure 4.4 shows the post SIR versus L curves at a DF-based RS when the original SIR is 0 dB and the coupling channel is jointly estimated from 4 and 8 ($N = 4$ and 8) recently received OFDM symbols. This figure verifies that the performance of cross-talk cancellation improves as the coupling channel turns more and more autocorrelated in the frequency-domain and in the time-domain. For example, as L decreases from 4 to 2 when $N = 4$, the SIR gain achieved by cross-talk cancellation increases from 15 dB to 18 dB; if

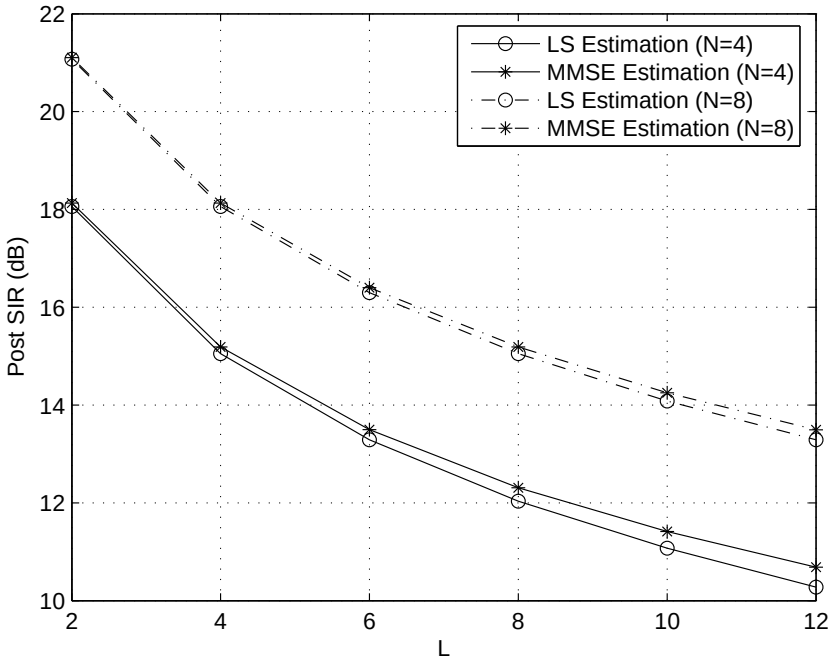

Figure 4.4. Post SIR versus the number of taps of the coupling channel (L) when SIR = 0 **dB.**

N increases from 4 to 8, the SIR gain further increases from 18 dB to 21 dB. Therefore, a higher SIR gain can be achieved by jointly estimating the coupling channel in more consecutive OFDM symbols if only the coupling channel remains unchanged during this period of time. Since no dedicated pilots are needed in the proposed scheme for coupling channel estimation, such joint estimation in consecutive OFDM symbols does not bring extra overhead.

Figure 4.5 shows the *symbol error rate* (SER) versus original SIR curves at a DF-based RS when $L = 4$ and $N = 4$. This figure verifies that the derived correlation matrix of the residual error vector after cross-talk cancellation can be utilized to further improve the detection of the desired signal at the RS. Both the ZF and the MMSE detection of the QPSK symbols based on perfect CSI from the SS to the RS are simulated at the RS and no error-correcting coding is applied. The correlation matrix of the residual error vector after cross-talk cancellation given in (4.37) or (4.38) is utilized for the MMSE detection. Figure 4.5 indicates that, whether the LS or the MMSE coupling channel estimation is

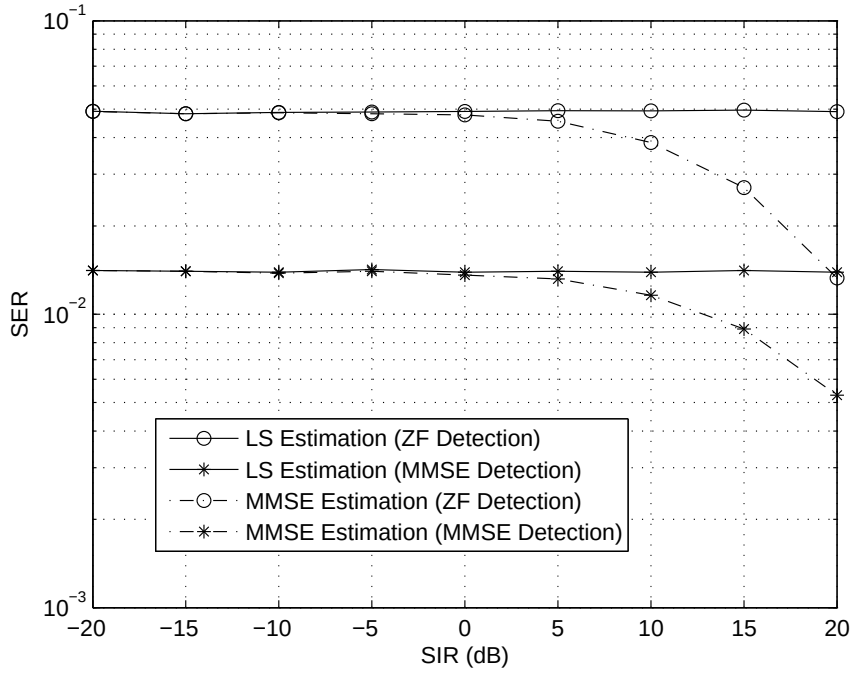

Figure 4.5. SER versus original SIR when the 4-tap ($L = 4$) coupling channel is jointly estimated from 4 ($N = 4$) recently received OFDM symbols.

applied, the MMSE detection based on the derived correlation matrix of the residual error achieves a significant performance gain over the ZF detection. For example, when the MMSE coupling channel estimation is applied, a performance gain of nearly 10 dB in terms of the original SIR is achieved when the SER is around 10^{-2}.

Finally we present a comparison between the proposed cross-talk cancellation scheme and the conventional low-power dedicated pilots assisted one at a DF-based RS. In the conventional scheme [15,21], the RS overlays its forwarded signals with specially designed pilots to help local coupling channel estimation. Since these dedicated pilots act like noise at the destination, they are of low power so as to guarantee an acceptable SNR level at the destination. Let the transmitted signal of the RS over each subcarrier be with unit average power; denote σ_p as the amplitude of each dedicated pilot, and then the *signal-to-pilot ratio* (SPR) is given by SPR $= \frac{1-\sigma_{\mathrm{p}}^2}{\sigma_{\mathrm{p}}^2}$. With the dedicated pilots, the composite received signal

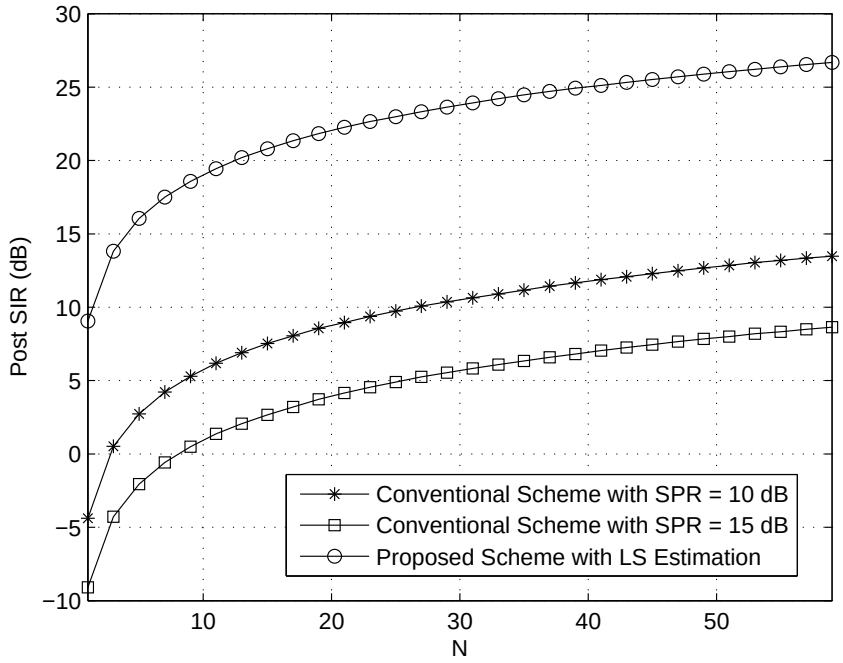

Figure 4.6. Comparison between the proposed cross-talk cancellation scheme and the conventional low-power dedicated pilots assisted one.

vector of the RS in the previous N OFDM symbols is given by

$$\mathbf{y}_N(n) = \hat{\mathbf{P}}_N(n)\,\mathbf{h}_c + \mathbf{i}_N(n) + \mathbf{s}_N(n) + \mathbf{w}_N(n), \tag{4.49}$$

where $\hat{\mathbf{P}}_N(n)$ denotes the dedicated pilot matrix and $\mathbf{i}_N(n) = \hat{\mathbf{X}}_N(n)\,\mathbf{h}_c$ denotes the cross-talk interference due to the forwarded signals of the RS. The dedicated pilot assisted coupling channel estimation treats $\mathbf{i}_N(n)$ as noise and gets the LS estimate of $\mathbf{h}_c$ as

$$\hat{\mathbf{h}}_{c,\mathrm{LS}}^{(\mathrm{P})}(n) = \left[\hat{\mathbf{P}}_N^H(n)\,\hat{\mathbf{P}}_N(n)\right]^{-1}\hat{\mathbf{P}}_N^H(n)\,\mathbf{y}_N(n), \tag{4.50}$$

based on which cross-talk cancellation can be performed accordingly. To optimize the estimation performance, the dedicated pilots are designed such that $\hat{\mathbf{P}}_N(n)$ has LM_rM_t orthogonal columns.

Figure 4.6 shows the post SIR versus N curves of the proposed cross-talk cancellation scheme and the conventional one at a DF-based RS when $L = 4$ and the original SIR is 0 dB. In the proposed scheme, the simple LS coupling channel estimation is applied. It

can be observed that to achieve a post SIR of 10 dB, the proposed scheme only needs one OFDM symbol while the conventional scheme with SPR = 10 dB needs 25 OFDM symbols. Moreover, when the SPR is 15 dB, the conventional scheme will take more than 70 OFDM symbols to achieve a post SIR of 10 dB. Compared to the conventional scheme, the proposed one is able to track the coupling channel more rapidly and achieves a much higher post SIR without causing any in-band interference at the DS.

4.5 Conclusion

In this chapter, we have proposed a new digital cross-talk canceller for a wireless CRRS. By utilizing the random forwarded signals of the RS as pilots for estimation of the coupling channel from the transmit to the receive antenna, the proposed scheme performs cross-talk reconstruction and cancellation without requiring the RS to transmit any dedicated pilots. Furthermore, joint estimation of the quasi-static coupling channel from multiple previously received OFDM symbols achieves an excellent estimation performance with low complexity. While the LS coupling channel estimation is applicable to a general RS with any relay mechanism, we further propose an MMSE coupling channel estimator for a DF-based RS when constant amplitude modulation is utilized, and derive the corresponding correlation matrix of the residual error vector after cross-talk cancellation, which can be utilized to further improve the desired signal detection at the RS. Both analytical and numerical results have demonstrated the excellent performance and various advantages of the proposed cross-talk canceller.

CHAPTER 5

ICI MITIGATION FOR OFDM-BASED WIRELESS RELAY ON HIGH-SPEED TRAINS

In the previous chapters, we have focused on advanced channel estimation and signal detection techniques for wireless relay to extend the communication coverage. In practice, wireless relay can also be utilized to shield a mobile terminal from adverse channel conditions over the direct link by transferring the burden of signal processing to the wireless relay. In this chapter, we are concerned with ICI mitigation at an OFDM-based wireless relay on a high-speed train when there exists a LOS propagation path between the BS and the train. With the burden of ICI mitigation transferred to the RS, mobile terminals on the train are shielded from the high Doppler frequency in the channel between the BS and the train. The proposed ICI mitigation schemes are based on the statistics of the wireless channel between the BS and the high-speed train, including the LOS factor, the Doppler frequency shift over the LOS path, and the Doppler spectrum over non-LOS paths. Specifically, we propose the Wiener filtering in the downlink transmission to maximize the post *signal-to-interference-plus-noise ratio* (SINR) by utilizing the correlation in and between the desired signals and the aggregate ICI over OFDM subchannels. In the uplink transmission, we further propose to preprocess the transmitted OFDM symbol to maximize the post SIR at the BS. Without the need for dedicated pilots, the proposed schemes do not sacrifice spectral efficiency and effectively mitigate ICI even in the presence of significant uncertainties in the channel statistics.

The remainder of this chapter is organized as follows. In Section 5.1, we describe the channel model and ICI in high-mobility OFDM. Then we develop the Wiener filtering in the downlink and the transmit preprocessing in the uplink for ICI mitigation in Sections 5.2 and 5.3, respectively. Finally Section 5.4 concludes this chapter.

5.1 System Model

In this chapter, we deal with ICI mitigation at an RS on a high-speed train. Such an RS forwards signals from the BS to mobile users on the train or vice versa to improve the QoS provided to passengers. While the involved relay mechanism is out of the scope of this chapter, we focus on ICI mitigation at the RS which is regarded as an ordinary OFDM transceiver throughout this chapter.

5.1.1 Channel Model

Since the high-speed train is traveling in the rural area most of the time and the antenna of the RS is located on top of the train, we assume there exists a LOS path between the BS and the RS in this chapter. Denote θ as the *angle of arrival* (AoA) of the LOS path, and then the baseband channel over the LOS path is [99]

$$h_{los}(t) = \alpha_{los} e^{j(2\pi f_D \cos(\theta) t + \varphi_0)}, \tag{5.1}$$

where α_{los} is the channel amplitude determined by path loss, φ_0 is the initial phase, and $f_D = \frac{v f_c}{c}$ is the maximum Doppler frequency with v the speed of the train, f_c the carrier frequency, and c the speed of light. Throughout this chapter, we denote $f_d = f_D \cos(\theta)$ as the *Doppler frequency shift* (DFS) over the LOS path and assume that it can be obtained at the RS based on the current speed and position of the train relative to the BS since these information is usually available on the high-speed train.

Consider an N-subcarrier OFDM modulation with the sampling interval T_s and the subcarrier spacing $\frac{N}{T_s}$. Assume that the maximum delay of the multipath channel relative to the LOS path is $(L-1)T_s$. Without loss of generality, we model the time-domain channel as an L-tap one with the first one corresponding to the LOS path and the rest $L-1$ ones non-LOS paths. Denote $h_{l,n}$ as the discrete-time channel over the lth path in the nth sampling interval, and then it can be obtained from (5.1) that

$$h_{0,n} = h_0 e^{j2\pi f_d n T_s}, \quad 0 \le n \le N-1, \tag{5.2}$$

where $h_0 = \alpha_{los} e^{j\varphi_0}$ and the power gain over the LOS path is given by $\xi_0 = |h_0|^2$. While the channel over the LOS path varies with time in a deterministic way for a given DFS, the channels over the non-LOS paths vary with time randomly with the correlation functions given by

$$r_l(m) = E\left\{h_{l,n+m} h_{l,n}^*\right\} = \xi_l \phi(mT_s), \quad 1 \le l \le L-1, \tag{5.3}$$

where ξ_l denotes the average power gain over the lth path and $\phi(\cdot)$ denotes the normalized correlation function of the time-varying channel with $\phi(0) = 1$. For the classical Doppler spectrum (Jakes' model) [99], $\phi(\tau) = J_0(2\pi f_D \tau)$ where $J_0(\cdot)$ denotes the zeroth-order Bessel function of the first kind. Without loss of generality, we assume that the average power gain of the multipath channel is unit throughout this chapter. Thus $\sum_{l=1}^{L-1} \xi_l = 1 - \xi_0$ and the LOS factor of the channel is defined as $K = 10\log_{10}\left(\frac{\xi_0}{1-\xi_0}\right)$. While the estimation of the LOS factor has been investigated in [100, 101] and the references therein, we assume that an estimate of K is available for statistics-based ICI mitigation.

5.1.2 ICI in High-Mobility OFDM

Denote X_k as the transmitted signal over the kth OFDM subchannel, and then the time-domain transmitted signal can be obtained as,

$$x_n = \frac{1}{\sqrt{N}} \sum_{k=0}^{N-1} X_k e^{j\frac{2\pi nk}{N}}, \quad -G \le n \le N-1, \tag{5.4}$$

where G denotes the length of cyclic prefix. Assume $G \ge L-1$ so that *intersymbol interference* (ISI) is avoided, and then the time-domain received signal can be obtained as

$$y_n = \sum_{l=0}^{L-1} h_{l,n} x_{n-l} + w_n, \quad 0 \le n \le N-1, \tag{5.5}$$

where w_n is the additive white Gaussian noise. According to (5.4) and (5.5), the corresponding frequency-domain received signal over the mth subchannel can be obtained as

$$\begin{aligned} Y_m &= \frac{1}{\sqrt{N}} \sum_{n=0}^{N-1} y_n e^{-j\frac{2\pi mn}{N}} \\ &= G(m,m) X_m + \sum_{k=0, k\ne m}^{N-1} G(m,k) X_k + W_m, \quad 0 \le m \le N-1, \end{aligned} \tag{5.6}$$

where W_k denotes the corresponding frequency-domain white noise and $G(m,k)$ denotes the channel gain from the kth to the mth subchannel given by

$$G(m,k) = \sum_{l=0}^{L-1} \frac{e^{-j\frac{2\pi kl}{N}}}{N} \sum_{n=0}^{N-1} h_{l,n} e^{-j\frac{2\pi(m-k)n}{N}}, \tag{5.7}$$

which indicates that when $m \neq k$, $G(m,k) = 0$ only if $h_{l,n} = h_l, 0 \leq n \leq N-1$, i.e., the variation of the wireless channel within an OFDM symbol causes ICI.

5.2 Wiener Filtering in the Downlink Transmission for ICI Mitigation

In this section, we develop the Wiener filtering at the RS for ICI mitigation in the downlink transmission from the BS to the high-speed train. Without the need for dedicated pilots, such a blind ICI mitigation scheme is performed before channel estimation based on the statistics of the wireless channel, including the LOS factor, the DFS over the LOS path, and the Doppler spectrum over the non-LOS paths.

According to (5.6), the frequency-domain received signal over the mth subchannel can be rewritten as

$$Y_m = S_m + I_m + W_m, \quad 0 \leq m \leq N-1, \tag{5.8}$$

where $S_m = G(m,m) X_m$ and $I_m = \sum_{k=0,k\neq m}^{N-1} G(m,k) X_k$ denote the desired signal from the mth subchannel and the aggregate ICI from the rest $N-1$ ones, respectively. Further define $\mathbf{s} = (S_0, S_1, \cdots, S_{N-1})^T$ and $\mathbf{i} = (I_0, I_1, \cdots, I_{N-1})^T$ as the desired signal and the aggregate ICI vectors in the current OFDM symbol, respectively, and then the received signal vector can be expressed as

$$\mathbf{y} = (Y_0, Y_1, \cdots, Y_{N-1})^T = \mathbf{s} + \mathbf{i} + \mathbf{w}, \tag{5.9}$$

where $\mathbf{w}$ denotes the white noise vector. The objective of the Wiener filtering is to estimate $\mathbf{s}$ from $\mathbf{y}$ with the minimum MSE by utilizing the correlation in and between the desired signal and the aggregate ICI vectors. To that end, we will first perform correlation analysis in the following.

5.2.1 Correlation Analysis

Throughout this chapter, we assume that the transmitted signals over different subchannels, X_k's, are independent with zero mean and unit variance and the channels over different paths are independent, and then, based on the channel model described in Section 5.1.1, the correlation among the desired signals can be obtained as

$$\begin{aligned} E\left\{S_{m_1}S_{m_2}^*\right\} &= E\left\{G\left(m_1,m_1\right)G^*\left(m_2,m_2\right)\right\}E\left\{X_{m_1}X_{m_2}^*\right\} \\ &= P_S\delta\left(m_1-m_2\right), \end{aligned} \tag{5.10}$$

where $E\{\cdot\}$ denotes expectation with respect to the transmitted signals and/or the random channel, $\delta(\cdot)$ denotes the Kronecker delta function, and

$$P_S = E\left\{\left|G\left(m,m\right)\right|^2\right\} = \frac{1}{N^2}\sum_{n_1=0}^{N-1}\sum_{n_2=0}^{N-1}\psi\left(n_1-n_2\right) \tag{5.11}$$

denotes the average desired signal power over each subchannel with

$$\psi\left(n_1-n_2\right) = \xi_0 e^{j2\pi f_d(n_1-n_2)T_s} + \left(1-\xi_0\right)\phi\left(\left(n_1-n_2\right)T_s\right). \tag{5.12}$$

On the other hand, the correlation among the aggregate ICI can be obtained as

$$\begin{aligned} E\left\{I_{m_1}I_{m_2}^*\right\} &= \sum_{k_1=0,k_1\neq m_1}^{N-1}\sum_{k_2=0,k_2\neq m_2}^{N-1} E\left\{G\left(m_1,k_1\right)G^*\left(m_2,k_2\right)\right\}E\left\{X_{k_1}X_{k_2}^*\right\} \\ &= \sum_{k=0,k\neq m_1,m_2}^{N-1} E\left\{G\left(m_1,k\right)G^*\left(m_2,k\right)\right\}. \end{aligned} \tag{5.13}$$

Based on (6.7), it can be shown that

$$\begin{aligned} \sum_{k=0}^{N-1} E\left\{G\left(m_1,k\right)G^*\left(m_2,k\right)\right\} &= \sum_{k=0}^{N-1}\frac{1}{N^2}\sum_{n_1=0}^{N-1}\sum_{n_2=0}^{N-1} e^{-j\frac{2\pi}{N}\left[\left(m_1-k\right)n_1-\left(m_2-k\right)n_2\right]}\psi\left(n_1-n_2\right) \\ &= \frac{1}{N^2}\sum_{n_1=0}^{N-1}\sum_{n_2=0}^{N-1}\psi\left(n_1-n_2\right)e^{-j\frac{2\pi}{N}\left(m_1n_1-m_2n_2\right)}\sum_{k=0}^{N-1} e^{-j\frac{2\pi}{N}\left(n_2-n_1\right)k} \\ &= \frac{1}{N}\sum_{n=0}^{N-1} e^{-j\frac{2\pi}{N}\left(m_1-m_2\right)n} \\ &= \delta\left(m_1-m_2\right). \end{aligned} \tag{5.14}$$

Thus, from (5.13) and (5.14), we obtain

$$E\left\{I_{m_1}I_{m_2}^*\right\} = \begin{cases} 1-P_S, & m_1 = m_2 = m \\ -\frac{1}{N^2}\sum\limits_{n_1=0}^{N-1}\sum\limits_{n_2=0}^{N-1}\left[e^{-j\frac{2\pi(m_1-m_2)n_1}{N}} + e^{-j\frac{2\pi(m_1-m_2)n_2}{N}}\right]\psi(n_1-n_2), & m_1 \neq m_2 \end{cases} \tag{5.15}$$

Furthermore, the cross correlation between the desired signal and the aggregate ICI can be obtained as

$$\begin{aligned} E\left\{S_{m_1}I_{m_2}^*\right\} &= \sum_{k=0,k\neq m_2}^{N-1} E\left\{G(m_1,m_1)G^*(m_2,k)\right\}E\left\{X_{m_1}X_k^*\right\} \\ &= \begin{cases} 0, & m_1 = m_2 \\ E\left\{G(m_1,m_1)G^*(m_2,m_1)\right\}, & m_1 \neq m_2 \end{cases} \\ &= \begin{cases} 0, & m_1 = m_2 \\ \frac{1}{N^2}\sum\limits_{n_1=0}^{N-1}\sum\limits_{n_2=0}^{N-1} e^{-j\frac{2\pi(m_1-m_2)n_2}{N}}\psi(n_1-n_2), & m_1 \neq m_2 \end{cases} \end{aligned} \tag{5.16}$$

Define $\mathbf{R_s} = E\left\{\mathbf{ss}^H\right\}$, $\mathbf{R_i} = E\left\{\mathbf{ii}^H\right\}$, and $\mathbf{R_{si}} = E\left\{\mathbf{si}^H\right\}$, and then they can be obtained from (5.10), (5.15), and (5.16), respectively, and utilized to perform the Wiener filtering in the downlink transmission for ICI mitigation.

5.2.2 Wiener Filtering

The proposed Wiener filtering minimizes the MSE of the desired signal vector estimate, $\hat{\mathbf{s}}$, which is given by [92] $\hat{\mathbf{s}} = \mathbf{R_{sy}}\mathbf{R_y}^{-1}\mathbf{y}$, where

$$\mathbf{R_{sy}} = E\left\{\mathbf{sy}^H\right\} = \mathbf{R_s} + \mathbf{R_{si}}, \tag{5.17}$$

$$\mathbf{R_y} = E\left\{\mathbf{yy}^H\right\} = \mathbf{R_s} + \mathbf{R_i} + \mathbf{R_{si}} + \mathbf{R_{si}}^H + \mathbf{R_w}, \tag{5.18}$$

and $\mathbf{R_w} = E\left\{\mathbf{ww}^H\right\} = \sigma_n^2\mathbf{I}$ with σ_n^2 the white noise power and $\mathbf{I}$ the $N \times N$ identity matrix. The corresponding MSE matrix is given by [92]

$$\mathbf{R_e} = E\left\{(\mathbf{s}-\hat{\mathbf{s}})(\mathbf{s}-\hat{\mathbf{s}})^H\right\} = \mathbf{R_s} - \mathbf{R_{sy}}\mathbf{R_y}^{-1}\mathbf{R_{sy}}^H. \tag{5.19}$$

Thus the post SINR after the Wiener filtering is given by $\text{SINR}_{\text{Post}} = \frac{\text{tr}\{\mathbf{R_s}\}}{\text{tr}\{\mathbf{R_e}\}}$, where $\text{tr}\{\cdot\}$ denotes the trace operator. In contrast, the original SINR before the Wiener filtering is given by $\text{SINR} = \frac{P_S}{1-P_S+\sigma_n^2}$.

5.2.3 Numerical Results

In this subsection, we present numerical results to demonstrate the SINR gain of the Wiener filtering. A 32-subcarrier ($N = 32$) OFDM transmission system is considered. Since the BS dedicated for high-speed trains is deployed along the railway, the AoA of the LOS path is usually close to 0 or π. Without loss of generality, we let $\theta = 0$ and define $F_d = NT_s f_d$ as the normalized DFS over the LOS path. Furthermore, we assume the classical Jakes' Doppler spectrum [99] over non-LOS paths. Focusing on ICI mitigation, we let $\sigma_n^2 = 0$ and thus the SINR reduces to the SIR floor. Besides the ideal Wiener filter, nonideal one based on inaccurate channel statistics is also considered to investigate the robustness of the Wiener filtering to uncertainties in the channel statistics. Two types of uncertainties are jointly considered here: the first one is inaccurate normalized DFS with a 30% uncertainty, corresponding to that the estimated normalized DFS, $F_{d,e}$, is a random variable uniformly distributed between $0.7F_d$ and $1.3F_d$; the second one is inaccurate LOS factor with a 6 dB uncertainty, corresponding to that the estimated LOS factor, K_e, is a random variable uniformly distributed between $K - 6$ and $K + 6$.

Figure 5.1(a) shows the SIR gain versus the LOS factor (K) when $F_d = 0.2$; Figure 5.1(b) shows the SIR gain versus F_d when $K = 6$ dB. We observe from Figure 5.1(a) that the SIR gain increases with K, which is reasonable since as K increases, the weight of the deterministic LOS path increases, the overall channel turns less random, the desired signals and the aggregate ICI are more correlated, and therefore the effect of ICI mitigation by the Winner filtering gets enhanced. Furthermore, it is also observed that the SIR gain increases slowly with the normalized DFS. Figures 5.1(a) and 5.1(b) demonstrate that the Wiener filtering significantly mitigates the ICI especially in the presence of a strong LOS path and a high normalized DFS. The two figures also indicate that the nonideal Wiener filter with significant uncertainties in the channel statistics still achieves similar SIR gains as the ideal one, which demonstrates the robustness of the proposed Wiener filtering.

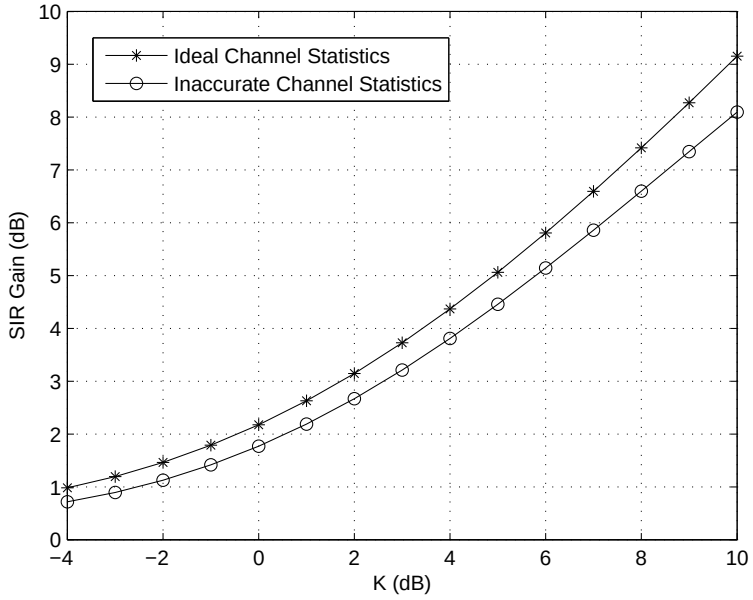

(a) SIR gain versus the LOS factor (K) when $F_d = 0.2$

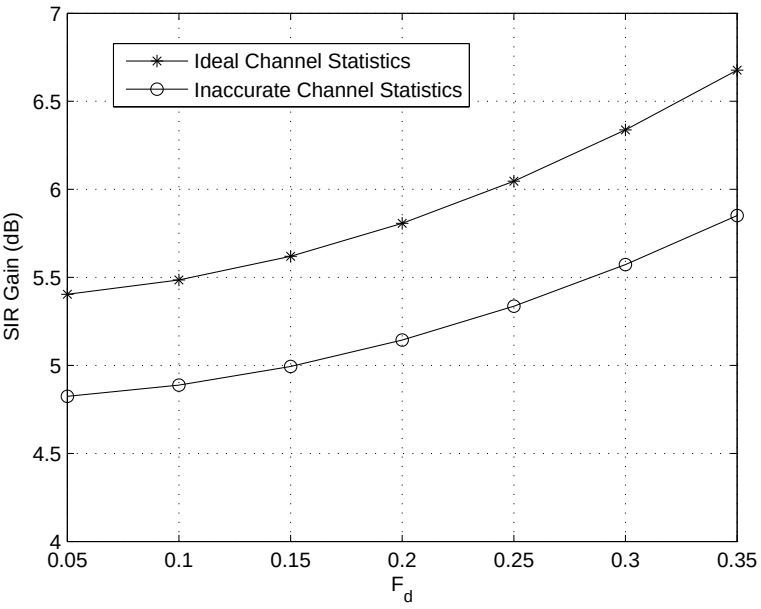

(b) SIR gain versus the normalized DFS (F_d) when $K = 6$ dB

Figure 5.1. SIR gain of the Wiener filtering

5.3 Transmit Preprocessing in the Uplink Transmission for ICI Mitigation

In Section 5.2, we have developed statistics-based Wiener filtering for ICI mitigation, which is suitable for the downlink transmission from the BS to the high-speed train since the DFS over the LOS path can be figured out locally at the RS based on the current speed and position of the train. However, obtaining this information at the BS is difficult. As a result, the Wiener filtering cannot be conveniently applied at the BS in the uplink transmission. Considering this, we further develop the transmit preprocessing in this section, which can be applied at the RS for ICI mitigation in the uplink transmission.

5.3.1 Principle of Transmit Preprocessing

Denote $\mathbf{x} = (X_0, X_1, \cdots, X_{N-1})^T$ as the frequency-domain transmitted signal vector, and then, based on (5.6), the received signal vector can be rewritten as

$$\mathbf{y} = \mathbf{G}\mathbf{x} + \mathbf{w}, \tag{5.20}$$

where $\mathbf{G}$ denotes the CFR matrix whose elements are defined in (6.7). With the transmit preprocessing, the actual frequency-domain transmitted signal vector is $\mathbf{z} = \mathbf{V}\mathbf{x}$ where $\mathbf{V}$ denotes the $N \times N$ transmit preprocessing matrix. Thus the corresponding received signal vector is given by

$$\mathbf{y} = \mathbf{G}\mathbf{z} + \mathbf{w} = \mathbf{H}\mathbf{x} + \mathbf{w}, \tag{5.21}$$

where $\mathbf{H} = \mathbf{G}\mathbf{V}$ denotes the equivalent CFR matrix after the transmit preprocessing. Denote $P(i, j) = E\left\{|H(i, j)|^2\right\}$; since the transmitted signals over different subchannels, X_k's, are independent with zero mean and unit variance, the post SIR over the ith subchannel after the transmit preprocessing can be obtained as

$$\mathrm{SIR}_{\mathrm{post}}^{(i)} = \frac{P(i, i)}{\sum\limits_{j=0, j\neq i}^{N-1} P(i, j)}. \tag{5.22}$$

Thus the objective of the transmit preprocessing is to design the preprocessing matrix, $\mathbf{V}$, based on the statistics of the wireless channel such that the post SIR is maximized.

5.3.2 Optimal Transmit Preprocessing

Because of the circular and symmetric structure of the OFDM modulation, it is expected that, with the optimal transmit preprocessing, the average power gain from the jth to the ith subchannel only depends on the distance between the two involved subcarriers, i.e., $P(i,j) = p\left((i-j)_N\right)$, where $(\cdot)_N$ denotes N modular and $p(\cdot)$ denotes a one-dimensional function, and all of the subchannels have the same post SIR given by

$$\mathrm{SIR}_{\mathrm{post}} = \frac{p(0)}{\sum_{n=1}^{N-1} p(n)}. \tag{5.23}$$

Since $\mathbf{H} = \mathbf{GV}$, it can be shown from (6.7) that

$$\begin{aligned} P(i,j) &= \sum_{k_1=0}^{N-1}\sum_{k_2=0}^{N-1} E\left\{G(i,k_1)G^*(i,k_2)\right\} V(k_1,j)V^*(k_2,j) \\ &= \sum_{k_1=0}^{N-1}\sum_{k_2=0}^{N-1} f\left((k_1-i)_N,(k_2-i)_N\right) V(k_1,j)V^*(k_2,j), \end{aligned} \tag{5.24}$$

where

$$f(c_1,c_2) = \frac{1}{N^2}\sum_{n_1=0}^{N-1}\sum_{n_2=0}^{N-1} e^{j\frac{2\pi}{N}(c_1n_1-c_2n_2)}\Upsilon(n_1-n_2,c_2-c_1), \tag{5.25}$$

with

$$\Upsilon(n,c) = \xi_0 e^{j2\pi f_d nT_s} + \phi(nT_s)\sum_{l=1}^{L-1}\xi_l e^{j\frac{2\pi cl}{N}}. \tag{5.26}$$

Based on (5.24), it can be shown that when

$$V(k_1,j)V^*(k_2,j) = g\left((k_1-j)_N,(k_2-j)_N\right), \tag{5.27}$$

where $g(\cdot,\cdot)$ denotes an arbitrary two-dimensional function, $P(i,j) = p\left((i-j)_N\right)$ holds. In light of this, we let $\mathbf{V}$ be a circulant matrix constructed from Vector $\mathbf{v} = (v_0, v_1, \cdots, v_{N-1})^T$ with $\sum_{i=0}^{N-1}|v_i|^2 = 1$, i.e.,

$$V(i,j) = v_{(i-j)_N}, 0 \le i,j \le N-1. \tag{5.28}$$

Since such a circular frequency-domain transmit preprocessing matrix corresponds to a time-domain window, it is of low-complexity. While receive time-domain windowing has been proposed for ICI mitigation in [87], we are concerned with a different scenario in this

chapter and focus on the transmit preprocessing, which, as analyzed above, is equivalent to transmit time-domain windowing.

For an arbitrary circular transmit preprocessing matrix constructed from $\mathbf{v}$, all of the subchannels have the same overall average received signal power given by

$$\begin{aligned} P_o = \sum_{n=0}^{N-1} p(n) &= \sum_{j=0}^{N-1} P_{0j} \\ &= \sum_{j=0}^{N-1} \sum_{k_1=0}^{N-1} \sum_{k_2=0}^{N-1} f(k_1, k_2)\, v_{(k_1-j)_N} v^*_{(k_2-j)_N} \\ &= \sum_{\Delta=0}^{N-1} h(\Delta) \sum_{k_2=0}^{N-1} f((k_2+\Delta)_N, k_2), \end{aligned} \tag{5.29}$$

where

$$h(\Delta) = \sum_{j=0}^{N-1} v_{(k_2+\Delta-j)_N} v^*_{(k_2-j)_N}. \tag{5.30}$$

Substitute (5.25) in (5.29), and then we obtain

$$\begin{aligned} P_o &= \frac{1}{N^2} \sum_{\Delta=0}^{N-1} h(\Delta) \sum_{n_1=0}^{N-1} \sum_{n_2=0}^{N-1} e^{j\frac{2\pi n_1 \Delta}{N}} \Upsilon(n_1 - n_2, -\Delta) \sum_{k_2=0}^{N-1} e^{j\frac{2\pi(n_1-n_2)k_2}{N}} \\ &= \frac{1}{N} \sum_{\Delta=0}^{N-1} h(\Delta) \left(\xi_0 + \sum_{l=1}^{l-1} \xi_l e^{-j\frac{2\pi\Delta l}{N}} \right) \sum_{n=0}^{N-1} e^{j\frac{2\pi n\Delta}{N}} \\ &= h(0) \left(\xi_0 + \sum_{l=1}^{l-1} \xi_l \right) \\ &= 1. \end{aligned} \tag{5.31}$$

On the other hand, all of the subchannels have the same desired signal power which varies with $\mathbf{v}$ and is given by

$$P_d = P(0,0) = \sum_{k_1=0}^{N-1} \sum_{k_2=0}^{N-1} v_{k_1} f(k_1, k_2)\, v^*_{k_2} = \mathbf{v}^T \mathbf{F} \mathbf{v}^*, \tag{5.32}$$

where $\mathbf{F}$ denotes an $N \times N$ matrix consisting of $f(k_1, k_2)$'s. Based on (5.31) and (5.32), the post SIR over each subchannel after the transmit preprocessing can be expressed as

$$\mathrm{SIR}_{\mathrm{post}} = \frac{P_d}{P_o - P_d} = \frac{\mathbf{v}^T \mathbf{F} \mathbf{v}^*}{1 - \mathbf{v}^T \mathbf{F} \mathbf{v}^*}. \tag{5.33}$$

Therefore, the optimal $\mathbf{v}$ can be obtained by maximizing $\mathbf{v}^T\mathbf{F}\mathbf{v}^*$ subject to $\|\mathbf{v}\|^2 = 1$. Since Equation (5.32) verifies that $\mathbf{F}$ is a semi-positive definite matrix, all of its eigenvalues are real and non-negative. Consequently, the optimal $\mathbf{v}$ maximizing the post SIR is the conjugate of the eigenvector of $\mathbf{F}$ associated with its largest eigenvalue, $\lambda_{\max}(\mathbf{F})$, and the corresponding maximum post SIR is given by

$$\mathrm{SIR}_{\mathrm{post}}^{(\max)} = \frac{\lambda_{\max}(\mathbf{F})}{1 - \lambda_{\max}(\mathbf{F})}. \tag{5.34}$$

In contrast, the original SIR over each subchannel before the transmit preprocessing is given by $\mathrm{SIR} = \frac{f(0,0)}{1-f(0,0)}$.

5.3.3 Numerical and Simulation Results

In this subsection, we present numerical and simulation results to demonstrate the performance of the transmit preprocessing. The simulation scenario described in Section 5.2.3 is considered again. Furthermore, we let $L = 4$ and the average power gains over the non-LOS paths decay with delay exponentially with the exponent factor $\beta = 0.5$. Since the transmit preprocessing also requires the power delay profile of the multipath channel, we further consider the third type of uncertainty in the channel statistics, which is inaccurate exponent factor with a 100% uncertainty, i.e., the estimated exponent factor, β_e, is a random variable uniformly distributed between 0 and 2β. This uncertainty, together with the other two in the normalized DFS and the LOS factor described in Section 5.2.3, are jointly considered to investigate the robustness of the transmit preprocessing to the uncertainties in the channel statistics.

Figure 5.2(a) shows the SIR gain versus the LOS factor (K) when the normalized DFS (F_d) is 0.2; Figure 5.2(b) shows the SIR gain versus F_d when $K = 6$ dB. Comparison between Figures 5.1 and 5.2 indicates that the transmit preprocessing behaves similarly to the Wiener filtering although they are based on different design criteria. Specifically, the transmit preprocessing effectively mitigates the ICI especially in high K and F_d regions. Similar to the Wiener filtering, the transmit preprocessing also exhibits robustness to uncertainties

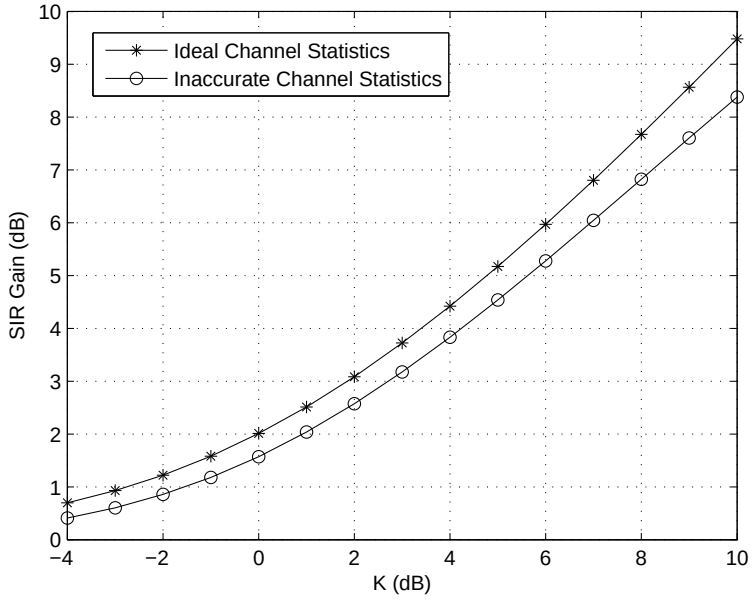

(a) SIR gain versus the LOS factor (K) when $F_d = 0.2$

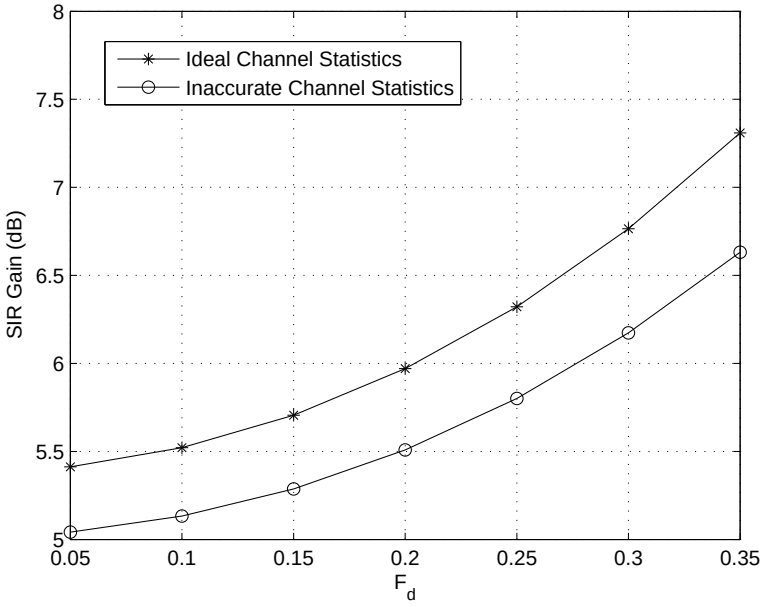

(b) SIR gain versus the normalized DFS (F_d) when $K = 6$ dB

Figure 5.2. SIR gain of the transmit preprocessing

in the channel statistics.

While the Wiener filtering and the transmit preprocessing have different design criteria and are implemented in the downlink and the uplink transmissions, respectively, both of them are based on the statistics of the wireless channel. Therefore, it is interesting to compare the performance of them. Figure 5.3(a) shows the BER versus K when $F_d = 0.2$;Figure 5.3(b) shows the BER versus F_d when $K = 8$ dB; Figure 5.4 shows the BER versus SNR when $F_d = 0.2$ and $K = 8$ dB. To avoid channel estimation, frequency-domain differential QPSK modulation is applied over OFDM subchannels and the conventional differential demodulation is employed without error-correcting coding. In Figure 5.3, we let $\sigma_n^2 = 0$ and thus the plotted BER corresponds to the BER floor caused by the residual ICI. For comparison, the BER curve of the conventional OFDM transmission without ICI mitigation is also plotted. Furthermore, the abovementioned three types of uncertainties in the channel statistics are also simulated to investigate the robustness of the Wiener filtering and the transmit preprocessing in the BER performance.

Figures 5.3 and 5.4 indicate that the Wiener filtering and the transmit preprocessing achieve almost the same BER performance. Figure 5.3(a) shows that both schemes achieve a larger and larger performance improvement as the LOS factor (K) increases gradually. As analyzed, when K increases, the effect of ICI mitigation gets enhanced and therefore the BER performance gets improved. From Figure 5.3(b), we observe that the performance improvement of the two ICI mitigation schemes also increases with the normalized DFS. Furthermore, it is also observed from Figure 5.4 that both schemes achieve a considerable performance improvement even before the BER floor occurs. The three figures verify that both the Wiener filtering and the transmit processing effectively lower the BER floor especially in the presence of a strong LOS path and a high Doppler frequency. However, we notice that the BER performance gains of both schemes are not as significant as their SIR gains. Essentially, this reflects the difference in the SIR, which depends only on the second-order statistics of the interference, and the BER, which depends on the complete

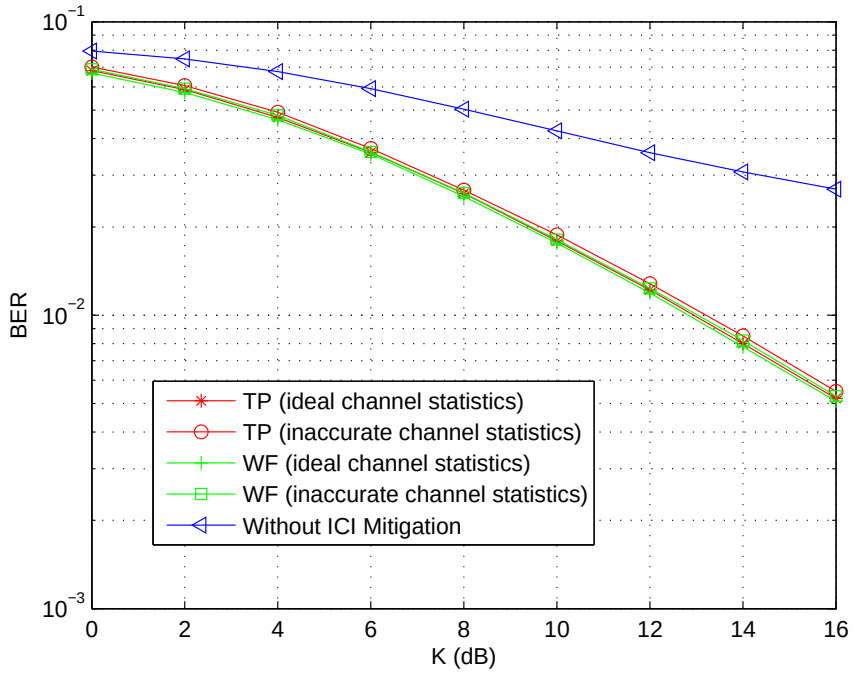

(a) BER versus the LOS factor (K) when $F_d = 0.2$

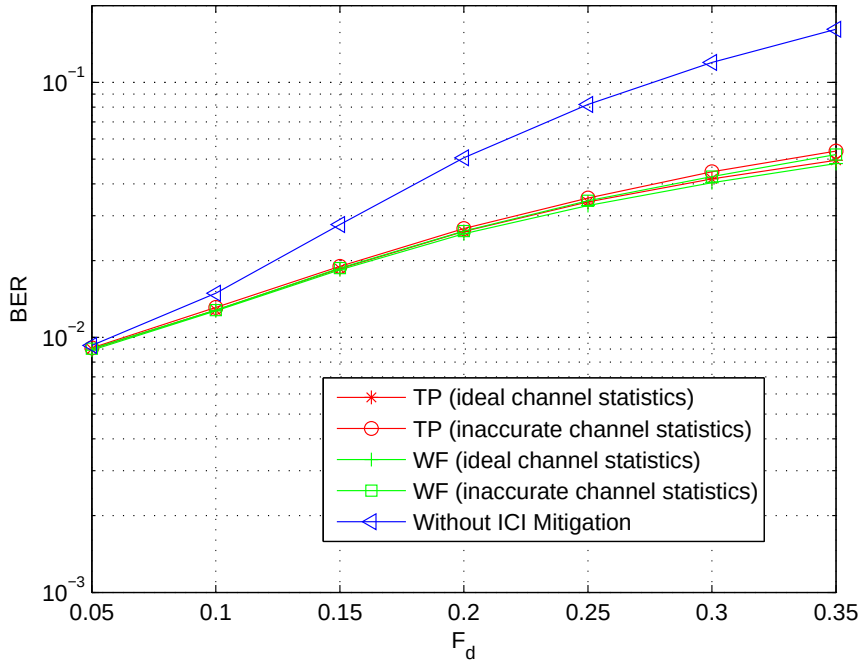

(b) BER versus the normalized DFS (F_d) when $K = 8$ dB

Figure 5.3. BER curves of the Wiener filtering (WF) and the transmit preprocessing (TP)

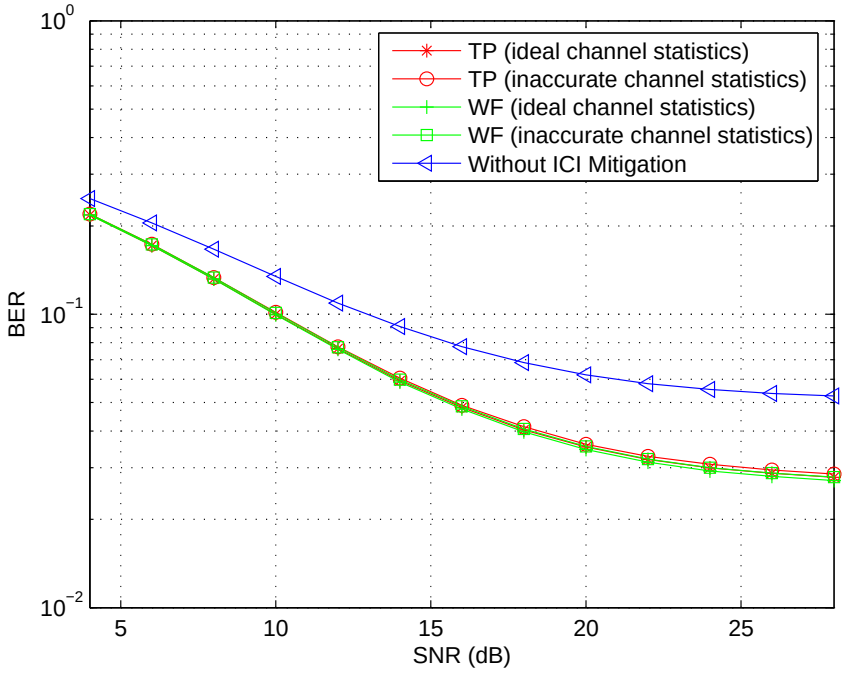

Figure 5.4. BER versus SNR when $K = 8$ dB and $F_d = 0.2$

statistical distribution of the interference. Last but not least, Figures 5.3 and 5.4 indicate that significant uncertainties in the channel statistics only cause negligible BER performance degradation, which verifies the robustness of the two statistics-based ICI mitigation schemes.

5.4 Conclusion

In this chapter, we have developed the Wiener filtering in the downlink and the transmit preprocessing in the uplink for ICI mitigation at an OFDM-based RS to improve QoS on a high-speed train. Without the need for dedicated pilots, the two schemes are based on the statistics of the wireless channel between the BS and the train. Numerical and simulation results have demonstrated that the proposed schemes effectively mitigate the ICI and lower the error floor even in the presence of significant uncertainties in the channel statistics.

CHAPTER 6

REDUCED-RATE OFDM TRANSMISSION FOR HIGH-MOBILITY WIRELESS RELAY

In Chapter 5, we have proposed statistics-based ICI mitigation for OFDM-based wireless relay on high-speed trains. In contrast with the pilot-assisted ICI cancellation schemes in literature [72,73,74,78], the proposed algorithms do not require any dedicated pilots and reduce ICI by taking advantages of the strong correlation in and between the desired signal and the ICI when there exists a LOS path between the BS and the train. However, like other pilot-free full-rate ICI mitigation schemes in literature [82, 83, 84], it only has limited ICI mitigation capabilities and still suffers considerable residual ICI, especially in the absence of a LOS path between the BS and the train.

To solve this problem, we extend the existing work in ICI self-cancellation [88,90] and develop a general reduced-rate OFDM transmission scheme with inherent ICI mitigation capabilities for OFDM-based wireless relay on high-speed trains. The proposed scheme in this chapter reduces ICI dramatically even in the absence of a LOS path. With transmit and receive preprocessing, the original N-subcarrier OFDM system is transformed into an equivalent K-subcarrier one with a general *rate reduction factor* (RRF) $\frac{N}{K}$. By reducing the transmission rate, we are able to design the transmitted signal structure with inherent ICI mitigation capability. Since the equivalent K-subcarrier OFDM system has significantly reduced ICI, no further processing is required for ICI mitigation at the receiver. Without requiring the instantaneous CSI, we develop a general structure of transmit and receive preprocessing matrices to ensure that all K subchannels in the equivalent OFDM system share a common average SIR. Given the developed structure, we further optimize the transmit and the receive preprocessing coefficients based on the channel statistics so as to maximize the SIR in the equivalent OFDM system. Numerical and simulation results demonstrate

that, for both integer and fractional RRFs, the proposed reduced-rate OFDM transmission achieves significant performance improvements over the existing ICI self-cancellation schemes even in the presence of significant uncertainties in the channel statistics.

The remainder of this chapter is organized as follows. In Section 6.1, we describe the channel model and ICI in high-mobility OFDM. Then we present the principle of reduced-rate OFDM transmission in Section 6.2 and design the transmit and the receive preprocessing matrices in Section 6.3, respectively. Numerical and simulation results are presented in Section 6.4. Finally Section 6.5 concludes this chapter.

6.1 High-Mobility OFDM

In this chapter, we deal with ICI mitigation in a high-mobility OFDM transmission system where ICI is caused by the time-domain variation of the wireless channel within an OFDM symbol. To illustrate ICI in high-mobility OFDM, we will first describe the channel model.

6.1.1 Channel Model

Consider an N-subcarrier OFDM modulation with the sampling interval T_s and the subcarrier spacing $\frac{1}{T_s N}$. Assume that the maximum delay of the multipath channel is $(L-1)T_s$. Without loss of generality, we model the discrete-time multipath channel as an L-tap one with each tap representing one path. In contrast with Chapter 5 where we focused on a LOS channel between the BS and the high-speed train, we assume random channels over L non-LOS paths throughout this chapter. Denote $h_{l,n}$ as the channel gain over the lth path in the nth sampling interval. In a high-mobility environment, $h_{l,n}$ varies with n randomly with the time-domain correlation functions given by

$$r_l(m) = E\left\{h_{l,n+m}h_{l,n}^*\right\} = \xi_l \phi(mT_s), \quad 0 \le l \le L-1, \tag{6.1}$$

where ξ_l denotes the average power over the lth path and $\phi(\cdot)$ denotes the normalized correlation function of the time-varying channel with $\phi(0) = 1$. For the classical Doppler

power spectrum (Jakes' model) [99], $\phi(\tau) = J_0(2\pi f_d \tau)$ where $J_0(\cdot)$ denotes the zeroth-order Bessel function of the first kind and f_d denotes the maximum Doppler frequency shift. Throughout this chapter, we assume that the channels over different paths are uncorrelated, i.e., if $l_1 \neq l_2$, $E\left\{h_{l_1,n+m} h^*_{l_2,n}\right\} = 0$ for any n and m. Without loss of generality, we further normalize the average power gain of the multipath channel to get $\sum_{l=0}^{L-1} \xi_l = 1$.

6.1.2 ICI in High-Mobility OFDM

Denote $\mathbf{X} = (X_0, X_1, \cdots, X_{N-1})^T$ as the frequency-domain transmitted signal vector and $\mathbf{F}_N$ as the $N \times N$ DFT matrix with the element at the n_1th row and the n_2th column given by

$$\mathbf{F}_N(n_1, n_2) = \frac{1}{\sqrt{N}} e^{-\frac{2\pi n_1 n_2}{N}}, 0 \leq n_1, n_2 \leq N-1, \tag{6.2}$$

and then the time-domain transmitted signal vector is given by $\mathbf{x} = \mathbf{F}_N^H \mathbf{X}$. Supposed that ISI is avoided by cyclic prefix, and then the time-domain received signal vector at the OFDM receiver is given by

$$\mathbf{y} = \mathbf{H}_N \mathbf{x} + \mathbf{w}_N, \tag{6.3}$$

where $\mathbf{w}_N$ denotes the additive white Gaussian noise vector and $\mathbf{H}_N$ is the $N \times N$ time-domain channel matrix, which, according to the channel model defined in Section 6.1.1, is given by

$$\mathbf{H}_N = \begin{bmatrix} h_{0,0} & & & h_{L-1,0} & \cdots & & h_{2,0} & h_{1,0} \\ h_{1,1} & h_{0,1} & & & h_{L-1,1} & & \cdots & h_{2,1} \\ \vdots & & \ddots & & & \ddots & & \vdots \\ h_{L-2,L-2} & & \cdots & h_{0,L-2} & & & & h_{L-1,L-2} \\ h_{L-1,L-1} & & \cdots & h_{1,L-1} & h_{0,L-1} & & & \\ & & \ddots & & & \ddots & & \\ & & h_{L-1,N-2} & & \cdots & & h_{0,N-2} & \\ & & & h_{L-1,N-1} & & \cdots & h_{1,N-1} & h_{0,N-1} \end{bmatrix} \tag{6.4}$$

The corresponding frequency-domain received signal vector can be obtained as

$$\mathbf{Y} = \mathbf{F}_N \mathbf{y} = \mathbf{G}_N \mathbf{X} + \mathbf{W}_N, \tag{6.5}$$

where $\mathbf{W}_N = \mathbf{F}_N\mathbf{w}$ denotes the frequency-domain white noise vector and

$$\mathbf{G}_N = \mathbf{F}_N\mathbf{H}_N\mathbf{F}_N^H \tag{6.6}$$

denotes the *channel frequency response* (CFR) matrix over the N OFDM subchannels. The element of $\mathbf{G}_N$ at the mth row ant the kth column denotes the channel gain from the kth to the mth OFDM subchannel and is given by

$$\mathbf{G}_N(m,k) = \sum_{l=0}^{L-1} \frac{e^{-j\frac{2\pi kl}{N}}}{N} \sum_{n=0}^{N-1} h_{l,n} e^{-j\frac{2\pi(m-k)n}{N}}, \tag{6.7}$$

which indicates that when $m \neq k$, $\mathbf{G}_N(m,k) = 0$ only if $h_{l,n} = h_l, 0 \leq n \leq N-1$, i.e., the time-domain variation of the wireless channel within an OFDM symbol causes ICI. As a result, $\mathbf{G}_N$ is no longer diagonal and the off-diagonal elements are the interference gains among OFDM subchannels.

6.2 Principle of Reduced-Rate OFDM Transmission

As described in Section 6.1.1, the time-domain variation of the wireless channel within an OFDM symbol causes ICI and will result in an error floor at the receiver. While it has been proposed to estimate the off-diagonal elements of the CFR matrix and perform ICI cancellation accordingly, this requires lots of pilots and significantly decreases spectral efficiency especially in a high-mobility environment. On the other hand, the existing pilot-free full-rate OFDM transmit preprocessing schemes [82, 83, 23] only have limited ICI mitigation capabilities and still suffer considerable residual ICI. In contrast, the half-rate OFDM transmission scheme with ICI self-cancellation capability proposed in [88] has been demonstrated to significantly reduce ICI. In this section, we extend the work in [88] and develop a general reduced-rate OFDM transmission scheme to trade spectral efficiency for ICI mitigation in a high-mobility environment.

6.2.1 Frequency-Domain

In the reduced-rate OFDM transmission, K data symbols are loaded over N subcarriers with $\eta = \frac{N}{K}$ defined as the RRF. By reducing the transmission rate, we are able to design the

structure of the transmitted signal vector so that it has inherent ICI mitigation capability. For a tradeoff between ICI mitigation and the spectral efficiency, we assume that $1 \leq \eta \leq 2$. Even so, the developed schematic framework and the presented analysis throughout this chapter can be easily extended to the case that $\eta > 2$.

Figure 6.1(a) shows the block diagram of the reduced-rate OFDM transmission scheme in the frequency-domain. In the figure, $\mathbf{S} = (S_0, S_1, \cdots, S_{K-1})^T$ denotes the frequency-domain signal vector over the K equivalent subchannels at the transmitter, $\mathbf{U}$ denotes the $N \times K$ transmit preprocessing matrix, and the actually transmitted signal vector over the N OFDM subchannels is given by

$$\mathbf{X} = \mathbf{US}. \tag{6.8}$$

At the receiver, we further perform receive preprocessing to get the frequency-domain received signal vector over the K equivalent subchannels as

$$\mathbf{R} = \mathbf{VY}, \tag{6.9}$$

where $\mathbf{V}$ denotes the $K \times N$ receive preprocessing matrix and $\mathbf{Y}$ denotes the received signal vector over the N OFDM subchannels given in (6.5). After that, channel estimation and signal detection algorithms are performed over the K equivalent subchannels. Based on (6.5), (6.8), and (6.9), we obtain the frequency-domain system equation over the K equivalent subchannels as

$$\mathbf{R} = \mathbf{G}_K\mathbf{S} + \mathbf{W}_K, \tag{6.10}$$

where $\mathbf{G}_K = \mathbf{VG}_N\mathbf{U}$ denotes the equivalent CFR matrix and $\mathbf{W}_K = \mathbf{VW}_N$ denotes the received noise vector. Equation (6.10) indicates that, by reducing the transmission rate via transmit and receive preprocessing, we transform the original N-subcarrier OFDM system into an equivalent K-subcarrier one.

6.2.2 Time-Domain

Denote $\mathbf{F}_K$ as the $K \times K$ DFT matrix, $\mathbf{s}$ and $\mathbf{r}$ as the time-domain transmitted and received signal vectors over the K equivalent subchannels, respectively, and then the time-domain

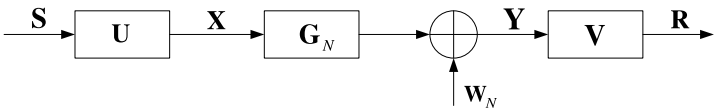

(a) Frequency-domain

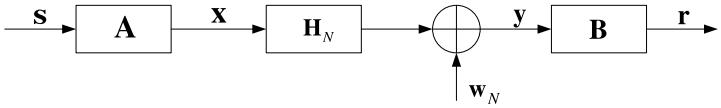

(b) Time-domain

Figure 6.1. Block diagram of the reduced-rate OFDM transmission

system equation of the equivalent K-subcarrier OFDM system can be obtained from (6.10) as

$$\mathbf{r} = \mathbf{H}_K\mathbf{s} + \mathbf{w}_K, \tag{6.11}$$

where $\mathbf{w}_K = \mathbf{F}_K^H\mathbf{W}_K$ and $\mathbf{H}_K = \mathbf{F}_K^H\mathbf{G}_K\mathbf{F}_K$ denotes the time-domain equivalent channel matrix.

Since $\mathbf{H}_K = \mathbf{F}_K^H\mathbf{G}_K\mathbf{F}_K$, $\mathbf{G}_K = \mathbf{V}\mathbf{G}_N\mathbf{U}$ and $\mathbf{G}_N = \mathbf{F}_N\mathbf{H}_N\mathbf{F}_N^H$, the mapping from the original to the equivalent time-domain channel matrices can be obtained as

$$\mathbf{H}_K = \mathbf{B}\mathbf{H}_N\mathbf{A}, \tag{6.12}$$

where $\mathbf{A} = \mathbf{F}_N^H\mathbf{U}\mathbf{F}_K$ denotes the $N \times K$ time-domain transmit preprocessing matrix and $\mathbf{B} = \mathbf{F}_K^H\mathbf{V}\mathbf{F}_N$ denotes the $K \times N$ time-domain receive preprocessing matrix. Denote $g_{l,n}, 0 \leq l, n \leq K-1$, as the channel gain over the lth path in the nth sampling interval of the equivalent K-subcarrier OFDM system, and then

$$\mathbf{H}_K(n_1, n_2) = g_{(n_1-n_2)_K, n_1}, \quad 0 \leq n_1, n_2 \leq K-1, \tag{6.13}$$

where $(\cdot)_K$ denotes K modular. Equation (6.12) indicates how the original time-domain channel is mapped to the equivalent one via transmit and receive preprocessing. Based on (6.11) and (6.12), we also show the time-domain block diagram of the reduced-rate OFDM transmission scheme in Figure 6.1(b).

6.3 Design of Transmit and Receive Preprocessing Matrices

Given the framework of the reduced-rate OFDM transmission, it is our objective to design the transmit preprocessing matrix, **U** or **A**, and the receive preprocessing matrix, **V** or **B**, so that the transformed K-subcarrier OFDM system has significantly reduced ICI.

6.3.1 Common SIR over Equivalent Subchannels

According to (6.10), the frequency-domain received signal over the mth equivalent subchannel can be expressed as

$$R_m = \mathbf{G}_K(m,m)S_m + \sum_{k=0,k\neq m}^{K-1} \mathbf{G}_K(m,k)S_k + W_{K,m}, \quad 0 \leq m \leq K-1, \tag{6.14}$$

where the first and second terms denote the desired signal and the ICI, respectively. Assume that the transmitted signals over different equivalent subchannels, S_k's, are independent with zero mean and variance σ_s^2, and then the average SIR over the mth equivalent subchannel can be obtained as

$$\text{SIR}_m = \frac{E\left\{|\mathbf{G}_K(m,m)|^2\right\}}{\sum_{k=0,k\neq m}^{K-1} E\left\{|\mathbf{G}_K(m,k)|^2\right\}} = \frac{P(m,m)}{\sum_{k=0,k\neq m}^{K-1} P(m,k)}, \tag{6.15}$$

where $P(m,k) = E\left\{|\mathbf{G}_K(m,k)|^2\right\}$ denotes the average power gain from the kth to the mth equivalent subchannel. The objective of reduced-rate OFDM transmission is to apply specially designed transmit and receive preprocessing so that the average SIR over each equivalent subchannel is maximized.

Because of the circular and symmetric structure of the OFDM modulation, it is expected that, with the optimal preprocessing matrices, the average power gain from the kth to the mth equivalent subchannel only depends on the distance between the two subchannels, i.e., $P(m,k) = p((m-k)_K)$, where $p(\cdot)$ denotes a one-dimensional function, and all of the equivalent subchannels have the common SIR given by

$$\text{SIR} = \frac{p(0)}{\sum_{n=1}^{K-1} p(n)}. \tag{6.16}$$

We notice that in [90], a common SIR is not guaranteed and as a result, the system performance is restricted by the equivalent subchannel with the smallest SIR if a common

modulation and coding scheme is applied. Furthermore, the fact that all equivalent subchannels have a common SIR also facilitates the optimization of the reduced-rate OFDM transmission since the common SIR works well as an objective to maximize, as will be discussed in Section 6.3.6.

Since $\mathbf{G}_K = \mathbf{F}_K \mathbf{H}_K \mathbf{F}_K^H$ and $\mathbf{H}_K(n_1, n_2) = h_{K,(n_1-n_2)_N,n_1}$, it can be obtained that

$$P(m,k) = \frac{1}{K^2} \sum_{l_1=0}^{M-1} \sum_{l_2=0}^{M-1} e^{-j\frac{2\pi k}{K}(l_1-l_2)} \sum_{n_1=0}^{K-1} \sum_{n_2=0}^{K-1} E\left\{h_{K,l_1,n_1} h_{K,l_2,n_2}^*\right\} e^{-j\frac{2\pi(m-k)(n_1-n_2)}{K}}, \tag{6.17}$$

which indicates that $P(m,k)$ generally depends on both m and k. However, if

$$E\left\{h_{K,l_1,n_1} h_{K,l_2,n_2}^*\right\} = 0, \tag{6.18}$$

for any $l_1 \neq l_2$, the above equation reduces to

$$P(m,k) = \frac{1}{K^2} \sum_{l=0}^{M-1} \sum_{n_1=0}^{K-1} \sum_{n_2=0}^{K-1} E\left\{h_{K,l,n_1} h_{K,l,n_2}^*\right\} e^{-j\frac{2\pi(m-k)(n_1-n_2)}{K}}, \tag{6.19}$$

i.e., $P(m,k)$ only depends on $(m-k)_K$. In light of this, we obtain the following first sufficient condition for a common SIR over equivalent subchannels.

Proposition 6.3.1 *The equivalent subchannels have a common SIR if different paths in the time-domain channel of the transformed K-subcarrier OFDM system are uncorrelated.*

6.3.2 Structure of A and B for a Common SIR

According to Proposition 6.3.1, it is our objective to design the time-domain preprocessing matrices, $\mathbf{A}$ and $\mathbf{B}$, so that different paths in the equivalent time-domain channel, $\mathbf{H}_K = \mathbf{B}\mathbf{H}_N\mathbf{A}$, are uncorrelated and a common SIR over all equivalent subchannels is guaranteed. For robustness of the design, we will utilize the least knowledge on the channel statistics when determining the structure of $\mathbf{A}$ and $\mathbf{B}$.

Since $\mathbf{H}_K = \mathbf{B}\mathbf{H}_N\mathbf{A}$, we have

$$\mathbf{H}_K(i,j) = \sum_{n_1=0}^{N-1} \sum_{n_2=0}^{N-1} \mathbf{B}(i,n_1)\, \mathbf{H}_N(n_1,n_2)\, \mathbf{A}(n_2,j), \quad 0 \leq i,j \leq K-1. \tag{6.20}$$

Define $i = (j + l)_K$ and $n_1 = (n_2 + \Delta)_N$ where l and Δ denote the path indexes in $\mathbf{H}_K$ and $\mathbf{H}_N$, respectively, and then the above equation can be rewritten as

$$\mathbf{H}_K\left((j+l)_K, j\right) = \sum_{\Delta=0}^{L-1} \sum_{n_2=0}^{N-1} \mathbf{B}\left((j+l)_K, (n_2+\Delta)_N\right) \mathbf{H}_N\left((n_2+\Delta)_N, n_2\right) \mathbf{A}\left(n_2, j\right), \qquad (6.21)$$

for $0 \leq l, j \leq K-1$, where L denotes the number of paths in $\mathbf{H}_N$ and $\mathbf{H}_N\left((n_2+\Delta)_N, n_2\right) = 0$ for any n_2 if $\Delta > L$. Since L is usually much smaller than N, we assume it is also smaller than K throughout this chapter. Equation (6.21) indicates how path Δ in $\mathbf{H}_N$ is mapped to path l in $\mathbf{H}_K$ for given preprocessing matrices, $\mathbf{A}$ and $\mathbf{B}$. Recall that different paths in the original time-domain channel, $\mathbf{H}_N$, are uncorrelated. Therefore, different paths in $\mathbf{H}_K$ will be still uncorrelated if, with specially designed $\mathbf{A}$ and $\mathbf{B}$, any path in $\mathbf{H}_N$ is mapped to at most one of the paths in $\mathbf{H}_K$. Thus we obtain the following second sufficient condition for a common SIR over equivalent subchannels.

Proposition 6.3.2 *The equivalent subchannels have a common SIR if any path in the original time-domain channel is mapped to at most one of the paths in the transformed one.*

Equation (6.21) indicates that, to guarantee channel sequence $\mathbf{H}_N\left((n_2+\Delta)_N, n_2\right), 0 \leq n_2 \leq N-1$, over path Δ in $\mathbf{H}_N$ is mapped to only one channel sequence, $\mathbf{H}_K\left((j+l)_K, j\right), 0 \leq j \leq K-1$, over path l in $\mathbf{H}_K$, we need to ensure that each row of $\mathbf{A}$ and each column of $\mathbf{B}$ have at most one non-zero element. Without loss of generality, we construct $\mathbf{A}$ so that the time-domain transmit preprocessing can be realized by simple periodic extension and windowing, i.e.,

$$\mathbf{A} = \begin{bmatrix} \alpha_0 & & & \\ & \ddots & & \\ & & \ddots & \\ & & & \alpha_{K-1} \\ \alpha_K & & & \\ & \ddots & & \\ & & \alpha_{N-1} & \end{bmatrix}, \qquad (6.22)$$

where $\alpha_0, \alpha_1, \cdots, \alpha_{N-1}$ denote the transmit preprocessing coefficients.

To find the structure of $\mathbf{B}$ corresponding to such an $\mathbf{A}$, we investigate how the first path in $\mathbf{H}_N$ contributes to $\mathbf{H}_K\left((j+l)_K, j\right)$ by extracting the first path ($\Delta = 0$) from the right side of Equation (6.21) as

$$\begin{aligned}&\textstyle\sum_{n_2=0}^{N-1} \mathbf{B}\left((j+l)_K, n_2\right) \mathbf{H}_N\left(n_2, n_2\right) \mathbf{A}\left(n_2, j\right) \\ &= \mathbf{B}\left((j+l)_K, j\right) \mathbf{H}_N\left(j, j\right) \mathbf{A}(j, j) + \mathrm{I}_{j<N-K} \mathbf{B}\left((j+l)_K, j+K\right) \mathbf{H}_N\left(j+K, j+K\right) \mathbf{A}(j+K, j),\end{aligned} \tag{6.23}$$

where $\mathrm{I}_{j<N-K}$ denotes the indicator function defined as

$$\mathrm{I}_{j<N-K} = \begin{cases} 1 & \text{if } j < N-K \\ 0 & \text{otherwise} \end{cases} \tag{6.24}$$

Without loss of generality, we let the first path in $\mathbf{H}_N$ be mapped to only the first path in $\mathbf{H}_K$. As a result, the contribution of the first path given in (6.23) must be nulled unless $l = 0$, i.e., $\mathbf{B}\left((j+l)_K, j\right)$ and $\mathbf{B}\left((j+l)_K, j+K\right)$ should be zero unless $l = 0$. In other words, the corresponding time-domain receive preprocessing matrix must have the following structure

$$\mathbf{B} = \begin{bmatrix} \beta_0 & & & \beta_K & & \\ & \ddots & & & \ddots & \\ & & \ddots & & & \beta_{N-1} \\ & & & \beta_{K-1} & & \end{bmatrix}, \tag{6.25}$$

where $\beta_0, \beta_1, \cdots, \beta_{N-1}$ denote the receive preprocessing coefficients.

Given the tentative structure of $\mathbf{A}$ and $\mathbf{B}$ in (6.22) and (6.25), respectively, we need to investigate whether it guarantees a one-to-one path mapping from $\mathbf{H}_N$ to $\mathbf{H}_K$ and a common SIR over all equivalent subchannels. To facilitate analysis, we will consider integer and fractional RRFs, respectively.

6.3.3 Design of A and B: Integer RRF

Given the structure of $\mathbf{A}$ and $\mathbf{B}$ in Section 6.3.2, we have proved the following proposition in Appendix D.1.

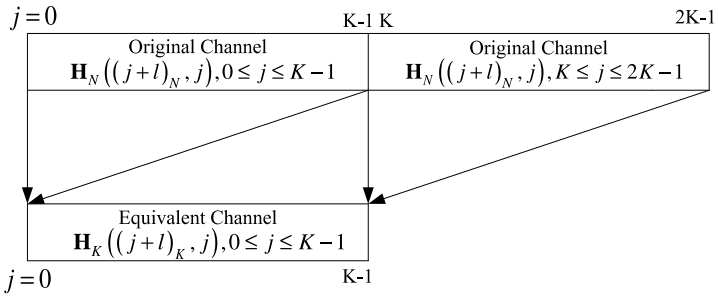

Figure 6.2. Mapping from the original channel to the equivalent one over path l when $K = \frac{N}{2}$

Proposition 6.3.3 *When $K = \frac{N}{2}$, there exists a one-to-one path mapping from $\mathbf{H}_N$ to $\mathbf{H}_K$ given by*

$$\mathbf{H}_K\left(\left(j+l\right)_K, j\right) = \alpha_j \beta_{j+l} \mathbf{H}_N\left(j+l, j\right) + \alpha_{j+K} \beta_{(j+K+l)_N} \mathbf{H}_N\left(\left(j+K+l\right)_N, j+K\right), \quad (6.26)$$

for $0 \le j, l \le K-1$, and a common SIR over K equivalent subchannels for arbitrary preprocessing coefficients $\alpha_0, \alpha_1, \cdots, \alpha_{N-1}$ and $\beta_0, \beta_1, \cdots, \beta_{N-1}$.

Equation (6.26) indicates that, for any path index l and time index j, $\mathbf{H}_K\left(\left(j+l\right)_K, j\right)$ is a linear combination of $\mathbf{H}_N\left(j+l, j\right)$ and $\mathbf{H}_N\left(\left(j+K+l\right)_N, j+K\right)$. Based on that, we show how the original time-domain channel is mapped to the equivalent one in Figure 6.2. As indicated, the equivalent channel sequence is obtained by dividing the original one into two segments with equal length and then performing a weighted summation of two segments with the weights determined by $\alpha_0, \alpha_1, \cdots, \alpha_{N-1}$ and $\beta_0, \beta_1, \cdots, \beta_{N-1}$. When the Doppler frequency is low, the original channel over each path usually varies with time linearly within an OFDM symbol. Therefore, it is possible to design $\alpha_0, \alpha_1, \cdots, \alpha_{N-1}$ and $\beta_0, \beta_1, \cdots, \beta_{N-1}$ appropriately so that the weighted summation of the two segments has the least time-domain variation. Therefore, with $K = \frac{N}{2}$, the reduced-rate OFDM transmission is expected to reduce ICI dramatically, as will be verified in Section 6.4.

6.3.4 Design of A and B: Fractional RRF

To guarantee a common SIR over all equivalent subchannels in the case of a fractional RRF, we design K so that $L \le N - K + 1$ and let $\alpha_n = 0$ for any $N - (L-1) \le n \le N-1$.

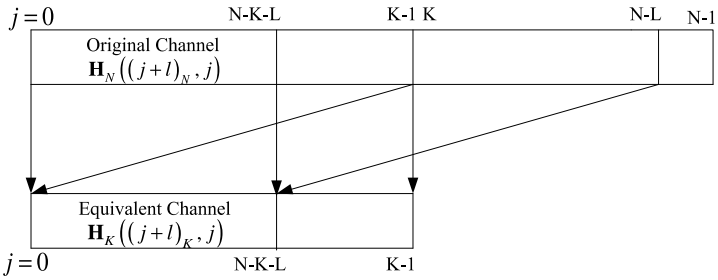

Figure 6.3. Mapping from the original channel to the equivalent one over path l when $\frac{N}{2} < K < N$

Then, given the structure of **A** and **B** in (6.22) and (6.25), respectively, we have proved the following proposition in Appendix D.2.

Proposition 6.3.4 *When $\frac{N}{2} < K < N$, there exists a one-to-one path mapping from $\mathbf{H}_N$ to $\mathbf{H}_K$ given by*

$$\mathbf{H}_K\left((j+l)_K, j\right) = \alpha_j \beta_{j+l} \mathbf{H}_N\left(j+l, j\right) + \mathrm{I}_{j \le N-K-L} \alpha_{j+K} \beta_{j+K+l} \mathbf{H}_N\left(j+K+l, j+K\right), \quad (6.27)$$

for $0 \le j, l \le K-1$, and a common SIR over K equivalent subchannels for arbitrary preprocessing coefficients $\alpha_0, \alpha_1, \cdots, \alpha_{N-L}$ and $\beta_0, \beta_1, \cdots, \beta_{N-1}$.

Based on (D.6), we show how the original time-domain channel is mapped to the equivalent one in Figure 6.3. Different from the case of an integer RRF, only the first part of the equivalent channel sequence, $\mathbf{H}_K\left((j+l)_K, j\right), 0 \le j \le N-K-L$, is a weighted summation of two original channel segments while the second part is not. As a result, even if the original channel over each path varies with time linearly, the variation of the equivalent channel in the second part cannot be eliminated entirely. Therefore, with $K > \frac{N}{2}$, the reduced-rate OFDM transmission increases spectral efficiency at the expense of degraded ICI mitigation capability, as will be verified in Section 6.4.

6.3.5 Structure of U and V

After determining the structure of the time-domain preprocessing matrices, **A** and **B**, we further investigate the corresponding frequency-domain preprocessing matrices, **U** and **V**.

Since $\mathbf{U} = \mathbf{F}_N \mathbf{A} \mathbf{F}_K^H$, it can be obtained that

$$\mathbf{U}(m,k) = \frac{1}{\sqrt{NK}} \sum_{n=0}^{N-1} \left(\alpha_n e^{j\frac{2\pi n}{N}\left(k\frac{N}{K}\right)} \right) e^{-j\frac{2\pi mn}{N}}, \quad 0 \le m \le N-1, 0 \le k \le K-1, \tag{6.28}$$

which indicates that the kth column vector of $\mathbf{U}$, $\mathbf{U}(:,k)$, is the DFT transform of the following sequence

$$\left\{ \frac{1}{\sqrt{NK}} \alpha_n e^{j\frac{2\pi n}{N}\left(k\frac{N}{K}\right)}, 0 \le n \le N-1 \right\}. \tag{6.29}$$

According to the properties of the DFT transform, this means that $\mathbf{U}(:,k)$ can be obtained by cyclically shifting the first column vector of $\mathbf{U}$, $\mathbf{U}(:,0)$, downwards by $k\frac{N}{K}$ times. When $\frac{N}{K} = 2$, $k\frac{N}{K}$ is always an integer and thus $\mathbf{U}$ becomes a quasi-circulant matrix in the sense that $\mathbf{U}(:,k)$ is a downward cyclic shift of $\mathbf{U}(:,k-1)$ by two times.

Similarly, it can be shown from $\mathbf{V} = \mathbf{F}_K \mathbf{Y} \mathbf{F}_N^H$ that

$$\mathbf{V}(k,m) = \frac{1}{\sqrt{NK}} \sum_{n=0}^{N-1} \left(\beta_n e^{-j\frac{2\pi n}{N}\left(k\frac{N}{K}\right)} \right) e^{j\frac{2\pi mn}{N}}, \quad 0 \le m \le N-1, 0 \le k \le K-1, \tag{6.30}$$

which indicates that the kth row vector of $\mathbf{V}$, $\mathbf{V}(k,:)$, is a rightward cyclic shift of the first row vector, $\mathbf{V}(0,:)$, by $k\frac{N}{K}$ times. Furthermore, $\mathbf{V}$ is also a quasi-circulant matrix when $\frac{N}{K} = 2$.

To illustrate the structure of the frequency-domain preprocessing matrices, here we show the $\mathbf{U}$ and $\mathbf{V}$ that are equivalently applied in [88] when $\frac{N}{K} = 2$.

$$\mathbf{U} = \begin{bmatrix} 1 & 0 & \cdots & 0 & 0 \\ -1 & 0 & \cdots & 0 & 0 \\ 0 & 1 & \cdots & 0 & 0 \\ 0 & -1 & \cdots & 0 & 0 \\ \vdots & \vdots & \ddots & \vdots & \vdots \\ 0 & 0 & \cdots & 0 & 1 \\ 0 & 0 & \cdots & 0 & -1 \end{bmatrix}, \mathbf{V} = \begin{bmatrix} 1 & -1 & 0 & 0 & \cdots & 0 & 0 \\ 0 & 0 & 1 & -1 & \cdots & 0 & 0 \\ \vdots & \vdots & \vdots & \vdots & \ddots & \vdots & \vdots \\ 0 & 0 & 0 & 0 & \cdots & 0 & 0 \\ 0 & 0 & 0 & 0 & \cdots & 1 & -1 \end{bmatrix} \tag{6.31}$$

An ICI self-cancellation scheme with the above $\mathbf{U}$ and $\mathbf{V}$ has been proposed in [88] where the actually transmitted signal vector over the N OFDM subchannels is

$$\mathbf{X} = (S_0, -S_0, S_1, -S_1, \cdots, S_{K-1} - S_{K-1})^T. \tag{6.32}$$

Essentially, this scheme is based on the conjecture that $\mathbf{G}_N(m,k) \approx \mathbf{G}_N(m,k-1)$ and as a result, with such transmitted signal structure, the interferences over the mth subcarrier from subcarriers k and $k-1$ cancel each other, resulting a significantly reduced ICI level. Although the ICI self-cancellation proposed in [88] is based on a different analysis framework, it can be equivalently regarded as a special reduced-rate OFDM transmission scheme with the above designed quasi-circulant $\mathbf{U}$ and $\mathbf{V}$. Therefore, the comparison between the optimized reduced-rate OFDM transmission and the existing ICI self-cancellation scheme will be insightful, as will be demonstrated in Section 6.4.

6.3.6 Optimization of A and B

Up to now, we have investigated the general structure of transmit and receive preprocessing matrices to ensure that all equivalent subchannels of the reduced-rate OFDM transmission system have a common SIR. Given the developed structure, we will further investigate the optimization of the two preprocessing matrices so as to maximize the common SIR based on the long-term channel statistics described in 6.1.1. Essentially, we will find the optimal preprocessing coefficient vectors, $\boldsymbol{\alpha} = \{\alpha_0, \alpha_1, \cdots, \alpha_{N-1}\}$ or $\{\alpha_0, \alpha_1, \cdots, \alpha_{N-L}, 0, \cdots, 0\}$ and $\boldsymbol{\beta} = \{\beta_0, \beta_1, \cdots, \beta_{N-1}\}$, so that the transformed time-domain channel has the least time-domain variation.

Recall that, with the developed structure of $\mathbf{A}$ and $\mathbf{B}$, the common SIR over K equivalent subchannels is given by

$$\text{SIR} = \frac{P(m,m)}{\sum_{k=0,k\neq m}^{K-1} P(m,k)} = \frac{p(0)}{\sum_{n=1}^{K-1} p(n)}, \tag{6.33}$$

for any $0 \leq m \leq K-1$, where $P(m,k) = p((m-k)_K)$. Without loss of generality, we consider the first equivalent subchannel over which the average desired signal power can be expressed as

$$\begin{aligned} P_d = P(0,0) &= E\left\{|\mathbf{G}_K(0,0)|^2\right\} \\ &= \sum_{r_1=0}^{N-1}\sum_{c_1=0}^{N-1}\sum_{r_2=0}^{N-1}\sum_{c_2=0}^{N-1} \mathbf{V}(0,r_1)\,\mathbf{U}(c_1,0)\,f(r_1,c_1,r_2,c_2)\,\mathbf{V}^*(0,r_2)\,\mathbf{U}^*(c_2,0), \end{aligned} \tag{6.34}$$

and the average ICI power can be expressed as

$$\begin{aligned} P_I &= \sum_{k=1}^{K-1} P(0,k) = \sum_{k=1}^{K-1} E\left\{|P(0,k)|^2\right\} \\ &= \sum_{k=1}^{K-1}\sum_{r_1=0}^{N-1}\sum_{c_1=0}^{N-1}\sum_{r_2=0}^{N-1}\sum_{c_2=0}^{N-1} \mathbf{V}(0,r_1)\,\mathbf{U}(c_1,k)\,f(r_1,c_1,r_2,c_2)\,\mathbf{V}^*(0,r_2)\,\mathbf{U}^*(c_2,k), \end{aligned} \tag{6.35}$$

where the elements of $\mathbf{U}$ and $\mathbf{V}$ are expressed in (6.28) and (6.30), respectively, and

$$f(r_1,c_1,r_2,c_2) = E\left\{\mathbf{G}_N(r_1,c_1)\,\mathbf{G}_N^*(r_2,c_2)\right\}, \tag{6.36}$$

which, based on the channel statistics described in 6.1.1, can be obtained as

$$f(r_1,c_1,r_2,c_2) = \frac{\sum_{l=0}^{L-1}\xi_l e^{j\frac{2\pi(c_2-c_1)l}{N}}}{N^2}\sum_{n_1=0}^{N-1}\sum_{n_2=0}^{N-1}\phi(n_1-n_2)\,e^{j\frac{2\pi}{N}[(r_2-c_2)n_2-(r_1-c_1)n_1]}. \tag{6.37}$$

Thus the optimization problem can be formulated as

$$\begin{aligned} \max_{\alpha,\beta} \quad & \text{SIR} = \tfrac{P_d}{P_I} \\ \text{s.t.} \quad & \sum_{n=1}^{N-1}|\alpha_n|^2 = N \text{ and } \sum_{n=1}^{N-1}|\beta_n|^2 = N \end{aligned} \tag{6.38}$$

Recall that the received noise vector over the K equivalent subchannels is given by $\mathbf{W}_K = \mathbf{V}\mathbf{W}_N$ where $\mathbf{W}_N$ denotes the original white noise vector over the N OFDM subcarriers. Denote σ_n^2 as the noise power over each OFDM subcarrier, and then the noise power over the kth equivalent subchannel can be obtained as

$$\sigma_k^2 = \sigma_n^2\sum_{m=0}^{N-1}|\mathbf{V}(k,m)|^2. \tag{6.39}$$

Substitute (6.30) in (6.39), and then we have

$$\begin{aligned} \sigma_k^2 &= \tfrac{\sigma^2}{NK}\sum_{n_1=0}^{N-1}\sum_{n_2=0}^{N-1}\beta_{n_1}\beta_{n_2}^* e^{-j\frac{2\pi k}{K}(n_1-n_2)}\sum_{m=0}^{N-1}e^{j\frac{2\pi m}{N}(n_1-n_2)} \\ &= \tfrac{\sigma^2}{K}\sum_{n_2=0}^{N-1}|\beta_n|^2 \\ &= \tfrac{N}{K}\sigma_n^2. \end{aligned} \tag{6.40}$$

Therefore, the second constraint on $\boldsymbol{\beta}$ in (6.38) ensures that all equivalent subchannels share a common constant received noise power and as a result, the optimal $\boldsymbol{\alpha}$ and $\boldsymbol{\beta}$ maximizing

the SIR also maximize the SINR and optimize the system performance. Assume that the transmitted signals over different equivalent subchannels are independent with zero mean and variance σ_s^2, and then it can be similarly shown that the first constraint on $\boldsymbol{\alpha}$ in (6.38) guarantees a constant total transmit power over N OFDM subcarriers, $N\sigma_s^2$. Therefore, the solution to (6.38) maximizes the common SIR for a constant total transmit power and a constant received noise power over each equivalent subchannel. Since the optimization problem given in (6.38) is rather complicated, a closed-form solution cannot be obtained. Therefore, we apply the gradient-based steepest descent algorithm to search for the optimal $\boldsymbol{\alpha}$ and $\boldsymbol{\beta}$ numerically. Since the optimization of $\mathbf{A}$ and $\mathbf{B}$ is based on the long-term channel statistics, it can be conducted offline, thus relieving the burden of computation complexity.

6.4 Numerical and Simulation Results

In this section, we present both numerical and simulation results to demonstrate the performance of the proposed reduced-rate OFDM transmission scheme. In our simulation, a 32-subcarrier ($N = 32$) OFMD system is considered. We model the time-varying wireless channel as a 4-tap one, i.e., $L = 4$, and assume that the average power gains over the 4 paths decay with delay exponentially with the exponent factor $\lambda = 0.5$. Furthermore, we assume the classical Jakes' Doppler power spectrum over all of the paths with the normalized Doppler frequency defined as $F_d = \frac{f_d}{f_s}$ where $f_s = \frac{1}{NT_s}$ denotes the subcarrier spacing and T_s denotes the sampling interval. The performance of the optimized reduced-rate OFDM transmission scheme is demonstrated in comparison with the ICI self-cancellation scheme specially proposed in [88] for integer RRFs, denoted as the Zhao's scheme, and the improved one proposed in [90] for general RRFs, denoted as the Chang's scheme.

Figure 6.4(a) shows the SIR versus the normalized Doppler frequency (F_d) curves of the proposed, the Zhao's, and the Chang's schemes when $K = \frac{N}{2}$. Such a half-rate OFDM transmission scheme is suitable for high Doppler frequencies to trade transmission rate for

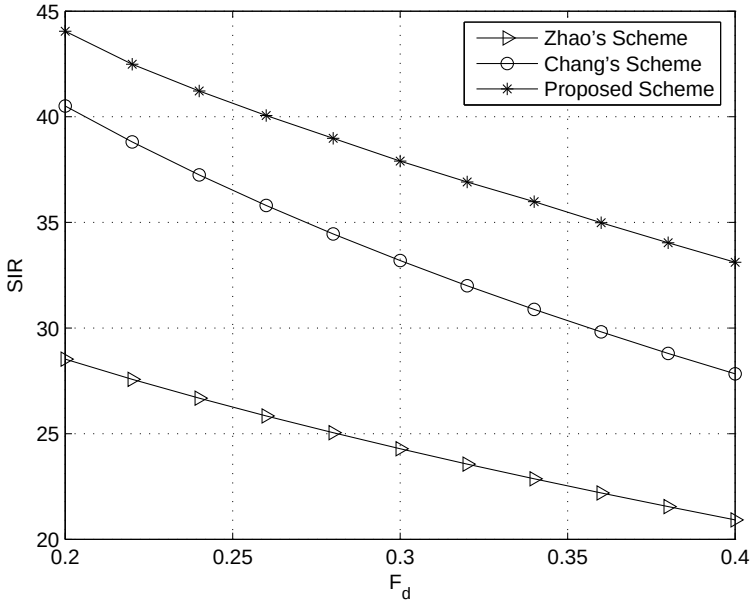

(a) $K = \frac{N}{2}$

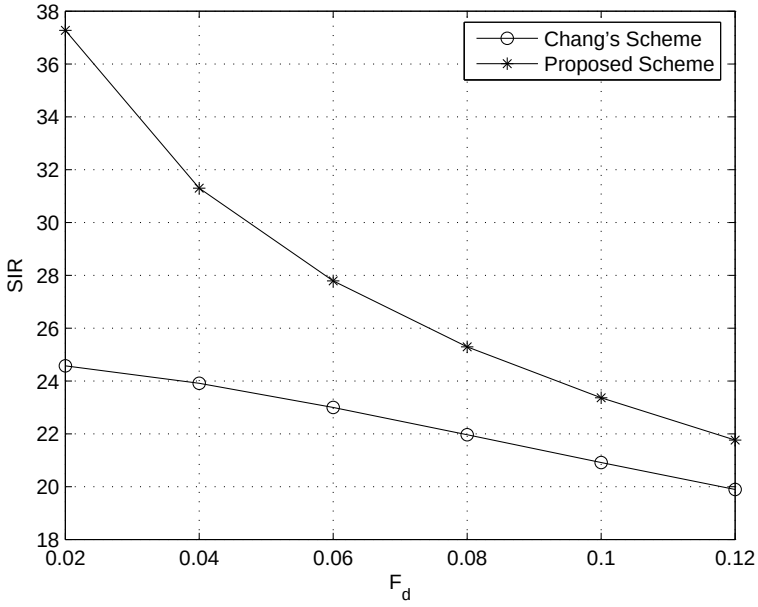

(b) $K = \frac{3}{4}N$

Figure 6.4. SIR versus the normalized Doppler frequency (F_d)

ICI mitigation in a high-mobility environment. As mentioned, the Zhao's scheme has quasi-circulant transmit and receive preprocessing matrices and thus has a common SIR over all equivalent subchannels. Furthermore, it can be shown that the Chang's scheme also has a common SIR over equivalent subchannels in the special case of half-rate transmission. As demonstrated in Figure 6.4(a), the optimized reduced-rate OFDM transmission achieves significant SIR gains of around 15 dB over the Zhao's scheme and around 5 dB over the Chang's scheme, respectively. Moreover, we observe that the SIR gain of the optimized reduced-rate transmission over the Chang's scheme increases with F_d slowly.

Figure 6.4(b) shows the SIR versus F_d curves of the proposed and the Chang's schemes when $K = \frac{3}{4}N$. In contrast with the half-rate scheme suitable for high Doppler frequencies, such a $\frac{3}{4}$-rate one is suitable for relatively low Doppler frequencies to achieve a tradeoff between spectral efficiency and ICI mitigation. Since the Chang's scheme does not guarantee a common SIR for fractional RRFs, we plot the minimum SIR over the equivalent subchannels in Figure 6.4(b) since it restricts the overall system performance. Figure 6.4(b) indicates that for fractional RRFs, the performance of the Chang's scheme degrades significantly in low F_d regions. Therefore, the SIR gain of the optimized reduced-rate transmission over the Chang's scheme increases considerably as F_d decreases. Moreover, it is observed that the $\frac{3}{4}$-rate scheme has a much lower SIR than the half-rate one. As explained in Section 6.3.4, the time-domain variation of the channel cannot be well eliminated by a fractional RRF. Therefore, the $\frac{3}{4}$-rate scheme increases the transmission rate at the expense of degraded ICI mitigation capability and is suitable for low Doppler frequencies.

Figure 6.5 shows the contrastive BER versus F_d curves of the proposed scheme, the Chang's scheme, and the Zhao's scheme when applicable. Focusing on the BER floor caused by residual ICI in this figure, we assume that there is no ambient noise and let $\sigma_n^2 = 0$. For both half-rate ($K = 16$) and $\frac{3}{4}$-rate ($K = 24$) schemes, 4 equally spaced equivalent subchannels are loaded with pilots for channel estimation at the receiver. Specifically, we first perform the liner LS estimation of the channel gains over the 4 pilots, and

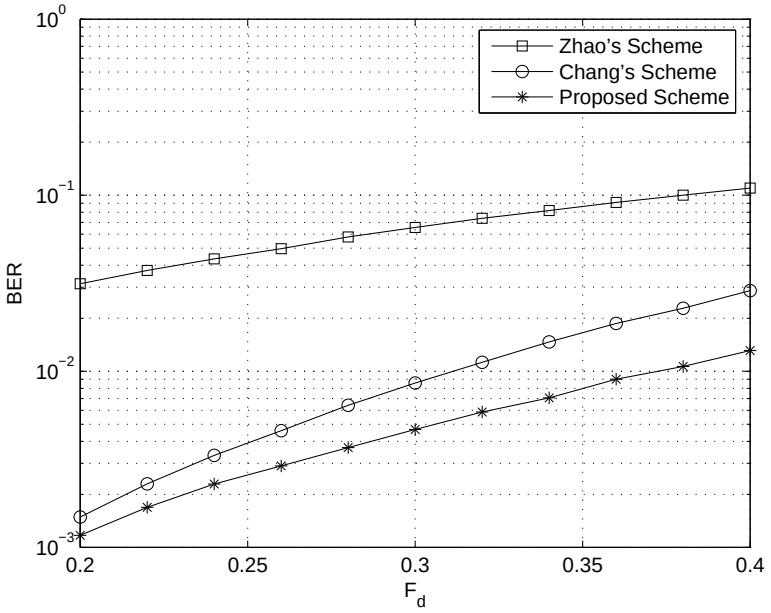

(a) $K = \frac{N}{2}$

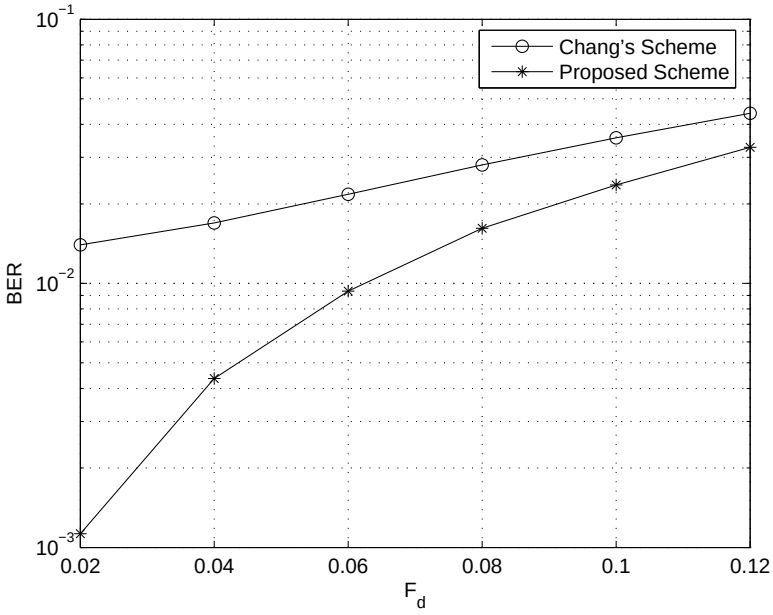

(b) $K = \frac{3}{4}N$

Figure 6.5. BER versus the normalized Doppler frequency (F_d)

then conduct the Wiener filtering based interpolation to estimate the channel gains over all equivalent subcannels based on the channel statistics. Furthermore, we apply the 64-QAM and the 16-QAM modulation means in the half-rate and the $\frac{3}{4}$-rate schemes, respectively. At the receiver, the zero-forcing detection is applied and no error-correcting coding is implemented. Figure 6.5 demonstrates that the optimized reduced-rate transmission achieves considerable BER improvements over the Zhao's and the Chang's schemes especially in high F_d regions for the half-rate and in low F_d regions for the $\frac{3}{4}$-rate, respectively, which is consistent with the observation from Figure 6.4.

Figure 6.6(a) further shows the contrastive BER versus SNR curves of the proposed, the Chang's, and the Zhao's scheme when $K = \frac{N}{2}$ and $F_d = 0.30$; Figure 6.6(b) shows the contrastive BER versus SNR curves of the proposed and the Chang's schemes when $K = \frac{3}{4}N$ and $F_d = 0.06$. To investigate the robustness of the proposed reduced-rate OFDM transmission to uncertainties in the channel statistics, we also plot the BER curves of the proposed schemes based on significantly inaccurate channel statistics where a uniform Doppler power spectrum [67] and a rectangular power delay profile (the estimate of the exponent factor is zero, i.e., $\lambda_e = 0$) are assumed. Similarly, we observe again that the optimized reduced-rate transmission effectively lowers the BER floor for both the half-rate and the $\frac{3}{4}$-rate schemes. Moreover, an SNR gain of around 2 dB over the Chang's scheme is observed even before the BER floor occurs. When $K = \frac{3}{4}N$, the non-ideal reduced-rate scheme based on the inaccurate channel statistics achieves almost the same BER performance as the ideal one; when $K = \frac{N}{2}$, the non-ideal scheme suffers an obvious performance degradation but still achieves a considerable performance improvement over the Chang's scheme. Therefore, Figure 6.6 verifies the robustness of the proposed reduced-rate OFDM transmission to uncertainties in the channel statistics.

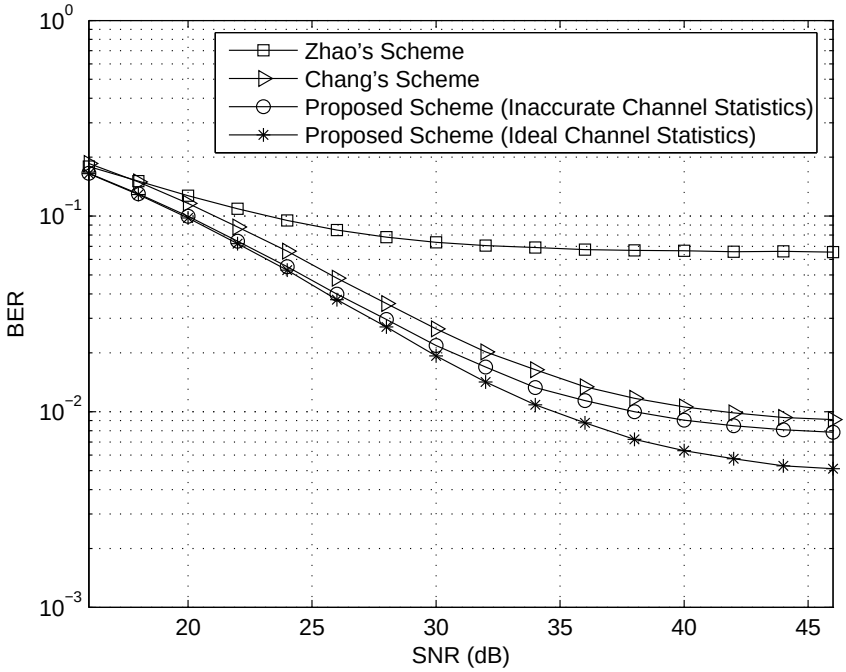

(a) $K = \frac{N}{2}$ and $F_d = 0.3$

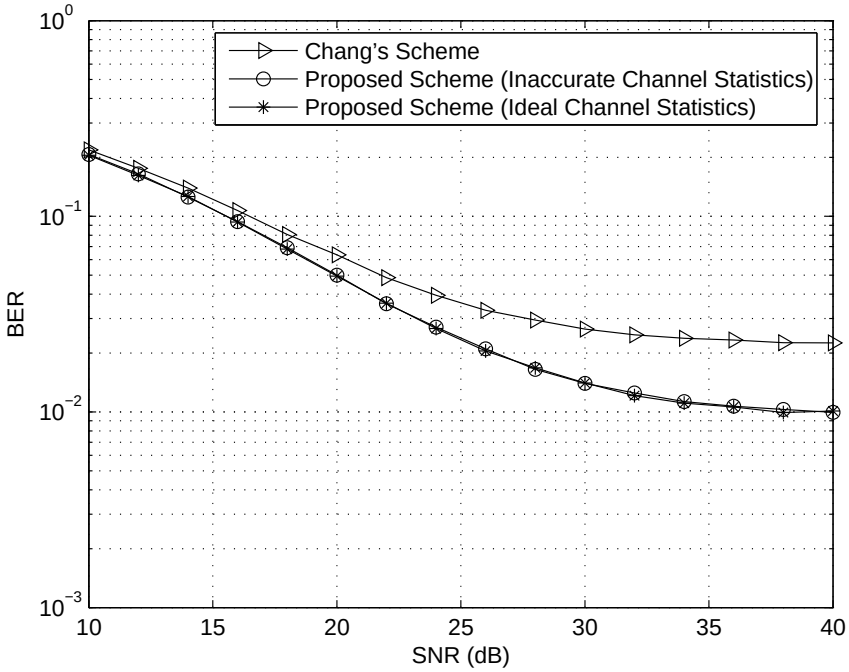

(b) $K = \frac{3}{4}N$ and $F_d = 0.06$

Figure 6.6. BER versus SNR

6.5 Conclusion and Future Work

In this chapter, we have developed a general reduced-rate OFDM transmission scheme for ICI mitigation at a high-mobility wireless relay. By transmit and receive preprocessing, we have transformed the original N-subcarrier OFDM system into an equivalent K-subcarrier one that has significantly reduced interference among the K equivalent subchannels. In particular, we have developed a general structure of transmit and receive preprocessing matrices to guarantee a common average SIR over all equivalent subchannels. By utilizing the long-term channel statistics, we have further optimized the preprocessing coefficients to maximize this common SIR. Both numerical and simulation results have demonstrated the considerable performance improvements of the optimized reduced-rate transmission over the existing ICI self-cancellation schemes even in the presence of significant uncertainties in the channel statistics. Furthermore, both analytical and simulation results have indicated that the time-domain variation of the wireless channel can be well eliminated by an integer RRF. When it comes to fractional RRFs, however, the equivalent channel of the transformed K-subcarrier OFDM system still contains considerable residual time-domain variation. Therefore, further development of fractional-rate-reduction OFDM transmission with better ICI mitigation capability will be an interesting future topic.

CHAPTER 7

CONCLUSION

In this dissertation, we have studied channel estimation and signal detection for wireless relay. The main contributions are summarized as follows.

We have established a two-hop MIMO AF relay system model consisting of an SS, a DS, and an RS that simply amplifies and forwards its received signals to the DS without any further processing. Such a system can be utilized to extend the coverage of wireless communications via low-complexity wireless relay. In this system, the overall noise vector at the DS is colored with its correlation matrix determined by the unknown forward relay channel over the RS-DS hop. To improve signal detection at the DS, we have proposed a blind noise correlation estimation algorithm by taking advantages of the frequency-domain correlation in the broadband wireless channel of an OFDM system. Without requiring any dedicated pilots, the proposed algorithm has been demonstrated to significantly improve signal detection at the DS especially over a spatially correlated MIMO forward relay channel. Since no pilots are inserted at the low-complexity RS to assist direct forward relay channel estimation at the DS, we have further proposed to estimate the two cascaded relay channels based on a predefined pilot amplifying matrix sequence at the RS and the corresponding overall channel sequence obtained at the DS through conventional channel estimation algorithms. We have found the necessary and sufficient conditions on the pilot amplifying matrix sequence to guarantee successful relay channel estimation at the DS. Based on these conditions, we have derived rules to design diagonal or quasi-diagonal pilot amplifying matrices so that the relay channels can be successfully estimated with minimum complexity at the RS. With the estimated relay channels at the DS, performance improvements in the signal detection have been demonstrated by simulation results.

For cross-talk interference at a CRRS, we have proposed to utilize the random forwarded signals of the RS as pilots to estimate the coupling channel from the transmit to the

receive antennas and then reconstruct and cancel the cross-talk interference accordingly. With such a coupling channel estimator, no modification is made to the signal structure in the physical layer and no in-band interference is caused at the DS. For an AF-based CRRS, we have developed the LS coupling channel estimator; for a DF-based CRRS, we have further developed the MMSE estimator and analyzed the correlation of the residual error after cross-talk cancellation, which can be utilized to improve desired signal detection at the RS.

To support the application of OFDM-based wireless relay on high-speed trains, we have developed Doppler compensation algorithms to improve the QoS provided to passengers. In particular, we have proposed to mitigate the ICI at an OFDM-based RS by taking advantages of the strong correlation in and between the desired signal and the ICI when there exists a LOS path between the BS and the train. Developed based on the channel statistics that can be estimated locally from the train system, the Wiener filtering and transmit preprocessing are applicable to ICI mitigation in the downlink and the uplink transmissions, respectively. Without sacrificing spectral efficiency, the proposed schemes have been demonstrated to effectively mitigate ICI and lower the error floor even in the presence of significant uncertainties in the channel statistics. To further reduce ICI over non-LOS channels, we have also extended the existing work in ICI self-cancellation and established a general reduced-rate OFDM transmission scheme to trade spectral efficiency for ICI mitigation in a high-mobility environment. We have designed the structure of transmit and receive preprocessing matrices so that the equivalent subchannels in the reduced-rate OFDM transmission system share a common average SIR, which is further maximized based on the statistics of the time-varying channel. Both numerical and simulation results have demonstrated the significant performance improvements of the developed reduced-rate OFDM transmission over the existing ICI self-cancellation schemes.

APPENDIX A

PROOF FOR CHAPTER 2

A.1 Derivation of $p_{ij}(k)$ and $o_{ij}(k)$

In this appendix, we show how to derive the expressions for $p_{ij}(k) = E\left\{r_{ij}(l+k)\widehat{r}^*_{ij}(l)\right\}$ and $o_{ij}(k) = E\left\{\widehat{r}_{ij}(l+k)\widehat{r}^*_{ij}(l)\right\}$ where $E\{\cdot\}$ denotes expectation with respect to both noise and the random channel over the RS-DS hop. Since $\widehat{r}_{ij}(k) = n_i(k)n^*_j(k)$ and $r_{ij}(k) = E_n\left\{n_i(k)n^*_j(k)\right\}$, where $E_n\{\cdot\}$ denotes expectation with respect to noise only, $p_{ij}(k)$ and $o_{ij}(k)$ can be regarded as the long-term correlation functions of the short-term correlation of the random overall noise,

$$\mathbf{n}(k) = g\mathbf{H}_2(k)\mathbf{n}_r(k) + \mathbf{n}_d(k), \tag{A.1}$$

where $\mathbf{H}_2(k)$ denotes the forward relay channel over the RS-DS hop and $\mathbf{n}_r(k)$ and $\mathbf{n}_d(k)$ denote the local white complex Gaussian noise vectors at the RS and the DS, respectively.

In [102], the authors have derived the long-term correlation functions of the short-term correlation of the random interference and noise,

$$\mathbf{v}(k) = \mathbf{C}(k)\mathbf{s}(k) + \mathbf{w}(k), \tag{A.2}$$

where the elements of $\mathbf{s}(k)$ are independent transmitted signals from different interferers with a constant amplitude, $\mathbf{C}(k)$ denotes the channel matrix between the interferers and the receiver, and $\mathbf{w}(k)$ denotes the local white complex Gaussian noise vector.

Noticing the differences in the statistics of $\mathbf{n}_r(k)$ and $\mathbf{s}(k)$, we follow the derivation in [102] and obtain the expressions for $p_{ij}(k)$ and $o_{ij}(k)$ in (2.23) and (2.24), respectively.

APPENDIX B

PROOF FOR CHAPTER 3

B.1 Proof of Proposition 3.2.1

According to (3.5), $\mathbf{Q}_l = \mathbf{H}_x^{-1}\mathbf{P}_l\mathbf{H}_x, 2 \le l \le L$, where $\mathbf{H}_x$ denotes the $N_r \times N_r$ relay channel matrix to estimate. Thus, according to the mixed-product property of the Kronecker product [97], we have

$$\begin{aligned}
\mathbf{A}_l &= \mathbf{I} \otimes \mathbf{P}_l - \mathbf{Q}_l^T \otimes \mathbf{I} \\
&= \mathbf{H}_x^T(\mathbf{H}_x^T)^{-1} \otimes \mathbf{P}_l - \mathbf{H}_x^T\mathbf{P}_l^T(\mathbf{H}_x^T)^{-1} \otimes \mathbf{I} \\
&= \left(\mathbf{H}_x^T \otimes \mathbf{I}\right)\left[(\mathbf{H}_x^T)^{-1} \otimes \mathbf{P}_l\right] - \left(\mathbf{H}_x^T \otimes \mathbf{I}\right)\left[\mathbf{P}_l^T(\mathbf{H}_x^T)^{-1} \otimes \mathbf{I}\right] \\
&= \left(\mathbf{H}_x^T \otimes \mathbf{I}\right)(\mathbf{I} \otimes \mathbf{P}_l)\left[\left(\mathbf{H}_x^T\right)^{-1} \otimes \mathbf{I}\right] - \left(\mathbf{H}_x^T \otimes \mathbf{I}\right)\left(\mathbf{P}_l^T \otimes \mathbf{I}\right)\left[\left(\mathbf{H}_x^T\right)^{-1} \otimes \mathbf{I}\right] \\
&= \left(\mathbf{H}_x^T \otimes \mathbf{I}\right)\left(\mathbf{I} \otimes \mathbf{P}_l - \mathbf{P}_l^T \otimes \mathbf{I}\right)\left(\mathbf{H}_x^T \otimes \mathbf{I}\right)^{-1}, \qquad \text{(B.1)}
\end{aligned}$$

where $\mathbf{I}$ denotes the $N_r \times N_r$ identity matrix. Define $\mathbf{W} = \mathbf{H}_x^T \otimes \mathbf{I}$; then, according to (B.1) and (3.11), $\mathbf{A}_l = \mathbf{W}\mathbf{B}_l\mathbf{W}^{-1}$, and therefore

$$\mathbf{A} = \begin{bmatrix} \mathbf{A}_2 \\ \mathbf{A}_3 \\ \vdots \\ \mathbf{A}_L \end{bmatrix} = \begin{bmatrix} \mathbf{W} & 0 & \cdots & 0 \\ 0 & \mathbf{W} & \cdots & 0 \\ \vdots & \vdots & \ddots & \vdots \\ 0 & 0 & \cdots & \mathbf{W} \end{bmatrix} \begin{bmatrix} \mathbf{B}_2 \\ \mathbf{B}_3 \\ \vdots \\ \mathbf{B}_L \end{bmatrix} \mathbf{W}^{-1}. \qquad \text{(B.2)}$$

Since $\mathbf{W}$ is invertible, (B.2) verifies that rank $(\mathbf{A})$ = rank $(\mathbf{B})$.

B.2 Proof of Proposition 3.2.3

For the equivalent problem, the original matrix equation w.r.t. $\mathbf{T}_1$ and $\mathbf{T}_2$ is given by

$$\mathbf{P}_l = \mathbf{T}_2\mathbf{P}_l\mathbf{T}_1, \quad 1 \le l \le L, \qquad \text{(B.3)}$$

Since $\mathbf{P}_1 = \mathbf{I}_{N_r}$ and $\mathbf{P}_1 = \mathbf{T}_2\mathbf{P}_1\mathbf{T}_1$, $\mathbf{T}_2 = \mathbf{T}_1^{-1}$. Therefore, (B.3) can be rewritten as

$$\mathbf{P}_l\mathbf{T}_1 = \mathbf{T}_1\mathbf{P}_l, \quad 2 \le l \le L, \qquad \text{(B.4)}$$

Similar to (3.10), Equation (B.4) can be rewritten in a compact manner as follows

$$\mathbf{B} \cdot \mathbf{t}_1 = 0. \tag{B.5}$$

where $\mathbf{B}$ is an $(L-1)N_r^2 \times N_r^2$ matrix defined in (3.11) and $\mathbf{t}_1 = \text{vec}(\mathbf{T}_1)$ denotes the vectorization of $\mathbf{T}_1$. Obviously the solutions to (B.5) have $N_r^2 - \text{rank}\,(\mathbf{B})$ DoF's. According to (3.10), the solutions to the original problem have $N_r^2 - \text{rank}\,(\mathbf{A})$ DoF's. Since $\text{rank}\,(\mathbf{A}) = \text{rank}\,(\mathbf{B})$ (See Appendix B.1), we conclude that the solutions to the original problem and those to the equivalent problem have the same DoF.

B.3 Proof of Invalidity of Permutated Pilot Matrices

In this Appendix, we will demonstrate that the two cascaded relay channels cannot be successfully estimated at the DN by setting $\{\mathbf{P}_l, 2 \le l \le L\}$ as the permutations of $\mathbf{P}_1$.

Without loss of generality, we let $\mathbf{P}_1 = \mathbf{I}_{N_r}$ and thus $\{\mathbf{P}_l, 1 \le l \le L\}$ will be a set of permutation matrices. Denote $\mathbf{E}$ to be an all-one $N_r \times N_r$ square matrix, and then obviously

$$\mathbf{P}_l\mathbf{E} = \mathbf{E}\mathbf{P}_l, \quad 1 \le l \le L. \tag{B.6}$$

Define $\mathbf{T} = a\mathbf{E} + b\mathbf{I}_{N_r}$, where $b \neq 0$ and $-N_r a$. Since $|\mathbf{T}| = b^{N_r-1}(b + N_r a) \neq 0$, $\mathbf{T}$ is invertible. According to (B.6),

$$\mathbf{P}_l\mathbf{T} = \mathbf{T}\mathbf{P}_l, \quad 1 \le l \le L. \tag{B.7}$$

which can be rewritten as

$$\mathbf{P}_l = \mathbf{T}\mathbf{P}_l\mathbf{T}^{-1}, \quad 1 \le l \le L. \tag{B.8}$$

Equation (B.8) indicates that, for permutation matrices $\{\mathbf{P}_l, 1 \le l \le L\}$, $\mathbf{T}_2 = \mathbf{T}$ and $\mathbf{T}_1 = \mathbf{T}^{-1}$ are solutions to the equivalent problem in (3.14). Since $\mathbf{T}$ has two DoF's embodied in the unknown a and b, respectively, successful relay channel estimation is impossible according to Proposition 3.2.3. Intuitively, suppose that $\mathbf{H}_1^*$ and $\mathbf{H}_2^*$ are solutions to

$$\mathbf{H}_{o,l} = \mathbf{H}_2\mathbf{P}_l\mathbf{H}_1, \quad 1 \le l \le L, \tag{B.9}$$

and then, according to (B.8), $\mathbf{T}^{-1}\mathbf{H}_1^*$ and $\mathbf{H}_2^*\mathbf{T}$ are also solutions to (B.9). Since $\mathbf{T}$ has two DoF's, the relay channels cannot be successfully estimated.

B.4 Proof of Proposition 3.2.4

Suppose K_{max} is the maximum number of eigenvector clusters of $\{\mathbf{P}_l, 2 \le l \le L\}$. We will first show that $K_{max} = 1$ is a necessary condition for successful relay channel estimation by constructing a $\mathbf{T}_2$ with K_{max} DoF's that satisfies Equation (3.16) in the equivalent problem.

Construct

$$\mathbf{U} = \left(\mathbf{e}_{11}, \mathbf{e}_{12}, \cdots, \mathbf{e}_{1n_1}; \cdots; \mathbf{e}_{K_{max}1}, \mathbf{e}_{K_{max}2}, \cdots, \mathbf{e}_{K_{max}n_{K_{max}}}\right), \tag{B.10}$$

as an eigenvector matrix of $\mathbf{T}_2$, where $\mathbf{e}_{kn}$ $(1 \le k \le K_{max}, 1 \le n \le n_k)$ denotes the nth base of the n_k-dimension space, S_k, which is spanned by the kth eigenvector cluster of each pilot matrix. Further let S_k be the kth eigenspace of $\mathbf{T}_2$ with the associated eigenvalue λ_k, i.e., $\forall \mathbf{v} \in S_k, \mathbf{T}_2\mathbf{v} = \lambda_k\mathbf{v}$. Define $\Lambda_k = \lambda_k\mathbf{I}_{n_k}$, then,

$$\mathbf{T}_2 = \mathbf{U}\Sigma\mathbf{U}^{-1}, \tag{B.11}$$

where $\Sigma = \text{diag}\{\Lambda_1, \Lambda_2, \cdots, \Lambda_{K_{max}}\}$ denotes the $N_r \times N_r$ diagonal eigenvalue matrix. According to the eigenvector grouping rule, for any $2 \le l \le L$, invertible transform $\mathbf{P}_l$ maps space S_k to itself, i.e., $\forall \mathbf{v} \in S_k, \mathbf{P}_l\mathbf{v} \in S_k$. As a result, $\mathbf{P}_l\mathbf{U}$ is still an eigenvector matrix of $\mathbf{T}_2$ for any $2 \le l \le L$, which indicates that $\mathbf{T}_2$ in (B.11), which has K_{max} DoF's embodied in K_{max} independent eigenvalues, satisfies Equation (3.16) and therefore is a solution to the equivalent problem. According to Proposition 3.2.3, successful relay channel estimation is guaranteed if and only if the solutions to the equivalent problem have only one DoF. Thus we conclude that $K_{max} = 1$ is a necessary condition for successful relay channel estimation.

To show that $K_{max} = 1$ is also a sufficient condition for successful relay channel estimation, we suppose that when $K_{max} = 1$, there exists an invertible $\mathbf{T}_2 \ne \alpha\mathbf{I}_2$, where α denotes an arbitrary complex scalar, that satisfies Equation (3.16). Since $\mathbf{T}_2 \ne \alpha\mathbf{I}_2$, it has J $(J \ge 2)$ different eigenvalues corresponding to J different eigenspaces, $S_j, 1 \le j \le J$. According

to (3.16), if $\mathbf{U}$ is an eigenvector matrix of $\mathbf{T}_2$, so is $\mathbf{P}_l\mathbf{U}, 2 \leq l \leq L$. In other words, for any $2 \leq l \leq L$, transform $\mathbf{P}_l$ maps S_j to itself, which means S_j for any j is a space spanned by eigenvectors of any pilot matrix, $\mathbf{P}_l$. According to the eigenvector grouping rule, the maximum number of eigenvector clusters of $\mathbf{P}_l$'s is greater than or equal to J, which is contradictory to the supposition that $K_{max} = 1$. Therefore, $\mathbf{T}_2 = \alpha\mathbf{I}_2$, where α denotes an arbitrary scalar, is the sole solution to Equation (3.16) when $K_{max} = 1$. According to Proposition 3.2.3, we conclude $K_{max} = 1$ is also a sufficient condition for successful relay channel estimation.

B.5 Proof of Validity of Design Rules

To prove that the design rules given in Section 3.3 ensure successful relay channel estimation, we will first show the following fact.

Fact 1 *Any eigenvector of $\boldsymbol{P}_3$ does not have zero elements if $\boldsymbol{P}_3$ is an indivisible permutation of $\boldsymbol{P}_2$.*

Proof According to the design rules given in Section 3.3,

$$\mathbf{P}_2 = \left(\mathbf{r}_1^T, \mathbf{r}_2^T, \cdots, \mathbf{r}_{N_r}^T\right)^T = \text{diag}\{\gamma_1, \gamma_2, \cdots, \gamma_{N_r}\}, \tag{B.12}$$

where $\mathbf{r}_i$ denotes the ith row vector of $\mathbf{P}_2$ and $\text{diag}\{\gamma_1, \gamma_2, \cdots, \gamma_{N_r}\}$ denotes a diagonal matrix with diagonal elements $\gamma_1, \gamma_2, \cdots, \gamma_{N_r}$. As a permutation of $\mathbf{P}_2$,

$$\mathbf{P}_3 = \left(\mathbf{r}_{f^{-1}(1)}^T, \mathbf{r}_{f^{-1}(2)}^T, \cdots, \mathbf{r}_{f^{-1}(N_r)}^T\right)^T, \tag{B.13}$$

where $f^{-1}(i) = j$ if i is directly reachable from j.

Suppose $\mathbf{v} = (v_1, v_2, \cdots, v_{N_r})^T$ is a non-zero eigenvector of $\mathbf{P}_3$ with the associated eigenvalue, λ, and then $\mathbf{P}_3\mathbf{v} = \lambda\mathbf{v}$, i.e.,

$$\mathbf{r}_{f^{-1}(i)} \cdot \mathbf{v} = \gamma_{f^{-1}(i)} v_{f^{-1}(i)} = \lambda v_i, \quad 1 \leq i \leq N_r. \tag{B.14}$$

Suppose $v_i = 0$ for an i. Since both $\mathbf{P}_2$ and $\mathbf{P}_3$ are unitary, $\gamma_{f^{-1}(i)} \neq 0$ and $\lambda \neq 0$. As a result, $v_{f^{-1}(i)}$ must be zero to satisfy Equation (B.14). For the same reason, it can be

shown that $v_j = 0$ for any j that reaches i. Since $\mathbf{P}_3$ is an indivisible permutation of $\mathbf{P}_3$, any $j \in \{1, 2, \cdots, N_r\}$ reaches i. As a result, $\mathbf{v}$ must be a zero vector, which is contradictory to the above supposition. Thus we conclude that any eigenvector of $\mathbf{P}_3$ does not have zero elements.

Since $\mathbf{P}_2$ is a diagonal matrix with N_r different non-zero elements, the standard bases of an N_r-dimension space, $\mathbf{e}_1 = [1, 0, \cdots, 0]^T, \mathbf{e}_2 = [0, 1, \cdots, 0]^T, \cdots, \mathbf{e}_{N_r} = [0, 0, \cdots, 1]^T$, constitute the N_r eigenvectors of $\mathbf{P}_2$. According to *Fact 1*, any eigenvector of $\mathbf{P}_3$ does not have zero elements and hence does not fall in any subspace spanned by a subset of the standard bases, $\{\mathbf{e}_1, \mathbf{e}_2, \cdots, \mathbf{e}_{N_r}\}$, which, according to the eigenvector grouping rule, means that $\mathbf{P}_2$ and $\mathbf{P}_3$ have only one eigenvector cluster. According to Proposition 3.2.4, we conclude that the design rules given in Section 3.3 ensure successful relay channel estimation.

APPENDIX C

PROOF FOR CHAPTER 4

C.1 Proof of Independence of $\mathbf{s}_N(n)$ and $\hat{\mathbf{X}}_N(n)$

In this appendix, we show that $\mathbf{s}_N(n)$ is statistically independent of $\hat{\mathbf{X}}_N(n)$ when the DF and constant amplitude modulation schemes are applied.

As before, denote

$$\mathbf{x}(n,k) = \left(x_{n,k}^0, x_{n,k}^1, \cdots, x_{n,k}^{M_s-1}\right)^T \tag{C.1}$$

and

$$\hat{\mathbf{x}}(n,k) = \left(\hat{x}_{n,k}^0, \hat{x}_{n,k}^1, \cdots, \hat{x}_{n,k}^{M_t-1}\right)^T \tag{C.2}$$

as the transmitted symbol vector of the SS and the corresponding forwarded symbol vector of the RS, respectively. Without loss of generality, we assume that elements of both of them have constant unit amplitude, i.e., $\left|x_{n,k}^j\right|^2 = \left|\hat{x}_{n,k}^l\right|^2 = 1$, where $0 \le j \le M_s - 1$ and $0 \le l \le M_t - 1$. Further define the received desired signal vector at the RS as

$$\mathbf{s}(n,k) = \left(s_{n,k}^0, s_{n,k}^1, \cdots, s_{n,k}^{M_r-1}\right)^T, \tag{C.3}$$

and then

$$s_{n,k}^i = \sum_{j=0}^{M_s-1} h_{n,k}^{i,j} x_{n,k}^j, \quad 0 \le i \le M_r - 1, \tag{C.4}$$

where $h_{n,k}^{i,j}$ denotes the element of $\mathbf{H}_r(n,k)$, the frequency-domain channel matrix from the SS to the RS on the kth subcarrier of the nth OFDM symbol, at the ith row and the jth column. Here we assume that the wireless channel from the SS to the RS is with Rayleigh fading and therefore $h_{n,k}^{i,j}$ is a *circularly symmetric complex Gaussian* (CSCG) random variable. Define $s_{n,k}^{i,j} = h_{n,k}^{i,j} x_{n,k}^j$; since $h_{n,k}^{i,j}$ is CSCG and $\left|x_{n,k}^j\right|^2 = 1$, obviously $s_{n,k}^{i,j}$ share exactly the same statistical distribution with $h_{n,k}^{i,j}$. In other words, $s_{n,k}^{i,j}$ is independent of $x_{n,k}^j$. Since $s_{n,k}^i = \sum_{j=0}^{M_s-1} s_{n,k}^{i,j}$, we can further show that $s_{n,k}^i$ and even $\mathbf{s}(n,k)$ are independent of $\mathbf{x}(n,k)$. As a result, $\mathbf{s}(n,k)$ is also independent of $\hat{\mathbf{x}}(n,k)$, the forwarded version of

$\mathbf{x}(n,k)$ at the RS. Considering that $\mathbf{s}_N(n)$ and $\hat{\mathbf{X}}_N(n)$ consist of $\mathbf{s}(n,k)$ and $\hat{\mathbf{x}}(n,k)$ with different k's and n's, respectively, we conclude that $\mathbf{s}_N(n)$ is statistically independent of $\hat{\mathbf{X}}_N(n)$, which completes the proof.

APPENDIX D

PROOF FOR CHAPTER 6

D.1 Proof of Proposition 6.3.3

When $K = \frac{N}{2}$, Equation (6.21) can be rewritten as

$$\begin{aligned}\mathbf{H}_K\left((j+l)_K, j\right) = & \sum_{\Delta=0}^{L-1} \mathbf{B}\left((j+l)_K, (j+\Delta)_N\right) \mathbf{H}_N\left((j+\Delta)_N, j\right) \mathbf{A}\left(j, j\right) \\ & + \sum_{\Delta=0}^{L-1} \mathbf{B}\left((j+l)_K, (j+K+\Delta)_N\right) \mathbf{H}_N\left((j+K+\Delta)_N, j+K\right) \mathbf{A}\left(j+K, j\right).\end{aligned} \tag{D.1}$$

According to the structure of $\mathbf{B}$, $\mathbf{B}\left((j+l)_K, n\right)$ is equal to zero unless $n = (j+l)_N$ or $(j+K+l)_N$. Since $0 \le \Delta \le L-1 \le K-1$, Equation (D.1) reduces to

$$\begin{aligned}\mathbf{H}_K\left((j+l)_K, j\right) = \mathrm{I}_{l \le L-1}\Big[& \mathbf{B}\left((j+l)_K, (j+l)_N\right) \mathbf{H}_N\left((j+l)_N, j\right) \mathbf{A}\left(j, j\right) \\ & + \mathbf{B}\left((j+l)_K, (j+K+l)_N\right) \mathbf{H}_N\left((j+K+l)_N, j+K\right) \mathbf{A}\left(j+K, j\right) \Big].\end{aligned} \tag{D.2}$$

Since $\mathbf{H}_N\left((j+l)_N, j\right) = 0$ for any j if $l > L-1$, the above equation can be rewritten as

$$\mathbf{H}_K\left((j+l)_K, j\right) = \alpha_j \beta_{j+l} \mathbf{H}_N\left(j+l, j\right) + \alpha_{j+K} \beta_{(j+K+l)_N} \mathbf{H}_N\left((j+K+l)_N, j+K\right), \tag{D.3}$$

for any $0 \le j, l \le K-1$. Equation (D.3) verifies that there is a one-to-one mapping from path l in $\mathbf{H}_N$ to path l in $\mathbf{H}_K$. According to Proposition 6.3.2, all of the equivalent subchannels have a common SIR, which completes the proof.

D.2 Proof of Proposition 6.3.4

With $L \le N-K+1$ and $\alpha_n = 0, N-(L-1) \le n \le N-1$, Equation (6.21) can be rewritten as

$$\begin{aligned}\mathbf{H}_K\left((j+l)_K, j\right) = & \textstyle\sum_{\Delta=0}^{L-1} \mathbf{B}\left((j+l)_K, j+\Delta\right) \mathbf{H}_N\left(j+\Delta, j\right) \mathbf{A}\left(j, j\right) \\ & + \mathrm{I}_{j \le N-K-L} \textstyle\sum_{\Delta=0}^{L-1} \mathbf{B}\left((j+l)_K, j+K+\Delta\right) \mathbf{H}_N\left(j+K+\Delta, j+K\right) \mathbf{A}\left(j+K, j\right).\end{aligned} \tag{D.4}$$

According to the structure of $\mathbf{B}$, $\mathbf{B}\left((j+l)_K, n\right)$ is equal to zero unless $n = j+l-K$, $j+l$, or $j+l+K$ depending on the specific values of j and l. Since $0 \leq \Delta \leq L-1 \leq N-K$, Equation (D.4) reduces to

$$\begin{aligned}\mathbf{H}_K\left((j+l)_K, j\right) = \mathrm{I}_{l\leq L-1}\Big[&\mathbf{B}\left((j+l)_K, j+l\right)\mathbf{H}_N\left(j+l, j\right)\mathbf{A}\left(j, j\right) \\ &+\mathrm{I}_{j\leq N-K-L}\mathbf{B}\left((j+l)_K, j+K+l\right)\mathbf{H}_N\left(j+K+l, j+K\right)\mathbf{A}\left(j+K, j\right)\Big].\end{aligned} \tag{D.5}$$

Since $\mathbf{H}_N\left(j+l, j\right) = 0$ for any j if $l > L-1$, the above equation can be rewritten as

$$\mathbf{H}_K\left((j+l)_K, j\right) = \alpha_j\beta_{j+l}\mathbf{H}_N\left(j+l, j\right) + \mathrm{I}_{j\leq N-K-L}\alpha_{j+K}\beta_{j+K+l}\mathbf{H}_N\left(j+K+l, j+K\right), \tag{D.6}$$

for any $0 \leq j, l \leq K-1$. Equation (D.6) verifies that there is a one-to-one mapping from path l in $\mathbf{H}_N$ to path l in $\mathbf{H}_K$. According to Proposition 6.3.2, all of the equivalent subchannels have a common SIR, which completes the proof.

REFERENCES

[1] D. Soldani and S. Dixit, "Wireless relays for broadband access," *IEEE Commun. Mag.*, vol. 46, pp. 58–66, Mar. 2008.

[2] S. W. Peters and R. W. Heath, "The future of WiMAX: multihop relaying with IEEE 802.16j," *IEEE Commun. Mag.*, vol. 47, pp. 104–111, Jan. 2009.

[3] A. H. Ali and J. G. Gardiner, "The performance of repeaters in UMTS networks," in *Proc. IEEE Mediterranean Electrotechnical Conf.*, pp. 465–468, May 2004.

[4] A. Nosratinia, T. E. Hunter, and A. Hedayat, "Cooperative communication in wireless networks," *IEEE Commun. Mag.*, vol. 42, pp. 74–80, Oct. 2004.

[5] P. Liu, Z. Tao, Z. Lin, E. Erkip, and S. Panwar, "Cooperative wireless communications: A cross-layer approach," *IEEE Wireless Commun. Mag.*, vol. 13, pp. 84–92, Aug. 2006.

[6] A. Scaglione, D. L. Goeckel, and J. N. Laneman, "Cooperative communications in mobile ad-hoc networks," *IEEE Signal Processing Mag.*, vol. 23, pp. 18–29, Sept. 2006.

[7] A. Sendonaris, E. Erkip, and B. Aazhang, "User cooperation diversity-part I: system description," *IEEE Trans. Commun.*, vol. 51, pp. 1927–1938, Nov. 2003.

[8] A. Sendonaris, E. Erkip, and B. Aazhang, "User cooperation diversity-part II: implementation aspects and performance analysis," *IEEE Trans. Commun.*, vol. 51, pp. 1939–1948, Nov. 2003.

[9] A. Sendonaris, E. Erkip, and B. Aazhang, "Increasing uplink capacity via user cooperation diversity," in *Proc. IEEE Int. Symposium on Inf. Theory*, p. 156, Aug. 1998.

[10] J. Laneman, D. N. C. Tse, and G. W. Wornell, "Cooperative diversity in wireless networks: efficient protocols and outage behavior," *IEEE Trans. Inf. Theory.*, vol. 50, pp. 3062–3080, Dec. 2004.

[11] J. Laneman and G. W. Wornell, "Distributed space-time-coded protocols for exploiting cooperative diversity in wireless networks," *IEEE Trans. Inf. Theory.*, vol. 49, pp. 2415–2425, Oct. 2003.

[12] T. E. Hunter and A. Nosratinia, "Diversity through coded cooperation," *IEEE Trans. Wireless Commun.*, vol. 5, pp. 283–289, Feb. 2006.

[13] T. E. Hunter, S. Sanayei, and A. Nosratinia, "Outage analysis of coded cooperation," *IEEE Trans. Inf. Theory.*, vol. 52, pp. 375–391, Feb. 2006.

[14] K. Salehian, M. Guillet, B. Caron, and A. Kennedy, "On-channel repeater for digital television broadcasting service," *IEEE Trans. Broadcasting*, vol. 48, pp. 97–102, June 2002.

[15] K. M. Nasr, J. P. Cosmas, M. Bard, and J. Gledhill, "Performance of an echo canceller and channel estimator for on-channel repeaters in DVB-T/H networks," *IEEE Trans. Broadcasting*, vol. 53, pp. 609–618, Sept. 2007.

[16] S. I. Park, S. R. Park, H. Eum, J. Y. Lee, Y. T. Lee, and H. M. Kim, "Equalization on-channel repeater for terrestrial digital multimedia broadcasting system," *IEEE Trans. Broadcasting*, vol. 54, pp. 752–760, Dec. 2008.

[17] O. M. Medina, J. Vidal, and A. Agustin, "Linear transceiver design in nonregenerative relays with channel state information," *IEEE Trans. Signal Processing*, vol. 55, pp. 2593–2604, June 2007.

[18] I. Hammerstrom and A. Wittneben, "Power allocation schemes for amplify-and-forward MIMO-OFDM relay links," *IEEE Trans. Wireless Commun.*, vol. 6, pp. 2798–2802, Aug. 2007.

[19] X. Tang and Y. Hua, "Optimal design of non-regenerative MIMO wireless relays," *IEEE Trans. Wireless Commun.*, vol. 6, pp. 1398–1407, Apr. 2007.

[20] J. Ma, P. Orlik, J. Zhang, and G. Y. Li, "Pilot matrix design for interim channel estimation in two-hop MIMO AF relay systems," in *Proc. IEEE Int. Conf. on Commun.*, 2009.

[21] M. Mazzotti, F. Zabini, D. Dardari, and O. Andrisano, "Performance of an echo canceller based on pseudo-noise training sequences," in *Proc. 58th Annual IEEE Broadcast Symposium*, Oct. 2008.

[22] J. Ma, G. Y. Li, J. Y. Zhang, T. Kuze, and H. Iura, "A new coupling channel estimator for cross-talk cancellation at wireless relay stations," in *Proc. IEEE Globecom 2009*, Nov. 2009.

[23] J. Ma, P. Orlik, J. Zhang, and G. Y. Li, "ICI mitigation in high-mobility OFDM over line-of-sight channels," *submitted to IEEE Trans. Wireless Commun.*

[24] S. Alamouti, "A simple transmit diversity technique for wireless communications," *IEEE J. Sel. Areas Commun.*, vol. 16, pp. 1451–1458, Oct. 1998.

[25] V. Tarokh, N. Seshadri, and A. Calderbank, "Space-time codes for high data rate wireless communications: Performance criterion and code construction," *IEEE Trans. Inf. Theory.*, vol. 44, pp. 744–765, Mar. 1998.

[26] V. Tarokh, H. Jafarkhani, and A. R. Calderbank, "Space-time block codes from orthogonal designs," *IEEE Trans. Inf. Theory.*, vol. 45, pp. 1456–1467, July 1999.

[27] G. J. Foschini and M. J. Gans, "On limits of wireless communications in a fading environment when using multiple antennas," *Wireless Personal Commun.*, vol. 6, pp. 311–335, Mar. 1998.

[28] I. E. Telatar, "Capacity of multi-antenna gaussian channels," *Europ. Trans. Telecommun.*, vol. 10, pp. 585–595, Nov. 1999.

[29] P. W. Wolniansky, G. J. Foschini, G. D. Golden, and R. A. Valenzuela, "V-BLAST: an architecture for realizing very high data rates over the rich-scattering wireless channel," in *Proc. Int. Symposium on Signals, Systems, and Electronics*, pp. 295–300, Oct. 1998.

[30] L. Zheng and D. N. C. Tse, "Diversity and multiplexing: A fundamental tradeoff in multiple-antenna channels," *IEEE Trans. Inf. Theory.*, vol. 49, pp. 1073–1096, May 2003.

[31] H. Shin and J. B. Song, "MRC analysis of cooperative diversity with fixed-gain relays in Nakagami-m fading channels," *IEEE Trans. Wireless Commun.*, vol. 7, pp. 2069–2074, June 2008.

[32] S. S. Ikki and M. H. Ahmed, "Performance of cooperative diversity using equal gain combining (EGC) over Nakagami-m fading channels," *IEEE Trans. Wireless Commun.*, vol. 8, pp. 557–562, Feb. 2009.

[33] A. Ribeiro, X. Cai, and G. B. Giannakis, "Symbol error probabilities for general cooperative links," *IEEE Trans. Wireless Commun.*, vol. 4, pp. 1264–1273, May 2005.

[34] G. Farhadi and N. C. Beaulieu, "On the performance of amplify-and-forward cooperative systems with fixed gain relays," *IEEE Trans. Wireless Commun.*, vol. 7, pp. 1851–1856, May 2008.

[35] A. Scaglione and Y.-W. Hong, "Opportunistic large arrays: cooperative transmission in wireless multihop ad hoc networks to reach far distances," *IEEE Trans. Signal Processing*, vol. 51, pp. 2082–2092, Aug. 2003.

[36] M. O. Hasna and M. S. Alouini, "A performance study of dual-hop transmissions with fixed gain relays," *IEEE Trans. Wireless Commun.*, vol. 3, pp. 1963–1968, Nov. 2004.

[37] M. O. Hasna and M. S. Alouini, "End-to-end performance of transmission systems with relays over Rayleigh-fading channels," *IEEE Trans. Wireless Commun.*, vol. 2, pp. 1126–1131, Nov. 2003.

[38] M. O. Hasna and M. S. Alouini, "Harmonic mean and end-to-end performance of transmission systems with relays," *IEEE Trans. Commun.*, vol. 52, pp. 130–135, Jan. 2004.

[39] H. A. Suraweera, R. H. Y. Louie, Y. Li, G. K. Karagiannidis, and B. Vucetic, "Two hop amplify-and-forward transmission in mixed Rayleigh and Rician fading channels," *IEEE Commun. Let.*, vol. 13, pp. 227–229, Apr. 2009.

[40] M. O. Hasna and M. S. Alouini, "Outage probability of multihop transmission over Nakagami fading channels," *IEEE Commun. Let.*, vol. 7, pp. 216–218, May 2003.

[41] G. K. Karagiannidis, "Performance bounds of multihop wireless communications with blind relays over generalized fading channels," *IEEE Trans. Wireless Commun.*, vol. 5, pp. 498–503, Mar. 2006.

[42] G. K. Karagiannidis, "Bounds for multihop relayed communications in Nakagami-m fading," *IEEE Trans. Commun.*, vol. 54, pp. 18–22, Jan. 2006.

[43] J. Boyer, D. D. Falconer, and H. Yanikomeroglu, "Multihop diversity in wireless relaying channels," *IEEE Trans. Commun.*, vol. 52, pp. 1820–1830, Oct. 2004.

[44] G. Farhadi and N. C. Beaulieu, "On the ergodic capacity of wireless relaying systems over Rayleigh fading channels," *IEEE Trans. Wireless Commun.*, vol. 7, pp. 4462–4467, Nov. 2008.

[45] G. Farhadi and N. C. Beaulieu, "On the ergodic capacity of multi-hop wireless relaying systems," *IEEE Trans. Wireless Commun.*, vol. 8, pp. 2286–2291, May 2009.

[46] M. O. Hasna and M. S. Alouini, "Optimal power allocation for relayed transmissions over Rayleigh-fading channels," *IEEE Trans. Wireless Commun.*, vol. 3, pp. 1999–2004, Nov. 2004.

[47] G. Farhadi and N. C. Beaulieu, "Power-optimized amplify-and-forward multi-hop relaying systems," *IEEE Trans. Wireless Commun.*, vol. 8, pp. 4634–4643, Sept. 2009.

[48] M. Dohler, A. Gkelias, and H. Aghvami, "2-hop distributed MIMO communication system," *Electronics Let.*, vol. 39, pp. 1350–1351, Sept. 2003.

[49] A. I. Sulyman, G. Takahara, H. S. Hassanein, and M. Kousa, "Multi-hop capacity of MIMO-multiplexing relaying systems," *IEEE Trans. Wireless Commun.*, vol. 8, pp. 3095–3103, June 2009.

[50] S. Jin, M. R. McKay, C. Zhong, and K. K. Wong, "Ergodic capacity analysis of amplify-and-forward MIMO dual-hop systems," in *Proc. IEEE Int. Symposium on Inf. Theory*, pp. 1903–1907, July 2008.

[51] A. Wittneben and B. Rankov, "Impact of cooperative relays on the capacity of rank-deficient MIMO channels," in *Proc. IST Summit on Mobile and Wireless Commun.*, pp. 421–425, June 2003.

[52] W. Guan and H. Luo, "Joint MMSE transceiver design in non-regenerative MIMO relay systems," *IEEE Commun. Let.*, vol. 12, pp. 517–519, July 2008.

[53] M. Herdin, "MIMO amplify-and-forward relaying in correlated MIMO channels," in *Proc. Int. Conf. on Inf., Commun. and Signal Processing*, pp. 796–800, 2005.

[54] C. S. Patel, G. L. Stüber, and T. G. Pratt, "Statistical properties of amplify and forward relay channels," *IEEE Trans. Veh. Tech.*, vol. 55, pp. 1–9, Jan. 2006.

[55] C. S. Patel and G. L. Stüber, "Channel estimation for amplify and forward relay based cooperation diversity systems," *IEEE Trans. Wireless Commun.*, vol. 6, pp. 2348–2356, June 2007.

[56] F. Gao, T. Cui, and A. Nallanathan, "On channel estimation and optimal training design for amplify and forward relay networks," *IEEE Trans. Wireless Commun.*, vol. 7, pp. 1907–1916, May 2008.

[57] A. S. Lalos, A. A. Rontogiannis, and K. Berberidis, "Channel estimation techniques in amplify and forward relay networks," in *Proc. IEEE Workshop on Signal Processing Advances in Wireless Commun.*, pp. 446–450, July 2008.

[58] B. Gedik and M. Uysal, "Two channel estimation methods for amplify-and-forward relay networks," in *Proc. IEEE Canadian Conf. on Electrical and Computer Engineering*, pp. 615–618, May 2008.

[59] W. T. Slingsby and J. P. McCeehan, "Antenna isolation measurements for on-frequency radio repeaters," in *Proc. 9th Int. Conf. on Antennas and Propag.*, vol. 1, pp. 239–243, Apr. 1995.

[60] A. S. M. Marzuki, A. R. Rahim, B. Mohmd, K. Khalil, A. Naemat, and A. Tee, "Antenna isolation considerations in WCDMA repeater deployment," in *Proc. 2006 Int. RF and Microwave Conf.*, pp. 347–350, Sept. 2006.

[61] S. J. Kim, J. Y. Lee, J. C. Lee, J. H. Kim, B. Lee, and N. Y. Kim, "Adaptive feedback interference cancellation system (AF-ICS)," in *IEEE Microwave Symposium (MTT-S) Digest*, pp. 627–630, 2003.

[62] J. Lee, S. Park, H. Choi, Y. Jeong, and J. Yun, "A design of co-channel feedback interference cancellation system using analog control," in *Proc. 36th European Microwave Conf.*, Sept. 2006.

[63] G. Y. Li and G. Stuber, *OFDM for Wireless Communications*. Boston, MA: Springer, Inc., 2006.

[64] M. Russell and G. L. Stüber, "Interchannel interference analysis of OFDM in a mobile environment," in *Proc. IEEE Veh. Tech. Conf.*, pp. 820–824, July 1995.

[65] P. Robertson and S. Kaiser, "The effects of Doppler spreads in OFDM(A) mobile radio systems," in *Proc. IEEE Veh. Tech. Conf.*, pp. 329–333, Sept. 1999.

[66] J. Li and M. Kavehrad, "Effects of time selective multipath fading on OFDM systems for broadband mobile applications," *IEEE Commun. Let.*, vol. 3, pp. 332–334, Dec. 1999.

[67] G. Y. Li and L. Cimini, "Bounds on the inter-channel interference of OFDM in time-varying impairments," *IEEE Trans. Wireless Commun.*, vol. 49, pp. 401–404, Mar. 2001.

[68] X. Cai and G. B. Giannakis, "Bounding performance and suppressing intercarrier interference in wireless mobile OFDM," *IEEE Trans. Commun.*, vol. 51, pp. 2047–2056, Dec. 2003.

[69] Z. J. Tang, R. C. Cannizzaro, G. Leus, and P. Banelli, "Pilot-assisted time-varying channel estimation for OFDM systems," *IEEE Trans. Signal Processing*, vol. 55, pp. 2226–2238, May 2007.

[70] S. Lu and N. Al-Dhahir, "Coherent and differential ICI cancellation for mobile OFDM with application to DVB-H," *IEEE Trans. Wireless Commun.*, vol. 7, pp. 4110–4116, Nov. 2008.

[71] S. Lu, R. Kalbasi, and N. Al-Dhahir, "OFDM interference mitigation algorithms for doubly-selective channels," in *Proc. IEEE Veh. Tech. Conf.*, Sept. 2006.

[72] W. Jeon, K. Chang, and Y. Cho, "An equalization technique for orthogonal frequency-division multiplexing systems in time-variant multipath channels," *IEEE Trans. Commun.*, vol. 47, pp. 27–32, Jan. 1999.

[73] Y. Mostofi and D. C. Cox, "ICI mitigation for pilot-aided OFDM mobile systems," *IEEE Trans. Wireless Commun.*, vol. 4, pp. 765–774, Mar. 2005.

[74] A. Stamoulis, S. Diggavi, and N. Al-Dhahir, "Intercarrier interference in MIMO OFDM," *IEEE Trans. Signal Processing*, vol. 50, pp. 2451–2464, Oct. 2002.

[75] W.-G. Song and J.-T. Lim, "Channel estimation and signal detection for MIMO-OFDM with time varying channels," *IEEE Commun. Let.*, vol. 10, pp. 540–542, July 2006.

[76] H. Hussein and R. Laurent, "Polynomial estimation of time-varying multipath gains with intercarrier interference mitigation in OFDM systems," *IEEE Trans. Veh. Tech.*, vol. 58, pp. 140–151, Jan. 2009.

[77] H. Senol, H. A. Cirpan, and E. Panayirci, "A low-complexity KL expansion-based channel estimator for OFDM systems," *EURASIP J. Wireless Commun. Netw.*, vol. 2005, pp. 163–174, Feb. 2005.

[78] T. Y. Al-Naffouri, K. M. Z. Islam, N. Al-Dhahir, and S. Lu, "A model reduction approach for OFDM channel estimation under high mobility conditions," *IEEE Trans. Signal Processing*, vol. 58, pp. 2181–2192, Apr. 2010.

[79] S. Tomasin, A. Gorokhov, H. Yang, and J.-P. Linnartz, "Iterative interference cancellation and channel estimation for mobile OFDM," *IEEE Trans. Wireless Commun.*, vol. 4, pp. 238–245, Jan. 2005.

[80] A. F. Molisch, M. Toeltsch, and S. Vermani, "Iterative methods for cancellation of intercarrier interference in OFDM systems," *IEEE Trans. Veh. Tech.*, vol. 56, pp. 2158–2167, July 2007.

[81] Z. Hong and L. Thibault, "A novel channel estimation and ICI cancellation for mobile OFDM systems," in *Proc. IEEE Int. Symposium on Personal, Indoor and Mobile Radio Commun.*, Sept. 2007.

[82] Y. Zhao and S. G. Haggman, "Intercarrier interference compression in OFDM communication systems by using correlative coding," *IEEE Commun. Let.*, vol. 2, pp. 214–216, Aug. 1998.

[83] H. Zhang and G. Y. Li, "Optimum frequency-domain partial response encoding in OFDM system," *IEEE Trans. Commun.*, vol. 51, pp. 1064–1068, July 2003.

[84] Y. Zhang and H. Liu, "Frequency-domain correlative coding for MIMO-OFDM systems over fast fading channels," *IEEE Commun. Let.*, vol. 10, pp. 347–349, May 2006.

[85] J. Armstrong, "Analysis of new and existing methods of reducing intercarrier interference due to carrier frequency offset in OFDM," *IEEE Trans. Commun.*, vol. 47, pp. 365–369, Mar. 1999.

[86] L. Rugini and P. Banelli, "Windowing techniques for ICI mitigation in multicarrier systems," in *Proc. Euro. Signal Process. Conf. (EUSIPCO)*, Sept. 2005.

[87] P. Schniter, "Low-complexity equalization of OFDM in doubly selective channels," *IEEE Trans. Signal Processing*, vol. 52, pp. 1002–1011, Apr. 2004.

[88] Y. Zhao and S. G. Haggman, "Intercarrier interference self-cancellation scheme for OFDM mobile communication systems," *IEEE Trans. Commun.*, vol. 49, pp. 1185–1191, July 2001.

[89] A. Seyedi and G. J. Saulnier, "General ICI self-cancellation scheme for OFDM systems," *IEEE Trans. Veh. Tech.*, vol. 54, pp. 198–210, Jan. 2005.

[90] M. X. Chang, "A novel algorithm of inter-subchannel interference self-cancellation for OFDM systems," *IEEE Trans. Wireless Commun.*, vol. 6, pp. 2881–2893, Aug. 2007.

[91] A. Papoulis, *Probability, Random Variables, and Stochastic Process 4th Ed*. New York: McGraw-Hill, 2002.

[92] S. M. Kay, *Fundamentals of Statistical Signal Processing: Estimation Theory*. Upper Saddle River, NJ: Prentice-Hall PTR, 1998.

[93] P. Kyosti, et al., "WINNER II Channel Models," in *IST-WINNER D1.1.2, ver 1.1, Available: https://www.ist-winner.org/WINNER2-Deliverables/D1.1.2v1.1.pdf*, Sept. 2007.

[94] A. J. Paulraj and C. B. Papadias, "Space-time processing for wireless communications," *IEEE Signal Processing Mag.*, vol. 14, pp. 49–83, Nov. 1997.

[95] J. H. Kotecha and A. M. Sayeed, "Transmit signal design for optimal estimation of correlated MIMO channels," *IEEE Trans. Signal Processing*, vol. 52, pp. 546–557, Feb. 2004.

[96] Y. G. Li, N. Seshadri, and S. Ariyavisitakul, "Channel estimation for OFDM systems with transmitter diversity in mobile wireless channels," *IEEE J. Sel. Areas Commun.*, vol. 17, pp. 461–471, Mar. 1999.

[97] C. R. Rao and S. K. Mitra, *Generalized Inverse of Matrices*. New York: John Wiley and Sons, 1971.

[98] J. Brewer, "Kronecker products and matrix calculus in system theory," *IEEE Trans. Circuits and Systems*, vol. 25, pp. 772–781, Sept. 1978.

[99] A. Goldsmith, *Wireless communications*. Cambridge, England: Cambridge University Press, 2004.

[100] C. Tepedelenlio, A. Abdi, and G. B. Giannakis, "The Ricean K factor: estimation and performance analysis," *IEEE Trans. Wireless Commun.*, vol. 2, pp. 799–810, July 2003.

[101] P. Y. Chen and H. J. Li, "An iterative algorithm for Doppler spread estimation in LOS environments," *IEEE Trans. Wireless Commun.*, vol. 5, pp. 1223–1228, June 2006.

[102] Y. Li and N. R. Sollenberger, "Adaptive antenna arrays for OFDM systems with co-channel interference," *IEEE Trans. Commun.*, vol. 47, pp. 217–229, Feb. 1999.

VITA

Jun Ma was born in Zaoyang, Hubei Province, China. He received the B.S. and M.S. degrees in Electrical Engineering from the University of Science and Technology of China, Hefei, China, in 2003 and 2006, respectively. In 2010, he received the Ph.D. degree in Electrical and Computer Engineering at Georgia Institute of Technology.